UNIVERSITÀ DEGLI STUDI DI MILANO

SCUOLA DI DOTTORATO IN MEDICINA MOLECOLARE

CICLO XXVI

Anno Accademico 2012/2013

TESI DI DOTTORATO DI RICERCA

MED04

The pathogenesis of Malaria Acute Respiratory Distress Syndrome (MA-ARDS): modification of the lipid profile, antioxidant defences and cytokine content in different tissues of malaria infected mice

Dottorando: Diletta SCACCABAROZZI

Matricola N°: R09156

TUTORE: Ch.ma Prof.ssa Donatella TARAMELLI
CO-TUTORE: Ch.ma Prof.ssa Fausta OMODEO SALE'

COORDINATORE DEL DOTTORATO: Ch.Mo Prof. Mario CLERICI

A Samuele

Ai miei genitori, ai fratelli, alla nonna

La scienza è fatta di dati, come una casa di pietre. Ma un ammasso di dati non è scienza più di quanto un mucchio di pietre sia una casa.

Henri Poincaré, *La scienza e l'ipotesi*, 1902

INDEX

SOMMARIO

INTRODUZIONE *La malaria insieme a tubercolosi e AIDS è una delle più diffuse malattie infettive al mondo con più di 650.000 morti e 200 milioni di casi clinici all'anno. Nei casi di malaria severa, si può manifestare nei pazienti la sindrome da insufficienza respiratoria acuta (MA-ARDS) caratterizzata da un'intensa e diffusa infiammazione a livello polmonare, con danni alla parete alveolare e vasale, edema e infiltrato cellulare, principalmente di monociti/macrofagi. Questi contengono pigmento malarico (o emozoina, Hz) noto per stimolare il rilascio di citochine e di altri mediatori dell'infiammazione. Nella MA-ARDS sono anche presenti disfunzioni a livello di diversi organi, tra cui il fegato.Nei casi di ARDS non malarica, sono state descritte alterazioni del surfattante polmonare che possono portare all'aumento della tensione superficiale e al collasso alveolare. I principali compiti del surfattante sono quelli di ridurre la tensione superficiale e regolare la risposta immune locale. Il surfattante è costituito da due frazioni: una definita LA e cioè "large aggregate", ritenuta la frazione attiva; e un'altra definita SA "small aggregate" che costituisce la frazione meno attiva. Non è noto se anche nella MA-ARDS siano presenti alterazioni del surfattante e come possano contribuire alla gravità della sindrome e influire sull'andamento della risposta infiammatoria.*

SCOPO *Lo scopo del lavoro è stato quello di descrivere i cambiamenti fisio-patologici nella MA-ARDS, studiare la risposta infiammatoria sistemica e locale e analizzare i cambiamenti lipidici del tessuto polmonare, del surfattante, del fegato e del plasma utilizzando due modelli di malaria nel topo con gravità simile, ma diverso interessamento di organi interni. In particolare, sono stati usati topi C57BL/6J infettati con due specie di Plasmodio: Plasmodium berghei NK65 (PbNK65) che causa la patologia polmonare e Plasmodium chabaudi (PcAS) che non causa complicanze polmonari. I due modelli hanno permesso di paragonare direttamente la stessa infezione e individuare gli aspetti caratteristici che potranno indirizzare nuove strategie terapeutiche nella MA-ARDS.*

RISULTATI E DISCUSSIONE

Analisi macroscopica e funzionale del tessuto polmonare nei due ceppi*. I polmoni dei topi infettati con PbNK65, ma non quelli con PcAS, si presentano edematosi, aumentati in peso e di color bruno a causa di microemorragie e della deposizione di aggregati di Hz. Solo nei polmoni dei topi con PbNK65 si è osservata un'aumentata espressione di citochine, tra cui TNF-α e IFN-γ, indotta quindi specificatamente durante la MA-ARDS e non dovuta all'infezione malarica. Questo è confermato dalla osservazione che nei topi trattati con desametasone (DEX) si registra un aumento della sopravvivenza, una diminuzione dell'edema polmonare e dell'infiltrato di cellule CD8+ senza una riduzione della parassitemia. Il tessuto polmonare dei topi con PbNK65 presenta un aumento dei fosfolipidi (PL) totali e degli esteri del colesterolo (ChoE) caratterizzati da un elevato rapporto acido linoleico/oleico tipico dei ChoE plasmatici. Il trattamento con DEX riporta il profilo lipidico alla norma. Questi risultati indicano che l'infiltrazione di lipoproteine plasmatiche e l'edema interstiziale sono responsabili delle variazioni del pattern lipidico del polmoni. Il trattamento con DEX migliora la patologia polmonare perché interviene sulla risposta infiammatoria.* ***Analisi proteica e lipidica del surfattante e del plasma dei topi infetti.*** *Il surfattante dei topi infettati con PbNK65 presenta un aumento delle proteine rispetto a quello dei topi controllo (CTR) o infettati con*

PcAS, probabilmente dovuto all'aumento delle proteine plasmatiche che vengono incorporate in microstrutture presenti nell'ipofase alveolare. È noto che questo comporta una diminuzione dell'attività del surfattante stesso. Il contenuto totale di PL non varia in nessun gruppo, ma cambia significativamente il profilo dei singoli PL in entrambe le frazioni di surfattante. Sia la frazione LA che SA dei topi con PbNK65 presentano un aumento di sfingomielina (SM) e una diminuzione di fosfatidilglicerolo (PG). Questi cambiamenti, presenti solo nei topi PbNK65, potrebbero essere dovuti ad una alterata sintesi e degradazione dei PL da parte delle cellule alveolari danneggiate.

I livelli plasmatici di PL e trigliceridi (TG) sono significativamente maggiori nei topi PbNK65 rispetto ai topi CTR o infettati con PcAS. Nei topi PbNK65 aumentano tutte le classi di PL ad eccezione della lisofosfatidilcolina. Queste alterazioni plasmatiche potrebbero essere dovute ad alterazioni dell'attività degli enzimi coinvolti nel metabolismo lipoproteico. Il profilo degli acidi grassi plasmatici presenta livelli elevati di acido docosaesanoico (DHA) sia nei topi PbNK65 che PcAS, e questo aumento è solo parzialmente diminuito dal trattamento con DEX. Questo suggerisce che l'aumento di DHA non sia dovuto alla complicanza polmonare ma piuttosto alla patologia malarica. ***Analisi del fegato di topi infetti.*** *L'ipotesi che l'aumento di TG e di PL plasmatici fosse dovuto ad un'aumentata lipogenesi epatica è stata confermata analizzando il fegato dei topi infetti e CTR. Il fegato dei topi PbNK65 presenta maggiori livelli di TG e ChoE e un aumento del rapporto acido linoleico/arachidonico probabilmente dovuto all'alterazione della via di allungamento/desaturazione degli acidi grassi. Sono anche presenti nel tessuto maggiori livelli di Hz che giustificano il TNF-α elevato. E' noto infatti che Hz stimola le cellule di Kuppfer a produrre citochine infiammatorie. Sia Hz che TNF-α promuovono perossidazione lipidica come confermato dagli elevati livelli di malonildialdeide trovati negli omogenati di tessuto epatico. Negli stessi campioni, negli stadi più avanzati della patologia, si sono osservati anche bassi livelli di glutatione e degli enzimi antiossidanti a conferma dell'elevato stress ossidativo a cui il tessuto è stato sottoposto.*

CONCLUSIONI *Lo studio presenta per la prima volta un'analisi approfondita delle alterazioni lipidiche e della risposta infiammatoria in diversi organi in due modelli murini di MA-ARDS. I dati suggeriscono che anche nella malaria, come in altre patologie non infettive, esiste un interplay patologico e metabolico polmone-fegato. Nei topi PbNK65, l'Hz depositata nei polmoni e il conseguente stato infiammatorio sono fondamentali per la patologia polmonare inducendo aumento di infiltrato e di citochine, e cambiamenti nella composizione lipidica del surfattante e del tessuto polmonare. La patologia polmonare è associata ad alterazioni delle lipoproteine plasmatiche che sembrano derivare dalla disfunzione epatica a sua volta causata dai depositi di Hz che inducono i macrofagi a produrre TNF-α e ROS. Ne consegue perdita di funzionalità epatica, aumento della lipogenesi e alterazione dei lipidi plasmatici a loro volta responsabili delle variazioni polmonari. Questi risultati confermano che la malaria è una malattia multisistemica e che la co-somministrazione di farmaci anti-infiammatori e anti malarici potrebbe essere utile nel combattere la malattia e le sue complicanze.*

ABSTRACT

INTRODUCTION *Malaria is a major health problem, with more than 650.000 deaths and 200 million clinical cases each year. Respiratory distress as malaria associated acute respiratory distress syndrome (MA-ARDS) is a common complication. The pathogenesis of MA-ARDS is mainly inflammatory and one of the main observation is the presence of abundant monocytes and macrophages inside the blood capillaries, in the interstitium and also in alveolar spaces. Malaria pigment or haemozoin (Hz) is often seen in these cells reflecting active phagocytosis and leads to the production of cytokines and other inflammatory mediators. Multiple organ dysfunctions are described in MA-ARDS, including liver damages. ARDS in non malarious patients is often associated with disorders of the lung surfactant, which can lead to the increase in surface tension, alveolar collapse and loss of the liquid balance in the lungs. Surfactant is known to reduce the surface tension at the air–liquid interface of lung epithelia and to regulate the local host immune response. It can be separated into a surface active Large Aggregate fractions (LA), representing a reservoir for the surface film located at the air-liquid interface of the alveoli and a less surface active, Small Aggregate fraction (SA). It is not known at present if alterations of the surfactant also exist in MA-ARDS and how they may contribute to the pathology and the development of the inflammatory response.*

AIM *The aim of our studies was to perform a comprehensive analysis of the local and systemic inflammatory response present in MA-ARDS and to analyse the lipid profile of the pulmonary surfactant, the lung and liver tissues and plasma using two different models of murine malaria of similar gravity, but different involvement of lungs or liver. In particular, we studied C57BL/6J mice infected with two different species of Plasmodium: Plasmodium berghei NK65 strain which induces MA-ARDS and Plasmodium chabaudi (PcAS), which does not. The two models allowed us to directly compare the different pathological manifestation of the same infection in order to identify peculiarities which could be exploited for novel therapeutic interventions.*

RESULTS AND DISCUSSION

Macroscopic and functional analysis of lung tissues in the two strains. *The lungs of PbNK65 infected mice were swollen, increased in weight and with a dark brown aspect due to micro haemorrhages and to the deposition of Hz clusters in concentrations significantly higher compared to the lungs of mice infected with PcAS. The expression of TNF-α and IFN-γ was increased only in PbNK65 mice, indicating that these cytokines are induced specifically during MA-ARDS and are not a consequence of malaria infection. This hypothesis was confirmed by the decrease of lung weight and of the $CD8^+$ cells infiltrate, and the reduction /delay in mortality rates seen in PbNK65 mice treated with DEX without a concomitant reduction in parasitaemia. Therefore, DEX seems to ameliorate MA-ARDS, not by inhibiting parasite growth but rather by modulating the immunopathology and the inflammatory response. A significant increase of the total phospholipid (PL) content and cholesterol esters (ChoE) was observed in PbNK65 lungs and was reverted by DEX. Moreover, compared to the control mice (CTR), the fatty acid distribution of lung ChoE was characterized by higher levels of the polyunsaturated fatty acid and an high linoleic/oleic ratio typical of plasma ChoE. All these features confirm a strict*

correlation between the interstitial oedema and the infiltration of plasma lipoproteins during MA-ARDS. ***Protein and lipid composition of surfactant and plasma of infected mice.*** *The total bronchoalveolar lavage (BAL) of PbNK65 mice showed a significant increase in the protein levels compared to CTR or PcAS mice, probably due to plasma derived proteins being incorporated into or associated with microstructures in the alveolar hypophase. This event is known to decrease the intrinsic surface activity of surfactant. The total content of PL was not different from CTR, whereas the PL profile of the LA and SA fractions in PbNK65 infected mice showed a significant increase in the amounts of sphingomyelin and a decrease in phosphatidylglycerol. These changes were absent in PcAS mice and may be related to the altered re-uptake and synthesis of PL by injured cells or to PL contamination due to inflammatory cells. The plasma levels of PL and triacylglycerol (TG) were significantly higher in PbNK65 mice than in CTR or PcAS mice. Compared to PcAS or CTR mice in PbNK65 group all the PL classes were significantly increased with the exception of lisophosphatidilcholine (LisoPC) that was decreased. These plasma alterations may be related to an impaired activity of the enzymes involved in the lipoprotein metabolism during infections or inflammatory diseases. The most important observation, both in PbNK65 and PcAS mice, was the significant increase of docosahexahenoic acid (C22:6 n-3, DHA) compared to CTR, which was only partially reverted by DEX treatment, suggesting that the increase of DHA is not related to lung pathology but rather to the malaria infection.* ***Analysis of the liver tissue of infected mice.*** *The hypothesis that the higher PL and TG content of PbNK65 plasma might be due to an enhanced hepatic lipogenesis was confirmed by the higher TG and ChoE content of the liver of PbNK65 mice compared to PcAS and CTR. An increased ratio linoleic (LA)/arachidonic acid (AA) was also present possibly due to the impairment of the elongation/desaturation pathway from LA to AA acid. Higher levels of Hz, compared to PcAS, were present in PbNK65 mice and, in agreement with the Hz capability of stimulating Kupffer cells, we found higher levels of TNF-α. Both Hz and TNF-α can induce lipoperoxidation as confirmed by the elevated levels of malondialdehyde (MDA) in the liver of PbNK65 mice. This finding was paralleled by the lower content of glutathione and of antioxidant enzymes particularly in the late stage of the pathology.*

CONCLUSIONS *This is the first time that a comprehensive analysis of the lipid content and inflammatory response of different organs in a model of murine MA-ARDS has been performed. All together the data suggest that in MA-ARDS as in other severe non infectious pathologies, a pulmonary-liver metabolic interplay exist which may contribute to the pathology. In PbNK65 mice, Hz and the derived inflammation play an important role in the lung pathology inducing changes in the lipid composition of lung and surfactant, cellular infiltration and cytokine production. Lung pathology is associated with liver disorders and alterations in the lipoprotein profile. Hz accumulation may induce macrophages to produce TNF-α and ROS that can interfere with liver functions by inducing lipogenesis and affecting the lipid profile of liver and plasma, which in turn contribute to the altered lipid composition of the lung tissue. These results confirm that severe malaria is a multi-organ dysfunction in which inflammation has an important role in different organs and thus, in addition to antimalarial treatment, adjunct therapies with anti-inflammatory drugs can be envisaged.*

ABBREVIATIONS

AA= arachidonic acid (C20: 4)

ALI= acute lung injury

ARDS= acute respiratory distress syndrome

BAL= bronchoalveolar lavage

BALF= bronchoalveolar lavage fluid

CAT= catalase

Cho= cholesterol

ChoE= cholesterol esters

CM= cerebral malaria

CTR= control

DEX= dexamethasone

DHA= docosahexanoic acid (C22:6, n-3)

FFA= free fatty acid

FP= ferric protoporphyrin IX

G6PD= glucose 6 phosphate dehydrogenase

GR= glutathione reductase

GSH+GSSG= total glutathione

Hb= haemoglobin

HDL= high density lipoprotein

HDP= haeme detoxification protein

HL= hepatic lipase

HPTLC= high performed thin layer chromatography

Hz= haemozoin

ICUs= intensive care units

IFN-γ= interferon γ

IL- = interleukin

iRBC= infected red blood cell

LA= large aggregate fraction

LCAT= lecihtin cholesterol acyltransferase

LDH= lactate dehydrogenase

LPC= lysophosphatidylcholine

MA-ARDS= malaria acute respiratory distress syndrome

MCP-1= monocyte chemoattractant protein

MMPs= matrix metalloproteinase

NF-kB= nuclear factor kappa B

NO= nitric oxide

PbANKA= Plasmodium berghei ANKA

PbNK65= Plasmodium berghei NK65

PbNK-DEX= Plasmodium berghei NK65 treated with dexamethasone

PC= phosphatidylcholine

PcAS= Plasmodium chabaudi AS

PE= phosphatidylethanolammine

Pf= Plasmodium falciparum

PG= phosphatidylglycerol

PI= phosphatidylinositol

PL= phospholipids

pRBC= parasite red blood cell

PS= phosphatidylserine

PVM= parasitophorous vacuolar membrane

RBC= red blood cell

ROS= reactive oxygen species

SA= small aggregate fraction

SM= sphingomyelin

SOD= superoxide dismutase

sPLA2= secretory phospholipase A2

TG= triglycerides

TGF-β= transforming growth factor β

TLR-9= toll like receptor-9

TNF-α= tumor necrosis factor α

VEGF= vascular endothelial growth factor

VLDL= very low density lipoprotein

1 INTRODUCTION

1.1 Malaria disease

Malaria is the most deadly parasitic infection of humans. Although economic development and the implementation of control measures during the twentieth century have eliminated malaria from many areas of the world, the disease is still rampant in the tropics and in the poorest regions of the globe, affecting 3 billion people and killing up to 1 million annually (World Health Organization, malaria report, 2012)

Malaria is a parasistic disease transmitted by the bite of an infected female mosquito of more than 30 *Anopheles* species and caused by five species of parasites of the genus ***Plasmodium*** that affect humans: ***P. falciparum***, ***P. vivax***, ***P. ovale***, ***P. malariae*** and ***P. knowlesi***. Malaria due to *P. falciparum* is the most deadly form and it predominates in Africa; *P. vivax* is less dangerous but more widespread, and the other three species are found much less frequently. Globally, an estimated 3,3 billion people were at risk of malaria in 2011, with populations living in sub-Saharan Africa having the highest risk of acquiring malaria: approximately 80% of cases and 90% of deaths are estimated occur in the African Region, with children under five years of age and pregnant women most severely affected (World Health Organization, malaria report, 2012).

In such areas, changes in environmental, economic, or social conditions (heavy rains after drought, large population movements together with a breakdown in malaria control and prevention services often because of armed conflicts) can result in epidemics, with substantial mortality in all age groups (*1*).

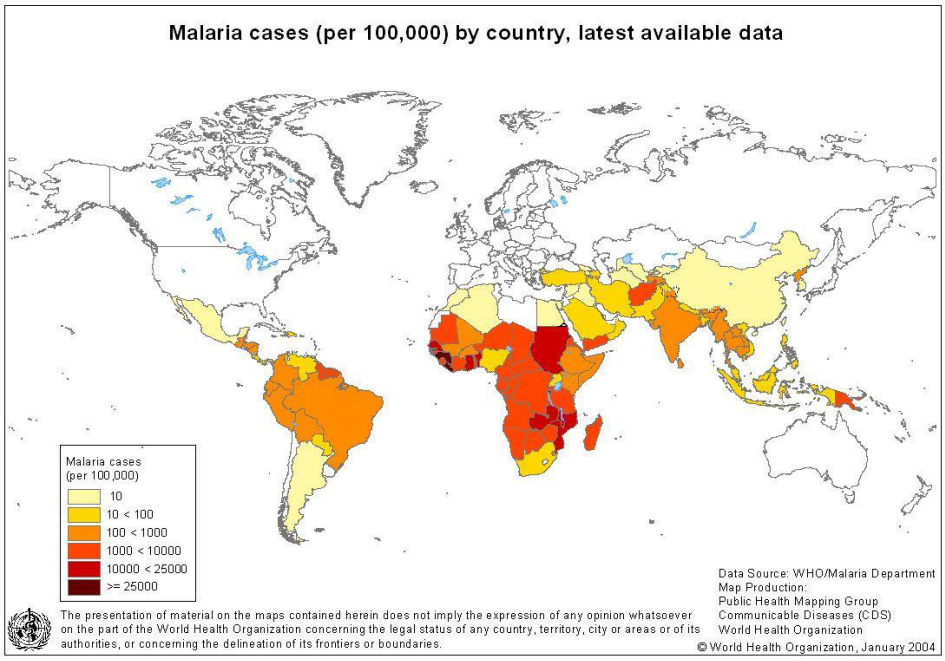

Figure 1- Malaria cases by country. Data source: WHO, Malaria Report 2012

Malaria is an entirely preventable and treatable disease, provided the currently recommended interventions are properly implemented. These include: vector control through the use of insecticide-treated nets, indoor residual spraying and, in some specific settings, larval control; chemoprevention for the most vulnerable populations, particularly pregnant women and infants; confirmation of malaria diagnosis through microscopy or rapid diagnostic tests for every suspected case; timely treatment with appropriate antimalarial drugs according to the parasite species and drug resistance.

1.2 The malaria parasite life cycle

The symptoms of malaria are caused by cycles of parasite multiplication inside host erythrocytes, and various complications, including cerebral malaria, result from cytoadherence of infected erythrocytes to endothelia.

The *P.falciparum* parasite life cycle comprises two stages: the first (sexual phase) takes place in the *Anopheles* mosquito vector and the second one in the human host (asexual phase) (Figure 2).

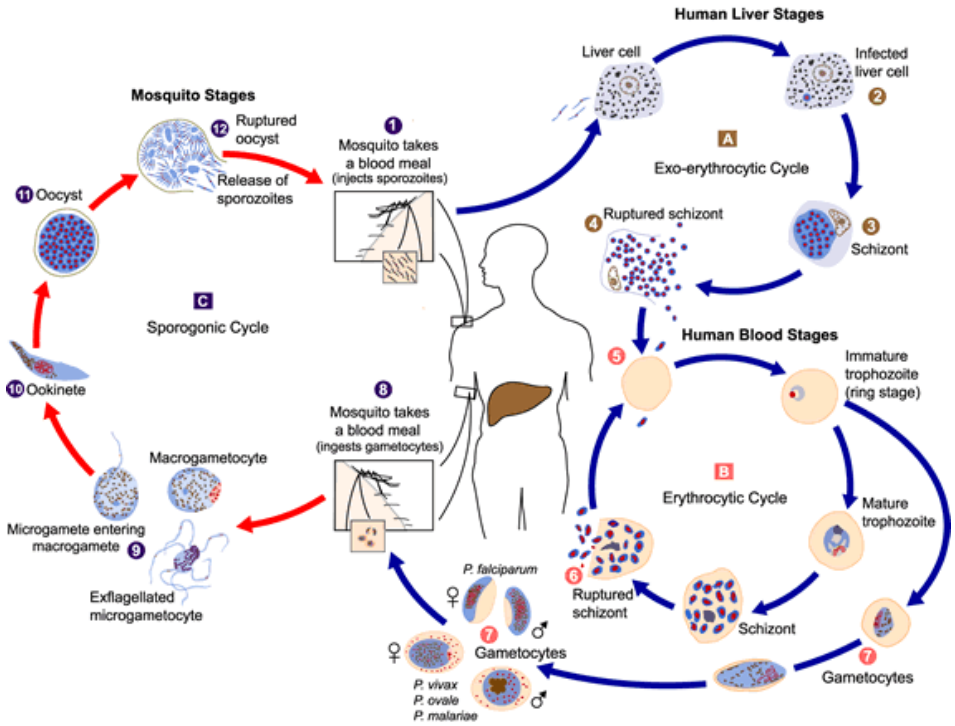

Figure 2- The malaria parasite life cycle (Parasite Image Library)

The malaria parasite life cycle involves two hosts. During a blood meal, a malaria-infected female Anopheles mosquito inoculates sporozoites into the human host (Point 1, Figure 2). Sporozoites infect liver cells (Point 2, Figure 2) and mature into schizonts (Point 3, Figure 2), which rupture and release merozoites (Point 4, Figure 2). After this initial replication in the liver (exo-erythrocytic schizogony; Point [A], Figure 2), the parasites undergo asexual multiplication in the erythrocytes (erythrocytic schizogony; Point [B], Figure 2). Merozoites infect red blood cells (Point 5, Figure 2). The ring stage trophozoites mature into schizonts, which rupture releasing merozoites (Point 6, Figure 2). Some parasites differentiate into sexual erythrocytic stages (gametocytes) (Point 7, Fiure 2). Blood stage parasites are responsible for the clinical manifestations of the disease. The gametocytes, male (microgametocytes) and female (macrogametocytes), are ingested by an Anopheles mosquito during a blood meal (Point 8, Figure 2). The parasites' multiplication in the mosquito is known as the sporogonic cycle; (Point [C], Figure 2). While in the mosquito's stomach, the microgametes penetrate the macrogametes generating zygotes (Point 9, Figure 2). The zygotes in turn become motile and elongated (ookinetes) (Point 10, Figure 2) which invade the midgut wall of the mosquito where they develop into oocysts (Point 11, Figure 2). The oocysts grow, rupture, and release sporozoites (Point 12, Figure 2), which make their way to the mosquito's salivary glands. Inoculation of the sporozoites into a new human host perpetuates the malaria life cycle (Point 1, Figure 2).

Malaria is transmitted when a female mosquito, infected with *P.falciparum*, takes a blood meal from a human. The parasites, at the stage of motile sporozoites, are injected from the salivary glands of the infected mosquito and travel to the liver via the microvasculature, a process that occurs over a few minutes. In the liver parasites develop into hepatic trophozoites and undergo asexual reproduction forming many merozoites which are

enclosed in small packages of host cell membrane termed merosomes. This asymptomatic hepatic stage of infection usually lasts about 10-12 days. Hepatic cell rupture leads to merozoites release into the blood stream where they invade circulating erythrocytes of the human host and embark upon the clinically important “intra-erythrocytic cycle” of asexual replication, which is ultimately responsible for all the clinical symptoms associated with the disease. This part of the parasite life cycle produces 8-20 new merozoites every 48-72 hours, causing parasite numbers to rise rapidly to level as high as 10^{13} per host. Following invasion of a red blood cell (RBC), the merozoite matures into a “ring stage” parasite, so called for the ring-like morphology of the parasite on a Giemsa smear. *P. falciparum* differs from other human malaria species in that parasitized erythrocytes do not remain in the circulating blood for their entire life cycle. In fact after 24-32 hours, when young parasites mature from the ring to the trophozoite stage, parasitized RBCs (pRBCs) adhere to endothelial cells in the microcirculation of various organs (sequestration), including the brain. Trophozoites in the host RBC degrade haemoglobin (Hb) and accumulate the breakdown product haemozoin (Hz), also called “malaria pigment”. At 36-48 hours trophozoites mature into schizonts which undergo the division (schizogony) of a single schizont into 16-32 individual merozoites. pRBC rupture leads to merozoite release that invade fresh erythrocytes to perpetuate the asexual life cycle. In response to poorly understood signals, some of the intra-erythrocytic parasites commit to sexual reproduction and differentiate into male and female gametocytes in the blood of their host. Gametocytogenesis can be triggered *in vitro* by cooler temperatures or an increase in pH, however, in nature, it may also involve a chemical cue from within the mosquito (*2*).

Upon ingestion by a feeding female mosquito, the gametocytes fuse in its midgut and the resulting ookinete invades the midgut wall where it will

develop into an oocyst. The cycle is completed when the division of the oocyst produces a large numbers of infective sporozoites which migrate to the salivary gland of the mosquito ready to be injected into a host during a blood meal, thereby ensuring the continuation of the parasite life cycle (Figure 2).

1.2.1 The intra-erythrocytic cycle of Plasmodium

How P.falciparum survives in the human host erythrocyte?

The mature human red blood cell (RBC) is a terminally differentiated cell. It lacks subcellular organelles (such as a nucleus or secretory structures) and de novo protein/lipid biosynthesis. RBCs contain high concentrations of cytoplasmic haemoglobin (about 5mM) and a deformable submembrane cytoskeleton, which reflects the specialized functions of erythrocytes for delivering oxygen to tissues and surviving repeated passage through capillaries. To maintain erythrocyte function in circulation, clearance of older RBC and production of new ones are carefully coordinated to optimize the delivery of oxygen to tissues. Because erythrocytes lack endocytic machinery, parasites attach and enter erythrocytes via several pathways by different ligand–receptor interactions. The study of the erythrocyte-malaria parasite interaction shows that both parasite and erythrocyte components regulate parasite entry and intracellular growth by extensively remodeling host membranes. These remodeling events include: the invagination of the host cell membrane during parasite entry that results in the creation and maintenance of a parasitophorous vacuolar membrane (PVM) that surrounds the intracellular organism; the development of antigenic, structural, and transport alterations during intracellular parasite development.

Malarial erythrocyte remodelling events presumably occur at a significant cost to the human host because many of the associated processes have

been linked to clinical evidence of severe disease. The malaria parasite has developed a number of ways to ensure its survival in the RBC. After invasion the parasite faces a number of biochemical challenges, some of which arise through its own metabolism. When merozoites invade the host RBCs they grow by ingesting the host cell cytoplasm. Haemoglobin (Hb), ingested via a cytostome through an endocytic process, is digested in a specialized acidic organelle (the digestive or food vacuole, analogous to phagolysosomes of mammalian cells) through the combined action of at least two aspartic proteases (plasmepsins I and II) and one cysteine protease (falcipain) (*3*).

It has been hypothesized that the parasite degrades Hb to obtain building blocks for protein synthesis, maintain osmotic balance and to provide space for its own growth (Figure 3). Four molecules of haem [ferrous-protoporphyrin IX, Fe(II)PPIX] are released from each molecule of Hb when digested by the malaria parasite. It is commonly accepted that, in the presence of molecular oxygen in the parasite food vacuole, Fe(II)PPIX is oxidized to form Fe(III)PPIX (FP) following a Fenton-Haber-Weiss-type reaction: at that time, a cascade of events begins, on one hand, to prevent haem toxicity and on the other hand, to scavenge the reactive oxygen species produced. Free FP is highly toxic, inhibiting enzymes and destabilising membranes via detergent-like effects and via catalysis of lipid peroxidation (*4*-*6*).

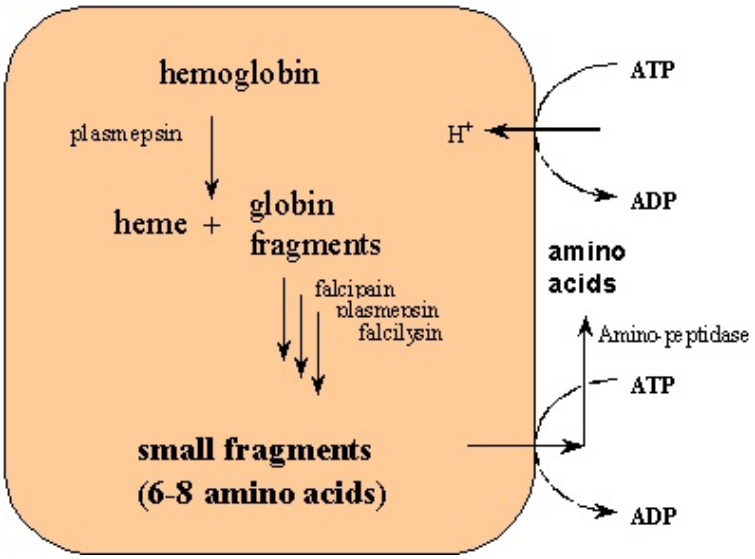

Figure 3- Haemoglobin degradation in the food vacuole of Plasmodium falciparum

To avoid the toxic effects of a product that arises through its own metabolism, the parasite sequesters free FP into a crystalline form termed haemozoin (Hz) or malaria pigment (Figure 4). The crystal forms via the coordination of the central iron atom of one molecule to one carboxyl of the adjacent molecule (*7*).

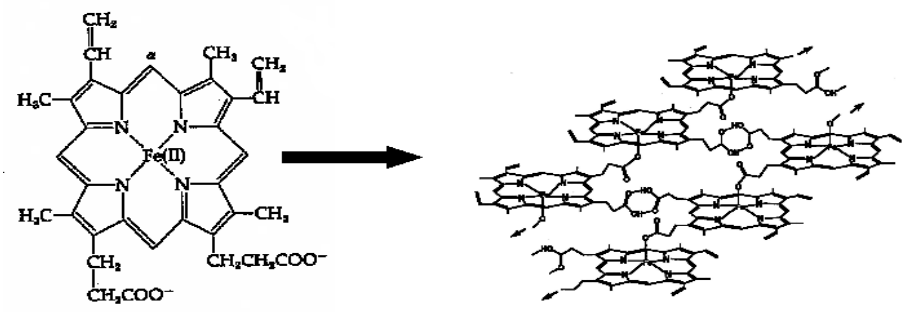

Figure 4-Haem detoxification: haemozoin formation

This non-enzymatic process is known as biocrystallization (*8*) and although it is not completely understood, it appears that lipids, the digestive vacuole membrane, and the acid environment play a crucial role for the organized aggregation of haem monomers into Hz crystals (*9, 10*).

Recently, a parasite protein, the Haem Detoxification Protein (HDP), has been described, which seems to be involved in accelerating the conversion of haem into Hz (*11*). With a 1–10% parasitaemia, as much as 0,2–2,0 g Hz may be produced by *P. falciparum* during each cycle (*12*). At the end of the cycle, erythrocytes rupture, and Hz crystals are liberated along with the daughter merozoites into the blood stream. Hz is rapidly ingested by phagocytic cells such as macrophages present in many organs, especially in the liver and spleen. HZ can be observed as a dark crystal by light microscopy (Figure 5).

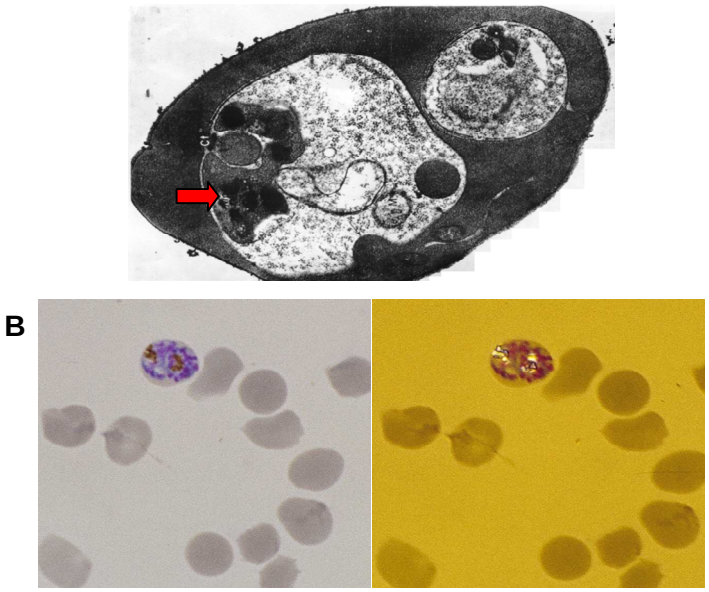

Figure 5-Hz in an infected red blood cell (red arrow). By light microscopy, HZ can be observed as a dark-brown crystal (B)

1.2.1.1 Why is Hz important?

Hz is important as an antimalarial drug target, in diagnostic applications and it appears to be biologically active, especially as an immune modulator. Hz formation is the target of the classic quinoline group of compounds (*13, 14*), and it may even play a role in the mode of action of artemisinins (*15, 16*). These drugs may act inhibiting Hz growth by formation of haem drug adducts (*17*) by interfering with nucleation of the crystal or by binding to the Hz crystal surface, thus preventing further growth (*13*). Different binding strengths or binding preferences of antimalarial drugs to the different faces of the crystal may explain the different inhibitory potency of antimalarial drugs on Hz growth (*13*).

The detection of Hz is also useful in the diagnosis of malaria, especially in methods that make use of its birefringent and paramagnetic properties (*18, 19*). Additionally, several studies reported a correlation of Hz-containing

monocytes and granulocytes with disease severity, especially an increase in the severe forms of malaria (*20-22*).

An increasing number of studies recently demonstrated that Hz has intrinsic biological activity especially on the immune system. Several groups reported an increased pro-inflammatory effect (*23, 24*). Other studies reported a positive correlation between Hz-containing monocytes or granulocytes and malarial anaemia (*25-27*) or an association between increased levels of Hz in pulmonary tissue with malaria-associated acute respiratory distress syndrome (MA-ARDS) in a mouse model (*28*). Hz has also been reported to have an adjuvant effect, possibly mediated through Toll-like receptor 9 (TLR9) (*29*). Some have questioned if biological effects are caused by Hz itself or by other bio-molecules that might be bound to Hz, especially DNA (*30*). For example, conflicting results were presented on whether Hz alone or DNA bound to Hz interacts with TLR9 to enhance innate responses (*30, 31*). Others reported that proteins, such as fibrinogen, bind to Hz and cause a strong initial stimulation of reactive oxygene species (ROS) production and an increase in the levels of TNF-α and MCP-1 (monocyte chemoattractant protein-1) in *in vitro* experiments (*32*). One study reported that synthetic Hz alone appeared inactive and only showed effects in the presence of RBC ghosts (which mainly consist of the membrane); this finding was interpreted as an interaction between Hz and RBC lipids (*33*). The finding that attached molecules, rather than the Hz crystal itself, cause biological effects finds support in the strong adsorptive properties of Hz (*34*). In fact, Hz crystals tend to stick to each other, and sometimes researchers resort to extensive sonication to disperse Hz before *in vitro* experiments (*29, 35*).

Other contradictory results have been reported, for example, concerning nitric oxide (NO) and ROS production (*33, 36, 37*). One study concluded that human monocytes containing Hz do not release NO (*36*), whereas a

different result was observed with murine macrophages (*37*). Hz was also found to either enhance or inhibit dendritic cell maturation (*38*).

Certainly, a possible explanation for these discrepant results could be the widely varying experimental protocols, including diverse types and origins of phagocytic cells, variable incubation times with Hz, or different types of Hz (*23, 24*).

1.3 Genetics of malaria disease

No infectious disease has shaped the human genome more than has malaria. The geographic distributions of sickle cell disease, haemoglobins C and E, ovalocytosis, thalassaemias, and glucose-6-phosphate dehydrogenase (G6PD) deficiency are roughly similar to that of malaria before the introduction of control measures, which suggests that these disorders confer a survival advantage in the presence of malaria (*39*). Malaria protective mechanisms include decreased parasite growth at low oxygen tensions (haemoglobin AS [HbAS]), reduced cytoadherence (haemoglobins AC [HbAC] and CC [HbCC] and HbAS), reduced invasion (ovalocytosis), reduced parasite densities (G6PD deficiency), and reduced multiplication at high densities (haemoglobin AE [HbAE]) (*40-42*). The immune response to malaria is incompletely understood. Non-specific host defence mechanisms control the infection initially. Subsequent strain-transcending and strain-specific immune responses then struggle against parasitic antigenic variation to eliminate the blood-stage infection. Both humoral and cellular immunity contribute to protection. Eventually, exposure to sufficient strains confers protection from illness, but not from infection (premonition). Asymptomatic parasitaemia is common in adults and older children living high-transmission areas (*43*).

1.4 Pathogenesis of malaria

In *P. falciparum* malaria, protuberances or knobs emerge on the infected erythrocyte's surface 12–15 h after invasion. These protuberances extrude high-molecular-weight, antigenically variant, strain-specific adhesive proteins (*Pf*EMP1) that mediate cytoadherence (attachment to endothelial surface receptors in veins and capillaries). Of the potential receptors identified, ICAM1 is probably the most important in the brain, chondroitin sulphate A in the placenta, and CD36 in most other organs (*44*). Infected erythrocytes adhere to the vessel walls and sometimes to each other (*45*) or to uninfected erythrocytes (rosetting) (*46*). Adherence causes sequestration of RBCs containing mature parasites into vital organs (particularly the brain), where the sequestered parasites interfere with microcirculatory flow and metabolism and the functioning of vascular endothelium (*47*). As a result, only the younger ring form *P. falciparum* parasites circulate in falciparum malaria, and thus peripheral parasite counts the total number of parasites in the body. Other malarias are not sequestered substantially, so all developmental stages are noted in peripheral blood smears.

P. vivax, *P. ovale*, and *P. malariae* invade RBC selectively (eg, *P. vivax* invades only young erythrocytes), and parasitaemias are usually less than 1%; *P. falciparum* and *P. knowlesi* are less selective and can reach very high parasite densities (*48*). The host responds to malaria by augmenting splenic immune function and filtrative clearance, accelerating removal of both parasitised and uninfected erythrocytes (*49*). Schizont rupture releases parasite and host cellular material into the blood, which activates monocytes and macrophages and induces the release of pro-inflammatory cytokines, causing fever and other pathological effects (*50, 51*).

1.5 Recurrent or persistent malaria

Blood-stage infection can persist for months or years (or decades in *P. malariae* infections) when untreated. Waves of asexual parasitaemia and gametocytaemia result from antigenic variation. In tropical regions, *P. vivax* relapses typically every 3–4 weeks (or every 6–8 weeks after treatment with slowly eliminated drugs, which suppress the first relapse). In temperate areas, *P. vivax* can remain latent for 8–10 months between primary infection and first relapse (*52*). Recurrent *falciparum* and *vivax* malaria have pronounced adverse effects in young children, and interfere with growth, development, and schooling.

1.6 Clinical features

In endemic areas malaria is often the most common cause of fever. The first symptoms of malaria are non specific, and include a vague absence of wellbeing, headache, fatigue, muscle aches, and abdominal discomfort, which are followed by irregular fever. Nausea, vomiting, and orthostatic hypotension occur frequently. Generalised seizures are associated specifically with *falciparum* malaria and might be followed by coma (cerebral malaria). Most patients with uncomplicated infections have few abnormal physical findings other than fever, mild anaemia, and, after several days, a palpable spleen. The liver can become enlarged, especially in young children, whereas mild jaundice is more likely in adults. In young children living in regions in which transmission is stable, recurrent infections cause chronic anaemia and splenomegaly. The manifestations of severe *falciparum* malaria depend on age (*53*). Severe anaemia and hypoglycaemia are more common in children, whereas acute pulmonary oedema, acute kidney injury, and jaundice are more common in adults; coma (cerebral malaria) and acidosis occur in all age groups (Figure 6).

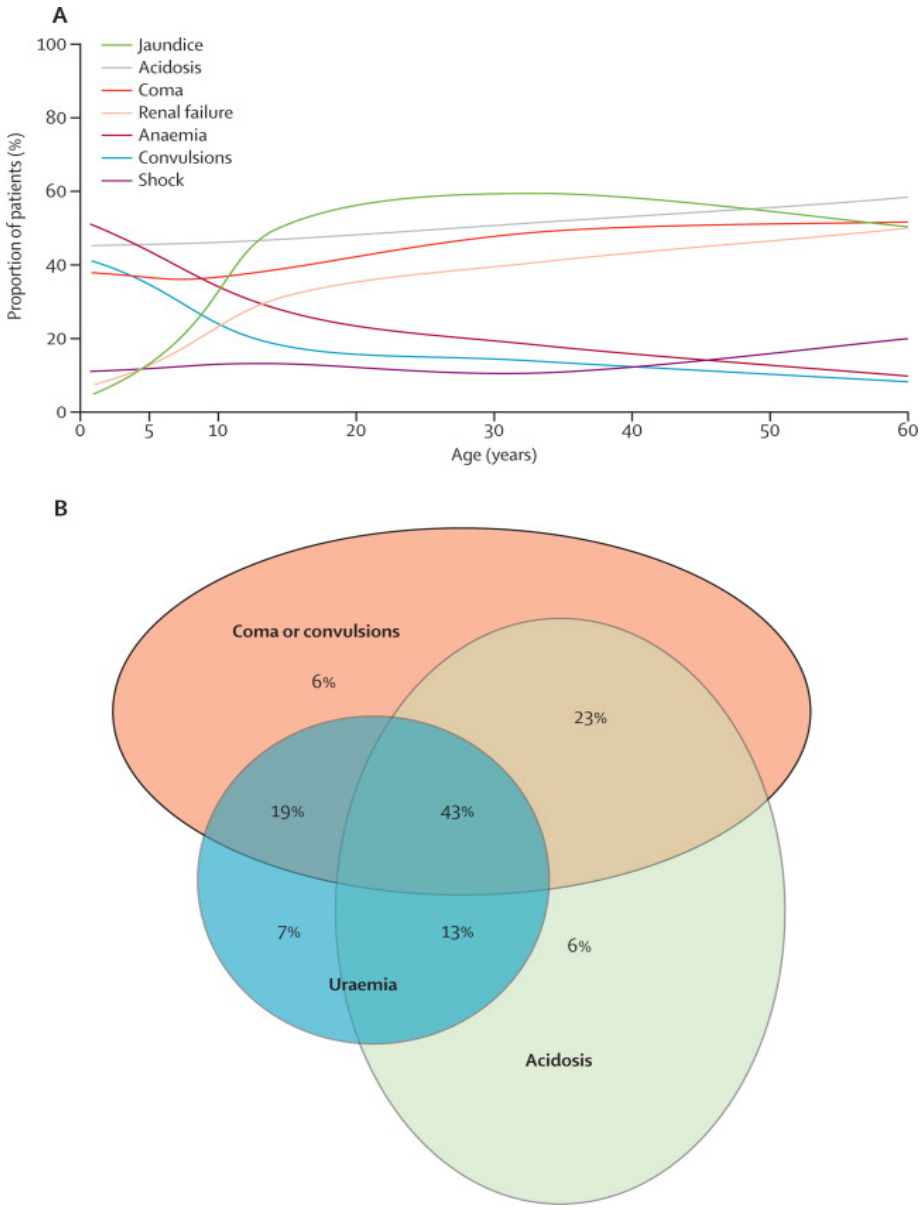

Figure 6-Manifestations of severe falciparum malaria by age (A) and mortality in children associated with coma, convulsion, acidosis and uraemia (B).

Mortality rises when the proportion of infected erythrocytes (parasitaemia) exceeds 2%, although the relation between parasite density and prognosis in *falciparum* malaria is very variable. When treated promptly with effective antimalarial drugs, uncomplicated *falciparum* malaria has a mortality of roughly 1%.

1.6.1 Cerebral malaria

In fatal cases of cerebral malaria, many cerebral capillaries and venules are packed tightly with parasitised erythrocytes, whereas other adjacent vessels are not obstructed (*1, 54, 55*). A distinct and specific malarial retinopathy with haemorrhages and retinal and vessel whitening occurs both in children and in adults. Organ-specific and systemic blood lactate–pyruvate ratios are increased in proportion to the severity of illness (a different profile compared to the hyper-metabolism of sepsis) (*56*). All these findings suggest that extensive microvascular obstruction and impaired perfusion are the crucial pathophysiological processes. Little histopathological evidence of inflammation is noted, although leucocytes are more prominent in the cerebral vessels of African children than in those of Asian adults who died from cerebral malaria (*57, 58*). A mild, generalised increase in systemic vascular permeability is noted. The blood–brain barrier is functionally intact (*59*) although the results of autopsies of African children suggest some increase in permeability, with disruption of endothelial intercellular tight junctions.

1.6.2 Severe anaemia

Severe anaemia is the main manifestation of severe malaria in young children in areas of high transmission (*60*) and is usually the cumulative result of repeated infections. Accelerated splenic removal of mainly the uninfected RBCs and erythrocyte destruction at parasite schizogony are compounded by ineffective erythropoiesis (*61, 62*). Slight coagulation

abnormalities are frequent, and thrombocytopenia is usual even in uncomplicated malaria (a normal platelet count should lead clinicians to question the diagnosis of malaria). Substantial bleeding from disseminated intravascular coagulation in severe malaria is rare. Haematemesis from stress ulceration or acute gastric erosions can occur. Malarial anaemias are classified as uncomplicated (Hb<110 g/l, haematocrit <33%) or severe (Hb<50 g/l, haematocrit <15%). Anaemia may become worse after treatment begins, particularly if the parasitaemia is high. The anaemia is typically normocytic and normochromic, with a notable absence of reticulocytes, although microcytosis and hypochromia may be present due to the very high frequency of α and β thalassaemia trait and/or iron deficiency in many endemic areas.

1.6.3 Pulmonary oedema

Acute respiratory distress syndrome (ARDS) is a feared complication in adults with severe *falciparum* malaria (particularly in pregnant women), which can also occur in *P. vivax* and *P. knowlesi* infections (*63, 64*). Increased pulmonary capillary permeability develops in as much as 30% of adult patients and often manifests after the start of antimalarial treatment (*65, 66*). Pathogenesis is not fully understood, but inflammation-mediated endothelial damage might have an important role. The role of pulmonary vascular parasite sequestration is unclear. Careful fluid management is essential; in the absence of mechanical ventilation, the mortality of acute respiratory distress syndrome exceeds 80%. With mechanical ventilation, case fatality still exceeds 50% in *falciparum* malaria.

1.6.4 Acute kidney injury

Acute kidney injury is common in adults with severe malaria (Figure 6). It behaves clinically and pathologically like acute tubular necrosis. Pathogenesis remains unclear, but reduced microcirculatory flow probably

contributes (*67*). Acute kidney injury is frequently associated with dysfunction of several other vital organs (leading to high mortality) or can develop more slowly as other disease manifestations resolve. Acute kidney injury is oliguric in 60–70% of cases. In survivors, urine flow resumes in a median of 4 days, and serum creatinine concentrations return to normal in a mean of 17 days (*68*). Early haemofiltration or dialysis substantially improves outcomes, especially in acute hypercatabolic renal failure (*69*). Oliguric renal failure is rare in children, although increased concentrations of blood urea are frequent and an independent risk factor for death in African children with severe malaria (Figure 6 b).

1.6.5 Malaria in pregnancy

In areas of high transmission, the risk of low birth weight (<2,5 kg) is roughly double when women have placental malaria; the effect is greatest during the first pregnancy. This lower birth weight is associated with increased infant mortality (*70*). Maternal anaemia is exacerbated, but most mothers remain asymptomatic despite intense accumulation of infected erythrocytes in the placental microcirculation. Congenital malaria occurs in roughly 5% of neonates but clears spontaneously in 62% of cases (*71*). Maternal HIV infection predisposes pregnant women to malaria and exacerbates reductions in birth weight (*72*). In areas with unstable malaria transmission, pregnant women are at increased risk of developing severe *falciparum* malaria with a very high mortality rate (roughly 50%). High parasitaemias, severe anaemia, hypoglycaemia, and acute pulmonary oedema are all more frequent in pregnant than in non-pregnant women. In severe disease, foetal distress, premature labour, and stillbirth often occur.
The risk of infant death is particularly high if maternal malaria occurs during late (near-term) pregnancy (*73*). Maternal death from haemorrhage at childbirth is correlated with malaria-induced anaemia (*74, 75*).

1.7 Diagnosis and assessment

Thick and thin blood film microscopy examination remains the gold standard for diagnosis, but simple, sensitive, and specific antibody-based rapid diagnostic tests that detect *Pf*HRP2, species-specific lactate dehydrogenase (LDH) or aldolase antigens in finger-prick blood are now used widely (World Health Organisation, Malaria Report 2011). *Pf*HRP2-based tests might remain positive for weeks after acute infection, which limits usefulness in high transmission areas, but can be used to diagnose severe malaria in patients who have taken artemisinin derivatives and cleared peripheral parasitaemia (tests remain strongly positive). *Pf*HRP2-based rapid diagnostic tests are as good as is routine microscopy in the diagnosis of *falciparum* malaria. The new-generation tests based on detection of plasmodium LDH are effective for diagnosis of both *falciparum* and *vivax* infections, although sensitivity is low at *P. vivax* densities of less than 200 µL. Aldolase based tests are less sensitive, especially for *non-falciparum* species (World Health Organisation, Malaria Report 2011). Because of their simplicity and speed, rapid diagnostic tests are particularly valuable in epidemic investigations and surveys. However, they are expensive and do not quantify parasitaemia.

1.8 Prevention

1.8.1 Vaccination

Much time, effort, and money have been spent on the development of malaria vaccines. The RTS,S subunit vaccine, which targets the circumsporozoite protein of *P. falciparum* and is boosted with the potent ASO1 adjuvant, is the most advanced vaccine in development. The active substance in RTS,S vaccine is a recombinant antigen expressed in *Saccharomyces cerevisiae* coded RTS,S. The RTS,S antigen consists of

two proteins, RTS and S, that spontaneously assemble into mixed polymeric particulate structures intracellularly. The results of a large multicentre study of RTS,S (A phase 3 trial of RTS,S/AS01 malaria vaccine in African infants) in infants aged 6–12 weeks at first immunisation (deployed as a monthly dose for three months in conjunction with an expanded programme of immunisation vaccines) showed good safety but only moderate efficacy, with 30% protection against clinical malaria and 26% protection against severe malaria in the 12 months after the last dose. Previously reported results (*76*) in slightly older children (aged 5–17 months) were better, with 55% protection against all *falciparum* malaria and 35% protection against severe malaria during 14 months.

1.8.2 Vector control

Vector control is an essential component of prevention. In areas of moderate or high transmission in Africa, employment of pyrethroid-insecticide-treated mosquito nets reduced all cause mortality by roughly 20% in children younger than 5 years (*77*). Wide-scale employment of such nets has contributed substantially to the fall in malaria morbidity and mortality. In addition of protecting the user, insecticide-treated nets protect the community by killing anopheline mosquitoes (the so-called mass effect) (*78, 79*), and should be employed in all areas where malaria is endemic. They are usually very effective; however, in some parts of Asia, the main mosquito vectors bite outside early in the evening or morning and so the protective effect is small. Use of pyrethroids in agriculture and widespread employment of insecticide-treated nets has put a tremendous selection pressure on anopheline mosquitoes and resistance has emerged.

Indoor residual spraying with insecticides that persist and kill mosquitoes is an important component of malaria control (*80-82*). Its efficacy strongly depends on the behaviour of the local *Anopheles* vectors (whether the

mosquitoes enter houses and rest there) and whether resistance has emerged. Dichlorodiphenyltrichloroethane (DDT) is still effective in parts of Asia and Africa and used for indoor residual spraying, which can result in high human exposure (*83*). Only four general insecticide classes exist, and, in some areas, the development of resistance is undermining the efficacy of insecticide-based measures (*84*).

1.8.3 Chemoprophylaxis and chemoprevention

Chemoprophylaxis is recommended for travellers during potential exposure to malaria (*85*). For drugs that do not have activity against the pre-erythrocytic (liver) stage, chemoprophylaxis is given during exposure and for four weeks thereafter to catch any blood-stage infections that emerge from the liver. Recommendations for chemoprophylaxis depend on local patterns of susceptibility to antimalarials and the likelihood of acquisition of malaria. When uncertainty exists, drugs that effectively prevent infection with resistant *P. falciparum* should be used: iatovaquone–proguanil, doxycycline, primaquine or mefloquine. Chemoprophylaxis is never completely reliable, and malaria should always be a possible diagnosis in febrile patients who have travelled to endemic areas.

Previously, chemoprophylaxis was recommended for pregnant women in endemic areas, but in most areas resistance has developed against the drugs approved for this indication (ie, chloroquine, proguanil). In Africa, intermittent preventive treatment with sulfadoxine–pyrimethamine was given instead. A full course of sulfadoxine–pyrimethamine twice during later pregnancy provided partial protection. A minimum of three doses of sulfadoxine–pyrimethamine are now recommended to provide continuous preventive effects. Resistance to sulfadoxine–pyrimethamine is increasing in Africa, and thus alternative drugs are being investigated for use in intermittent preventive treatment in pregnancy.

All pregnant women in endemic areas should be encouraged to attend regular antenatal clinics (when available). Pregnant women travelling to endemic areas should be advised of the potential risks. Mefloquine is the only drug recommended for chemoprophylaxis in pregnant women travelling to areas with drug-resistant malaria, and is thought to be safe in the second and third trimesters of pregnancy; data for first-trimester exposures (although few) are reassuring (*86*).

The safety of other prophylactic antimalarials in pregnancy has not been established, although no harmful effects have been associated with atovaquone–proguanil (WHO: Guidelines for the treatment of malaria, 2nd edn. Geneva: WHO Press, 2010)

The intermittent treatment approach has been extended to infancy, where it can be delivered to all at-risk infants via the system in place for the expanded programme on immunisation. However, many malaria-related diseases and deaths in Africa occur in children aged 3 months-5 years in the Sahel sub-region during 4 months of the rainy season. WHO has recommended administration of monthly amodiaquine and sulfadoxine–pyrimethamine (maximum four doses) to all children aged 3 months-5 years in this region from the start of the yearly transmission season (WHO: Guidelines for the treatment of malaria, 2nd edn. Geneva: WHO Press, 2012). This seasonal malaria chemoprevention has superseded intermittent preventive treatment in infants. Intermittent preventive therapy is effective when delivered through schools or to adults at high risk of malaria (*87*).

Since the 1930s, various approaches to treatment of whole populations have been taken. Mass drug administration to millions of people was effective in some settings but not in others and gained a poor reputation (perhaps undeservedly); thus this approach has been little used in recent years (*88*).

1.9 Treatment

1.9.1 Severe disease

Severe *falciparum* malaria is a medical emergency, and necessitates intensive nursing care and careful management. In Asia, parenteral artesunate significantly reduced mortality from 22,4% to 14,7% compared with quinine. In Africa, artesunate significantly reduced mortality from 10,9% to 8,5% compared with quinine (*89*). Intravenous or intramuscular artesunate is thus the treatment of choice for severe malaria worldwide (including in patients with severe *vivax* and *knowlesi* malaria) (World Health Organisation: Guidelines for the treatment of malaria, 2nd edn. Geneva). Artesunate has no important local or systemic adverse effects, although high cumulative doses (≥6 mg/kg per day) can temporarily suppress bone marrow. Delayed haemolysis starting a week after artesunate treatment for severe malaria has been noted in travellers (particularly those initially presenting with high parasitaemias) returning to hospitals in non-endemic countries (*90*). This haemolysis is probably partly caused by the loss of once-infected erythrocytes, which results from splenic pitting of parasites killed by artesunate.

In a large placebo-controlled trial community-based pre-referral treatment with a rectal formulation of artesunate for patients unable to take oral medications decreased malaria mortality in severely ill children by 25% (*91*).

In acute renal failure or severe metabolic acidosis, haemofiltration or haemodialysis should be started early (*69*). Dose reduction of artemisinin derivatives is unnecessary, even in renal failure. Prophylactic anticonvulsants are potentially dangerous; high-dose phenobarbital (20 mg/kg) doubled mortality in children with cerebral malaria—patients died mainly from respiratory arrest (*92*).

In unconscious patients, blood glucose should be measured every 4–6 h and dextrose continuously infused to maintain concentrations higher than 4 mmol/l. Hypoglycaemia (<2,2 mmol/l) should be treated immediately with bolus glucose. Parasite counts and haematocrit concentrations should be measured every 6–12 h. Anaemia develops rapidly in severe malaria; if haematocrit falls to less than 20% (haemoglobin <70 g/l), then packed cells or whole (preferably fresh) blood should be transfused carefully. The transfusion threshold for children in Africa (where anaemia is very common and safe blood for transfusion is scarce) is a haematocrit concentration of 15% or less (haemoglobin concentrations less than 50 g/l). Renal function should be checked daily. Management of fluids is difficult, especially in adults, because the risks of overhydration (pulmonary oedema) have to be balanced against those of underhydration (exacerbation of renal impairment and tissue hypoperfusion). Large fluid boluses are harmful at all ages (*66, 93*). Early enteral feeding in non-intubated comatose adults can cause aspiration pneumonia, so feeding should not start until the third day of the coma (*94*). When the patient can take tablets reliably, a full course of artemisinin combination treatment should be given (World Health Organisation: Guidelines for the treatment of malaria, 2nd edn. Geneva).

Intravenous antimicrobials should be given to all children with suspected severe malaria in areas of moderate or high transmission (*95*). Convulsions should be treated with intravenous or rectal benzodiazepines and respiratory support provided when necessary. Aspiration pneumonia should be suspected in any unconscious child or adult patient with convulsions, particularly when persistent hyperventilation is noted. Hypoglycaemia or septicaemia should be suspected after sudden deterioration for no obvious reason during treatment. Patients who bleed spontaneously should be given packed red blood cells with fresh frozen plasma or, when unavailable, fresh blood and parenteral vitamin K.

1.9.2 Uncomplicated falciparum malaria

Artemisinin combination treatment is the recommended first-line therapy for uncomplicated *falciparum* malaria in all endemic areas, and is highly efficacious against the other human malarias. The artemisinin component (artesunate, artemether, or dihydroartemisinin) is given for 3 days with a slowly eliminated antimalarial, preferably in a fixed-dose combination. Artemisinin combination treatment is rapidly and reliably effective, associated with few adverse effects, and curative in more than 90% of cases (except in foci of artemisinin resistance) (International Artemisinin Study Group, 2004, Lancet). The price of such treatment has dropped substantially, making it more generally affordable. Unfortunately, fake or substandard antimalarials are widespread in many Asian and African countries, which compromises effectiveness, selects for resistance, and diminishes confidence in the health sector. Atovaquone–proguanil is highly effective everywhere, but seldom used in endemic areas because of the cost and propensity for high-grade resistance to emerge from single mutations in the *cyt b* gene. The duration of post-treatment prophylaxis after artemisinin combination treatment varies. Slowly eliminated partner drugs, such as mefloquine and piperaquine, provide 4–6 weeks prophylaxis, whereas reinfections after treatment with artemether–lumefantrine often emerge within a month. In low transmission areas, a single gametocytocidal dose of primaquine (0,25 mg/kg) should be added to all artemisinin combination treatments for *falciparum* malaria (except for those in infants and pregnant women, in whom primaquine is not recommended) to sterilise the infection and prevent onward transmission (World Health Organisation, Global Malaria programme, 2012). Testing for G6PD deficiency is not necessary with this dose. Patients should be monitored for vomiting for 1 h after any oral antimalarial dosing. If the patient vomits, another dose should be given. Minor adverse effects (eg,

nausea, abdominal discomfort, headache, dizziness) occur frequently in malaria, and often result from the illness rather than the treatment. Three days artemisinin combination regimens are well tolerated, although mefloquine is associated with increased rates of vomiting and dizziness. The frequency of serious adverse neuropsychiatric reactions to mefloquine is around one per 1000 patients treated in Asia but as high as one per 200 in African and white patients. All the antimalarial quinolines (ie, chloroquine, mefloquine, and quinine) exacerbate orthostatic hypotension, and are tolerated better by children than by adults.

1.10 Resistance

Western Cambodia and the Thailand–Myanmar border, where artemisinin-resistant *P. falciparum* has emerged, (*96, 97*) are the regions of greatest concern. Resistance to both chloroquine and sulfadoxine–pyrimethamine emerged previously in this area, and in both cases the resistance genes spread to Africa and caused millions of deaths. Artemisinin-resistant parasites are cleared slowly from the blood after artemisinin combination treatment. Parasite clearance times exceed 3 days, and treatment failure occurs more often. Resistance to amodiaquine, sulfadoxine–pyrimethamine, and, to a lesser extent, mefloquine, limits deployment of artemisinin combinations containing these drugs in several areas.

1.11 Malaria and lung involvement

Lung involvement in malaria has been recognized for more than 200 hundred years, yet our knowledge of its pathogenesis and management is limited.

The lung contributes crucially to two stages of the *Plasmodium* life cycle. First, the initial generation of hepatocyte derived merozoites is released into the pulmonary microvasculature, which places the lung at the intersection

between the clinically silent liver phase and the symptomatic blood phase of the infection (*98*). Second, the lung is subject to a severe manifestation of malaria: Acute lung injury (ALI)/Acute Respiratory Distress Sindrome (ARDS), which is characterized by impairment of oxygen exchange due to widespread inflammation of the alveolar microvasculature.

After the maturation of *Plasmodium* in the infected hepatocytes, the first generation of merozoites is released into the microvasculature of the liver as merosomes, and they are shuttled out of the liver unharmed, by-passing the gauntlet of highly phagocytic Kupffer cells, and travel to the lungs where they are arrested and efficiently cleared from the bloodstream. After a period of most likely several hours, the merozoites are released from the merosome into the pulmonary bloodstream. One possible explanation for the high efficiency with which the lung clears merosomes from the blood is mechanical trapping (*98*). Merosomes may be arrested, based on their large size, within the pulmonary arterioles, i.e. before being able to enter the narrow alveolar capillary bed of the lung. This hypothesis is supported by the fact that the average diameter of extrahepatic merosomes (around 13-18 µm) clearly exceeds the 1–4 µm functional diameter of alveolar capillaries. However, merozoites that bud from hepatocytes are also much larger than the hepatic sinusoids (around 7 µm), but exit the liver nevertheless (*98, 99*). Mechanical trapping could result if merosomes were to become more rigid prior to entering the lungs. Arguing against this, are *ex vivo* lung imaging data showing merosomes easily adapting to the narrow vascular lumen of small pulmonary vessels (Leberl and Frevert, unpublished data), suggesting that merosomes retain the flexibility needed to squeeze through the pulmonary capillary bed if otherwise unrestricted. Alternatively, the merosomal membrane may contain *Plasmodium*-derived adhesion molecules that bind to the microvascular endothelium. This mechanism, even if not selective for the pulmonary endothelium, would

explain the high efficiency of merosome clearance from the blood, as the lung represents the first capillary bed, merosomes encounter after leaving the liver. The exact site of merosome arrest in the alveolar microvasculature is currently under investigation (*98, 99*).

1.11.1 Respiratory symptoms and signs of MA-ARDS

A dry cough may be present in 20% to 50% of patients with malaria (*100-102*). Tachypnea may result from high fever, anaemia, and lung involvement. Lung function tests have demonstrated small airways obstruction and a decrease in diffusion capacity in uncomplicated *falciparum* and *vivax* malaria (*63, 101, 103*). The reduced diffusion capacity is attributed to a reduction in the pulmonary capillary vascular component of gas transfer, which could be related to the sequestration of parasitized erythrocytes in the pulmonary microcirculation. The alveolar-capillary membrane component of gas transfer was reduced progressively in the days following treatment, consistent with the development of pulmonary interstitial and alveolar oedema. Pulmonary oedema is the most severe form of lung involvement. Increased alveolar capillary permeability leading to intravascular fluid loss into the lungs is the main pathophysiologic mechanism (*65*). Pulmonary oedema has been described most often in non-immune individuals with *Plasmodium falciparum* infections as part of a severe systemic illness or as the main feature of acute malaria.

P. vivax and *P. ovale* have also rarely caused pulmonary oedema. It was presumed that *P. vivax* infection may lead to severe consequences only when possibility of mixed infections exists and the pulmonary manifestations were so far under-diagnosed (*104*). Different types of respiratory distress may be present in malaria patients. Hyperventilation occurs as a consequence of metabolic acidosis, mainly due to lactic acid accumulation (*105*). The pathogenesis of a raised blood lactate in severe

malaria is almost certainly multifactorial. High levels of TNF are associated with high blood lactates in childhood malaria but the relationship between TNF-α and the presence of acidosis remains unclear (*106, 107*).

Lactate production by the parasite is also considered to be quantitatively of only minor importance and the lack of association between peripheral parasitaemia and blood lactate supports this conclusion (*108*). Lactate in addition can be produced by peripheral tissues, in particular when anaemia and/or blood vessel obstruction by sequestering parasites cause hypoxia.

Metabolic acidosis may be aggravated by renal dysfunction and insufficient clearance of lactic acid. The lower blood pH stimulates the brain stem to increase the respiratory rate to expel more carbon dioxide, resulting in hyperventilation. Currently, it is not clear whether hyperventilation may contribute to pulmonary oedema (e.g., by prolonged high tidal volume breathing), although both may occur simultaneously (*104*). Hyperventilation is the main type of respiratory distress in African children with malaria and is also frequent in adults (*109, 110*).

A completely different type of respiratory distress are ALI and ARDS. ARDS is a disease with a high mortality and is a common cause of admission into intensive care units (ICUs) all over the world.

ALI and ARDS have well-defined criteria for diagnosis based on reduced ratio of partial pressure of arterial oxygen/inspired fraction of oxygen -PaO_2 /FiO_2 ratios- (PaO2/FiO2 < 200 mm Hg, or PaO2/FiO2 < 300 mm Hg for the less severe ALI), bilateral infiltrates on the chest radiograph, and absence of left atrial hypertension. ARDS is the most cruel pulmonary manifestation of severe malaria, irrespective of the infecting species. ALI/ARDS may be seen as part of a severe multisystem illness or may be the main clinical feature and often occurs within a few days of starting treatment when parasitaemia is falling. This is illustrated well by Krishnan and Karnad, who showed that at presentation, 84 of 301 patients (28%) had mild hypoxia

(PaO_2 /FiO_2 ratios, 400 mm Hg), 18 ALI, and 10 ARDS. ARDS developed in a further 33 patients within 48 hours and in 36 patients after 48 hours (*111*). Dyspnea in patients developing ARDS may start abruptly, progress rapidly, and causes death within hours of onset. Physical signs include sweating, tachypnea, labored breathing, peripheral and central cyanosis, inspiratory crepitations, expiratory wheezes, and frothy sputum. An increased respiratory rate and dyspnea are usually the earliest signs. The jugular venous pulse is not raised unless there is concomitant fluid overload. Hypoxia-related confusion and agitation may also be seen.

1.11.2 Epidemiology of MA-ARDS

Reliable epidemiological data are not available regarding the prevalence of ALI/ARDS in patients with malaria. Data from different studies suggest that about 5% patients with uncomplicated *falciparum* malaria and 20% – 30% patients with severe and complicated malaria requiring ICU admission, may develop ARDS. It should be remembered, however, that different denominators have been used in various publications and meaningful comparison of such data is not possible. Furthermore, in many of the previously reported studies, the precise definition used for the diagnosis of ARDS is also not mentioned (*112*).

MA-ARDS occurs mainly in adults; most reported ARDS cases are from low-transmission area or from non immune travellers, as resident adults from high transmission areas are semi-immune and protected against severe disease. Also pregnant women with placental malaria are prone to develop MA-ARDS (*65, 113*).

1.11.3 Role of concomitant bacterial sepsis

Bacterial sepsis is an important contributor to the genesis of ALI/ARDS in severe *falciparum* malaria. In patients with severe *falciparum* malaria, the prevalence of bacteraemia in published studies has varied from 6% –15% (*112*). However, an obviously evident focus of sepsis may not be discernible in many patients. Further research is required to understand the contribution made by bacterial sepsis in patients with severe *falciparum* malaria. This important observation implies that, in endemic areas, practicing clinicians should have a low threshold to initiate broad spectrum antibiotics in *falciparum* malaria patients with ALI/ARDS and shock as it can be life-saving (*113, 114*).

1.11.4 Pathophysiology of MA-ARDS

The pathogenesis of ALI/ARDS in severe malaria is not understood. There are multiple potential causes that may result in lung injury during malaria, which may also be interrelated. These include the effects of sequestration of parasitized erythrocytes, host immunologic reactions to lung specific sequestration or systemic malaria infection, superimposed pulmonary infections (community acquired, nosocomial, or opportunistic in immunocompromised patients), aspiration, coexistent sepsis and bacteremic induced ARDS, or the effects of treatment such as fluid resuscitation.

The sequestration of pRBCs in the pulmonary microcirculation may initiate lung damage via direct endothelial activation and recruitment of host inflammatory responses, but these can continue after treatment with antimalarial drugs. The occurrence of ALI/ARDS when a parasite is declining or has been cleared suggests a post-treatment inflammatory effect as a contributory cause, since parasite products such as malaria haemozoin pigment can persist in the vessels either bound to endothelial

cells in ghosted ruptured erythrocyte membranes postschizogony or phagocytosed by host leukocytes (*115*). A combination of parasitized erythrocyte sequestration and lung inflammatory changes are considered the main cause of *falciparum* malaria induced ALI/ARDS.

Some workers (*103*) have proposed that ALI/ARDS in malaria is likely to be a continuous spectrum from subclinical lung involvement in uncomplicated malaria and severe malaria through to ALI/ARDS in severe malaria. The authors postulated that in patients with severe malaria without ALI, endovascular obstruction caused by erythrocytes with reduced deformability, parasitised erythrocytes, and leucocytes; endothelial injury and interstitial oedema result in ventilation-perfusion mismatch and impairment of gas exchange. Furthermore, worsening or persistence of these gas exchange abnormalities after treatment and beyond the expected time of clearance of parasitised erythrocytes reflects a prolonged inflammatory response and the genesis of ALI/ARDS (*103*).

Severe *falciparum* malaria is characterized by an upregulation of pro inflammatory cytokines eg, TNF-α (which causes an increase in endothelial intracellular adhesion molecule-1 expression), and IL-1, IL-6, and IL-8 which have also been implicated in the pathogenesis of ARDS. Anti inflammatory cytokines such as IL-4 and IL-10 are also upregulated, and an imbalance between IL-10 and the proinflammatory cytokine IL-6 has prognostic significance for death (*116*).

However, none of the cytokine profiles in severe *falciparum* malaria is specifically associated with capillary leakage in the lung. A decrease in pulmonary NO production in adults with severe malaria (*117*), could be significant for pulmonary capillary leakage, because pulmonary NO is central in the modulation of pulmonary vascular tone and pulmonary hypertension (*118*).

A relative L-arginine deficiency (the precursor of NO) with increased levels of asymmetric dimethylarginine (an inhibitor of NO synthase) and an increase in free haemoglobin caused by intravascular hemolysis all contribute to the decrease in NO bioavailability (*119*).

Data from a murine model of severe malaria caused by *Plasmodium berghei* indicate that vascular endothelial growth factor (VEGF) may also be involved in damaging alveolar capillary endothelium (*120*), but levels of plasma VEGF in patients with human *falciparum* malaria are significantly lower in severe versus uncomplicated cases (*121*), and in patients with fatal cerebral malaria in India, (*122*), arguing against high levels of VEGF being directly associated with lung injury in severe human *falciparum* malaria.

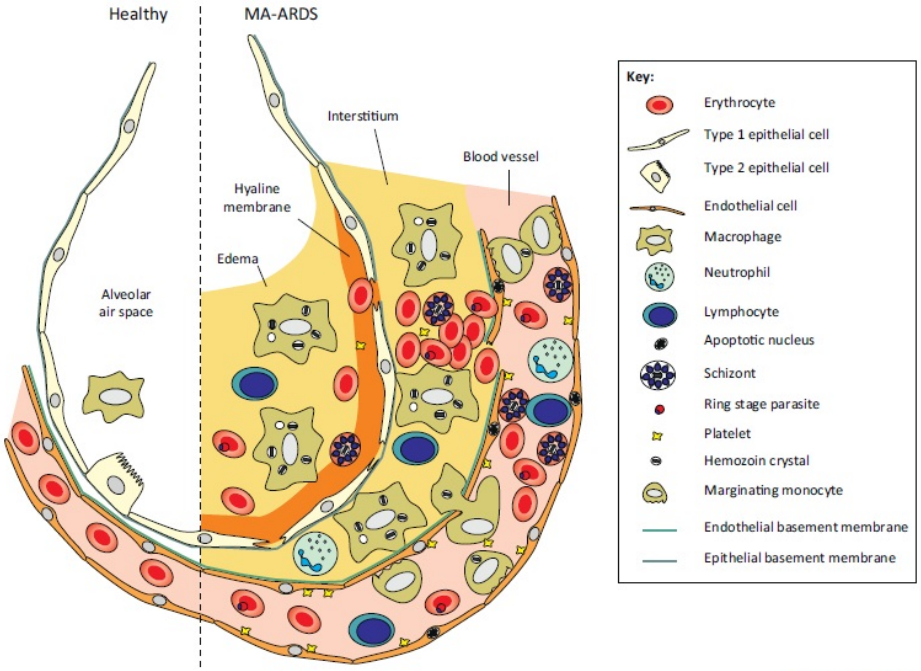

Figure 7-Cellular components involved in the pathogenesis of malaria-associated acute respiratory distress syndrome (MA-ARDS)

The sequestration of infected red blood cells (mainly in the schizont stage) is supposed to play an important role in the initiation and amplification of local immunopathology. Haemozoin crystals are produced by sequestering parasites, are also found in phagocytes, and are able to induce pulmonary inflammation. Margination and infiltration of inflammatory cells (mainly monocytes or macrophages, lymphocytes, and some neutrophils) and platelets in blood vessels, interstitial tissue, and alveoli of the lungs are crucial determinants of the pathogenesis of MA-ARDS. Damage to and apoptosis of endothelial cells results in increased vascular permeability and microhaemorrhages. As alveolar oedema and haemorrhages are also frequent, it may be inferred that the epithelium is also damaged, which is presumably further amplified by the deposition of proteinaceous debris (hyaline membrane formation). Alveolar oedema, thickened interstitium, and presumably also decreased blood flow result in impaired gas exchange and severe hypoxemia.

1.11.5 Role of inflammation in MA-ARDS

Variable levels of inflammation are observed in malaria. During MA-ARDS abundant leukocyte recruitment and inflammation is evident. Since MA-ARDS often appears after therapeutic clearance of parasites, it's supposed to result from excessive inflammation. Central to the onset of MA-ARDS is a shift of the normal anti-thrombotic and anti-inflammatory state of the (tolerant) pulmonary endothelia towards an activated pro-thrombotic and pro-inflammatory phenotype with expression of activators of the clotting system and adhesion molecules for platelets and leukocytes (*123*).

Unlike ALI/ARDS induced by sepsis, the infiltration of inflammatory cells into the microvasculature and interstitium of the lung during human malaria appears histopathologically as predominantly mononuclear with a lesser contribution of polymorphonuclear cells (*63, 99, 103, 124*).

Specifically, during MA-ARDS there is an accumulation of monocytes, macrophages and lymphocytes, whereas only limited numbers of neutrohils are present (*105*). Initially, *P. falciparum* iRBCs bind and roll along the microvascular endothelium via interactions with ICAM-1,VCAM-1, PECAM-1, as well as P and E-selectins, then firmly adhere to endothelial CD36 (*125, 126*). The binding of infected RBCs to the pulmonary microvasculature activates the endothelium and leukocytes, although the relative contribution of the various leukocyte subpopulations remains unclear. Endothelial activation results in the release of cytokines and up-regulation of adhesion molecules, thus perpetuating the inflammatory cell recruitment. This then leads to the accumulation of monocytes, which also release pro-inflammatory cytokines such as TNF-α and IL-1. TNF-α and IL-1, in turn, induce IL-6 and IL-8 as well as endothelial cytoadherence by up-regulating ICAM-1 and VCAM-1, but not CD36 (*112, 125, 127*). Furthermore it's known that TNF-α and IL-6 increase vascular permeability (*128*), TNF-α reduces the pulmonary expression of the amiloride sensitive epithelial sodium channel (ENaC) in the alveoli, altering alveolar fluid clearance. Additionally, TNF-α triggers the release of NO, which can reduce alveolar epithelial sodium transport by impairing the function of ENaC and the sodium/potassium ATPase (*129*).

The release and activation of cytokines, such as TNF-α and IL-1 from macrophages and monocytes can be due also to Hz deposition in the lung.

Van de Steen et al demonstrated the important role of Hz in pulmonary inflammation by the injection of *Plasmodium falciparum*-Hz in malaria free C57BL/6J mice. Injection of *Pf* Hz induced the pulmonary expression of the neutrophil-attracting chemokine; and stimulated the pulmonary expression of cytokines (*130, 131*).

Furthermore, Hz inside the phagocytes cannot be degraded and interacts with polyunsaturated fatty acids present in membranes resulting in

accumulation of different lipoperoxidation products including 4-hydroxynonenal (4-HNE) and hydroxyeicosatetraenoic acids (HETEs). HETEs augment the inflammatory response by inducing the expression of pro-inflammatory cytokines and chemokines through the induction of NF-kB (*132*).

1.11.6 Murine models for MA-ARDS

Several studies have employed mouse models to study lung pathology prior to death from cerebral malaria (CM) (*133, 134*) or in concert with CM (*135*). Selective models for murine malaria-associated ALI/ARDS have provided valuable insights into various pathogenetic mechanisms (*120, 136*) and possible interventions (*130, 133*).

The most common model to study MA-ALI/ARDS is the infection of mice with *P.berghei ANKA.* This parasite strain causes lethal CM in several mouse strains (C57Bl/6, DBA/1, CBA/J) culminating in coma and death when peripheral parasitaemia reaches around 10%(*137*). At the same time, mice develop pulmonary pathology characterized by oedema, interstitial infiltration of inflammatory cells and limited haemorrhages. However, due to CM, mice usually die before completely developing pulmonary pathology. An important strategy to avoid the problem of early death and to study MA-ALI/ARDS is the use of parasite strains that do not cause CM. Infection of C57Bl/6J mice with *P.berghei NK65* resulted in severe MA-ARDS with initial interstitial oedema and cell infiltration and progression to severe alveolar oedema, cell infiltration and haemorrhages (*130*). This model has a high incidence and the pathology develops to a full extent without CM, creating a sufficient time window to test candidate therapeutic treatments. Furthermore, the *P.berghei NK65* MA-ARDS model has a high degree of similarity with human MA-ALI/ARDS. In particular, leukocyte infiltrations consist mainly of inflammatory macrophages and lymphocytes, with only a

limited number of neutrophils; hyaline membranes are formed in the alveoli and abundant microhemorrages develop.

The infection of C57Bl/6J mice with *Plasmodium chabaudi* may cause limited pulmonary pathology with lymphocyte infiltration 20 days post infection, after the main parasitaemia peak (*138*). This animal model can be useful as negative control to understand if the changes are due to malaria disease or to MA-ARDS.

1.11.7 Interventions and treatment

There are no ALI/ARDS treatment trials in malaria, so management strategies follow non malaria ARDS guidelines (*139-141*). Mechanical ventilation is often difficult in the severely diseased lung. Lung compliance is markedly reduced and unevenly distributed, ventilation/perfusion is mismatched, and gas diffusion is compromised. Guidelines include the application of volume- or pressure- support ventilation with positive end-expiratory pressure, avoidance of both high tidal volumes (6 mg/kg ideal body weight) and an initial plateau pressure, 30 cm H_2O (*142*).

An early study in murine MA-ARDS indicated a possible beneficial effect of phenoxybenzamine, an alpha-blocker and vasodilator. This is in line with the oedema promoting role of catecholamines (*143*). Furthermore, indomethacine, an inhibitor of cyclooxygenase-1 and -2, effectively blocked the pulmonary oedema, suggesting an important role for prostaglandins in murine MA-ARDS. More recently, anti-inflammatory treatments have been evaluated in the mentioned mouse models. Inhalation of carbon monoxide (CO), which has strong anti-inflammatory effects, decreased serum VEGF levels and protected against MA-ALI (*120*). The same effect was obtained by pharmacological treatment with a novel CO-releasing molecule, ALF492 (*144*).

Treatment with 80 mg/kg dexamethasone, an inexpensive glucocorticoid, greatly inhibited *P.berghei NK65* induced MA-ARDS, even when administered after appearance of the pathology (*130, 139*). The problem in the use of dexamethasone is the high dosage (80 mg/kg), which exceeds the maximum dosage for patients (3-5 mg/kg). More research to understand the therapeutic effects of dexamethasone in MA-ARDS is underway.

2 AIMS

Malaria associated acute respiratory distress syndrome (MA-ARDS) is a deadly complication and its pathophysiology is insufficiently understood. In particular, little is known about the biochemical alterations contributing to lung dysfunction. The most commonly used animal model for malaria-associated ALI/ARDS is infection of susceptible mice (e.g., C57BL/6 mice) with *Pb*ANKA, in which the critical roles of IFN-γ, IL-12, intercellular adhesion molecule-1, urokinase receptor, CD40 and lymphotoxin-a were documented (*133-135, 145-147*). As susceptible mice infected with *Pb*ANKA die quite rapidly from cerebral malaria, the study of ALI/MA-ARDS is possible only in the early phase of the complication.

Therefore, it was critical to analyze whether MA-ARDS might also develop in other mouse models of malaria, for example, without cerebral pathology or with a broader time window for the evaluation of the pathology.

In this study, the occurrence of MA-ARDS in C57BL/6 mice infected with *P. berghei* NK65 (*Pb*NK65) is described and investigated at different levels. To deepen our understanding of the complexity of the pathological changes in malaria-ARDS we have explored in the murine model of C57BL/6J mice infected with *Pb*NK65 the lipid profile of lung tissue and the molecular organization and lipid composition of the pulmonary surfactant.

In parallel, to understand the metabolic networks/pathways related to MA-ARDS caused by the *Pb*NK65 infection, we have also explored the liver and plasma changes in lipid profile. In fact, severe malaria is often characterized by multi-organ failure and in particular significant hepatic pathology (*148-151*) and host homeostasis is achieved at the cost of a cascade of events in different tissues with liver playing a major role in toxic control and helping the organism maintain homeostasis.

Plasma/serum composition on the other hand, reflects the status of this homeostasis and is also an excellent reporter of disturbances caused by environmental stressors.

The analyses performed on *Pb*NK65 mice have been also performed in mice infected with *Plasmodium chabaudi (Pc*AS), a Plasmodium strain that does not induce lung pathology.

3 MATERIALS AND METHODS

3.1 Chemical reagents

Solvents and plates silica gel for High Performance Thin Layer Chromatography were purchased from MERCK (Darmstad, Germany). All the others chemicals were from Sigma-Aldrich (Italia) unless otherwise stated.

3.2 Mice and parasites

3.2.1 Infection of Mice with rodent malaria Parasites

C57Bl/6J mice were infected by intraperitoneal injection of 10^4 *Plasmodium berghei* NK65 (*Pb*NK65) or *Plasmodium chabaudi* AS (*Pc*AS) infected red blood cells (iRBCs) by serial passage of tail vein blood obtained from a mouse that had been infected with *Pb*NK65 or *Pc*AS. The percentage of infected erythrocytes in the peripheral blood (parasitaemia) was determined by microscopic analyses after Giemsa staining. Mice were sacrificed at day 8 or 10 post infection, euthanasia was performed by intraperitoneal injection of Nembutal and every effort was made to minimize suffering.
All experiments were approved by the local ethics committee (License LA121251, Belgium).

3.2.2 Treatment of infected mice with dexamethasone (DEX)

Dexamethasone sodium phosphate (DEX; CERTA, Braine-l'Alleud, Belgium) was dissolved in phosphate-buffered saline (PBS) and a volume of 200 µl, containing the indicated dose, was injected intraperitoneally daily starting at day 6 or 7 post infection, before the onset of MA-ARDS.
Control mice were treated with the same volume of PBS.

3.3 Preparation of biological specimens

Blood was drawn by cardiac puncture into heparin coated syringes and centrifuged at 1850xg for 5 minutes to separate plasma and RBC.

To asses pulmonary pathology, left lungs were pinched off before bronchoalveolar lavage (BAL) and perfusion and were used for lung weight and RNA extraction.

Bronchoalveolar lavage (BAL) fluids was collected from right lungs by intratracheal instillation of an isotonic NaCl solution (3 x 0.6 ml) through a trachea cannula and immediately centrifuged at 150xg for 10 min at 4°C to pellet cells. The cell-free supernatant (total fraction) was collected and immediately centrifuged at 12000xg for 30 min to obtain a Large aggregate fraction (LA, pellet) and a Small aggregate fraction (SA, supernatant) according to Davidson et al. (*152*). LA and SA fractions were lyophilized, resuspended in an appropriate volume of distilled water and stored at - 80°C until further processing.

The percentages of lymphocytes, monocytes/macrophages, and neutrophils in the totale BAL were determined by microscopy analysis of Cytospin slides (Thermo Shandon, Cheshire, UK).

To remove circulating iRBCs, mice were perfused with 0.15 M NaCl containing 0.2 mM butylhydroxytoluene (BHT) as an antioxidant, and lungs and livers were removed and weighed. A small piece of the liver was stored at -80°C for Hz quantification, whereas the other parts of the liver and right lungs were mechanically homogenized in Precellys tubes in 600 µl of a solution containing 20 mM Tricine pH 7.5, 250 mM sucrose, 5 mM EDTA, 0.2 mM BHT and a protease inhibitor cocktail (Sigma).

Lung homogenates were further centrifuged at 1000xg for 10 min at 4°C, washed three times in the same buffer and the pooled supernatants were

ultracentrifuged at 100000xg for 1 hour at 4°C. Pellets, representing an enriched membrane fraction, were resuspended in a proper volume of distilled water added of 0.2 mM BHT and stored at -80°C until further analyses.

3.4 Total lipid extraction and fractionation

Lipids in plasma, BAL fluids, lung and liver samples were extracted and partitioned according to Folch (*153*). Briefly: lipids were extracted once by chloroform/methanol (2:1, v/v), once by chloroform/methanol (1:2, v/v) and once by chloroform/methanol (1:1, v/v) . After centrifugation at 20000xg for 15 minutes at 4°C, the supernatants containing the lipid fraction were isolated, dried under a stream of N_2, dissolved in a proper volume of chloroform and saved at -80°C until further analyses.

An aliquot of the total lipid extract was fractionated in the different lipid components by silicic acid column chromatography according to Vance et al. (*154*), and the neutral fraction was further fractionated according to a slightly modified procedure of Horning et al. (*155*). Briefly: about 1 g of silicic acid was resuspended in hexane and slurried in a column of about 1.0 cm diameter. About 300 to 350 mg of lipids in hexane were separated by stepwise elution with the following benzene-hexane mixtures: benzene-hexane 18% (v/v) and benzene-hexane, 60% (v/v).

3.4.1 Phospholipid and neutral lipid analyses

Phospholipid (PL) phosphorus was determined by the Bartlett procedure (*156*). Briefly: dried samples were added with 0.5 ml 80% perchloric acid and heated for 90 minutes at 200°C. After the incubation 1.2 ml of Fiske solution (30 g of monobasic sodium sulphite + 6 g of dibasic sodium sulphite + 0.5 g of 1.2.4 amino naphthol sulfonic acid dissolved in 250 ml of distillated water and filtered after 3 hours) and 1 ml of Molibdate solution

(200 ml of 2.2 % ammonium molybdate + 14 ml 96 % sulphuric acid diluted to 1 l with distilled water) were added, mixed thoroughly and heated for 10 minutes at 100°C. The optical density at 625 nm was recorded with the use of spectrophotometer UV-Visible Cary 50 Scan against a standard curve (2 µg/0.1 ml of potassium phosphate).

The individual classes of PL were separated by High Performance Thin Layer Chromatography (HPTLC) plates by chloroform/methanol/acetic acid/water 60:40:4:2 (v/v/v/v) as developing solvent. Spots were visualized by a solution of anisaldehyde (*157*) and quantified by densitometric analysis (Camag Reprostar 3). Cholesterol (Cho), free fatty acids (FFA), triglycerides (TG) and cholesterol esters (ChoE) were quantified by densitometric analysis after separation by HPTLC in hexane/diethyl ether/acetic acid (90:10:1 v/v/v) and visualized with a solution of 10% $CuSO_4$ in 8% H_3PO_4.

The fatty acid composition of the lipid fractions was analyzed by gas liquid chromatography according to Corsetto et al. (*158*).

Briefly: the fatty acid methylesters were obtained after derivatization with sodium methoxide in methanol 3.33% w/v and injected into gas chromatograph (Agilent Technologies 6850 Series II) equipped with a flame ionization detector (FID) under the following experimental conditions: capillary column: AT Silar length 30 m, film thickness 0.25 µm; gas carrier: helium; temperature injector 250°C; detector 275°C, oven 50°C for 2 min, rate of 10°C min^{-1} until 200°C for 20 min. A standard mixture containing methyl ester fatty acids was injected for calibration.

The degree of unsaturation of fatty acids was calculated and expressed as double bond index (DBI). DBI represents the sum of the values obtained by multiplying the percentage of each fatty acid by the number of double bonds in that acid, divided by 100.

3.4.2 Lipid peroxidation

Lipid peroxidation was measured by determining the levels of thiobarbituric acid reactive substances (TBARS) in the sample homogenates according to the method of Wey slightly modified as previously reported (*159*). Briefly, sample homogenates (200 µg protein) were added to 500 µl of 2-thiobarbituric acid (TBA) reagent (6 g TBA dissolved in 4 ml of NaOH 5 N and brought to 100 ml in 3% $HClO_4$) and heated at 100 °C for 10 min. After cooling TBARS were extracted with 1 N buthanol (Merck). Fluorescence of the upper alcoholic phase, separated by a brief centrifugation at 2000 g for 5 minutes, was determined in a Varian Cary Eclipse spectrofluorimeter (Varian instruments, CA, USA) (λ exc= 520 nm; λ em= 553 nm). A standard curve was obtained by dissolving tetraethoxypropane in 0.01 N HCl (Merck) to produce malondialdehyde (MDA), used as standard compound. Data are expressed as pmoles of MDA per micrograms of proteins, evaluated by the Bradford protein assay (*160*).

3.5 Antioxidant enzymes and other analyses

Liver homogenates were centrifuged at 12000xg for 10 minutes and supernatants were used to determine the activity of antioxidant enzymes and total glutathione (GSH+GSSG). Catalase (CAT), glutathione reductase (GR) and superoxide dismutase (SOD) activity was determined according to Aebi et al (*161*), Pinto et al. (*162*), and by a CAYMAN assay kit (Cayman chemical, Michigan, USA), respectively, and expressed as mU or U/mg protein.

Catalase: Catalase catalyzes the breakdown of H_2O_2 according to the following reaction:

$$2\ H_2O_2 \rightarrow 2\ H_2O + O_2$$

The rate of decomposition of H_2O_2 is determined spectrophotometrically by measuring the decrease of absorbance at 240 nm (spectrophotometer UV-Visible Cary 50 Scan).

Glutathione reductase: Glutathione reductase catalyzes the reduction of oxidized glutathione (GSSG) by NADPH or NADH to reduced glutathione (GSH):

$$GSSG + NAD(P)H \rightarrow 2\ GSH + NAD(P)^+$$

The activity of the enzyme is measured by following the oxidation of NAD(P)H spectrophotometrically at 340 nm (spectrophotometer UV-Visible Cary 50 Scan).

SOD: The assay utilizes a tetrazolium salt for the detection of superoxide radicals generated by xanthine oxidase and hypoxantine. One unit of SOD is defined as the amount of enzyme needed to exhibit 50% dismutation of the superoxide radical.

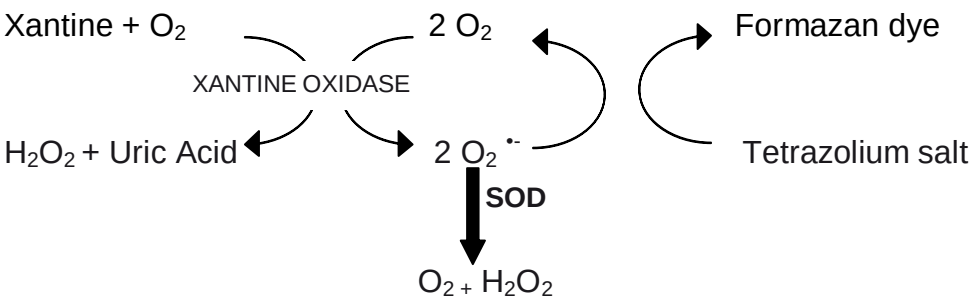

Scheme of the Superoxide Dismutase Assay

Total Glutathione (GSH + GSSG): An aliquot of total homogenate was precipitated, immediately after preparation, with 1 % (w/v) picric acid. Total glutathione was spectrophotometrically determined in the supernatant by titration with 5-5'-dithiobis-2 nitro benzoic acid (DTNB) according to Beutler (*163*) and to the following reactions:

$$2\,GSH + DTNB \xrightarrow{\text{Gluthatione Reductase}} GSSG + 2\,TNB$$

$$GSSG + NADPH + H^{+} \longrightarrow 2\,GSH + NADP+$$

$$DTNB + NADPH + H^{+} \xrightarrow[\text{GSH-GSSG}]{} 2\,TNB + NADP^{+}$$

Total antioxidant power (PAO): PAO was assessed by the Sigma Antioxidant Assay Kit. The principle of the antioxidant assay is the formation of a ferryl myoglobin radical from metamyoglobin and hydrogen peroxide, which oxidizes the 2,2'-azino-bis (3-ethylbenzthiazoline-6-sulfonic acid (ABTS) to produce a radical cation, $ABTS^{\circ+}$, a soluble green chromogen that can be determined spectrophotometrically at 450 nm (spectrophotometer UV-Visible Cary 50 Scan).

Hydroxyproline content: The assay was performed according to Tager AM et al. (*164*)**.** Biefly, 0.5 ml of lung/liver total homogenates were hydrolyzed in an equal volume of 6 N HCl at 110°C for 12 h and proper aliquots were added with 0.5 ml of chloramine T (Sigma, St. Louis, MO), (1.4% chloramine T, 10% *n*-propanol, and 25% 1 M sodium acetate). After 20 min of incubation at room temperature, 0.5 ml of Erlich's solution (14% 1 M *p*-dimethylaminobenzaldehyde in 70% *n*-propanol, 20% perchloric acid) was added and a 15 min incubation at 65°C performed. Absorbance was

measured at 550 nm and the amount of hydroxyproline was determined against a standard curve.

3.6 Quantitative reverse transcription ‐ polymerase chain reaction (RT- qPCR)

RT-qPCR was performed in collaboration with the laboratory of Professor Philippe Van Den Steen (Leuven, Belgium). In brief, after mechanical homogenization of perfused livers, total RNA was extracted with RNAeasy Minikit (Qiagen, Hilden, Germany) and quantified with the Nanodrop ND-1000 (Isogen ife Science, Temse, Belgium). For each sample, cDNA was synthesized with the High Capacity cDNA Reverse Transciptase kit and quantitative PCR (qPCR) was performed on 25 ng and 12.5 ng cDNA with the following mouse-specific primer and probe sets from Apllied Byosistems or Integrated DNA Technologies (Leuven, Belgium): IP-10/CXCL10 (NM_021274.1), TNF (NM_013693.2), IL-10 (NM_010548.1). The qPCR was performed with the TraqMan Fast Universal PCR Master Mix (Applied Biosystems) on an ABI Prism 7500 Fast Real-Time PCR System (Applied Biosystem). As a control form mRNA quantification, 18S ribosomal RNA (X03205.1) was also quantified. Since 18S ribosomal RNA levels were found to remain stable during the infection, was used to normalize the data.

3.7 TNF protein determination

Liver homogenates were centrifuged at 15000 x g for 15 minutes and TNF-α was assayed in supernatants using the mouse ELISA kit (R&D Systems, Minneapolis, MN, USA) following the manufacturer's instructions. The quantity of cytokine was plotted against a standard curve provided by the distributor.

3.8 HZ extraction and determination

To assess lung and liver injury, perfused livers and lungs were used for the determination of the Hz content by heme-enhanced chemoluminescence according to Deroost et al (*165*). Analyses were performed in collaboration with the laboratory of Professor Van Den Steen (Leuven, Belgium). Briefly, 30-60 mg of perfused liver or lung were homogenized in minimum 5 volumes of a solution containing 50 mM Tris/HCl pH 8.0, 5 mM $CaCl_{2,}$ 50 mM NaCl and 1% of Triton X-100. The homogenate was supplemented with 1% Proteinase K and incubated overnight at 37°C. The next day the proteinase K digest was sonicated (VialTweeter, Hielscher ultrasonics GmbH, Germany) for 1 minute (10W, pulse 0.5 sec) and centrifugated at 11000xg for 45 min. The supernatant was discarded and the pellet was washed three times in 100 mM $NaHCO_{3,}$ pH 9 and 2% SDS with subsequent sonication and centrifugation for 30 min to remove degraded tissue, free haeme and Hb. After the third wash, the pellet (Hz) was dissolved and sonicated in 100 mM NaOH, 2% SDS and 3 mM EDTA to form haematin and centrifuged to pellet the any remaining insoluble material. To confirm that the isolated was indeed Hz, it was examined for its birefringence character. The extracted Hz was measured in different diluitions by luminescence method: 100 µl luminal (100 µg/ml 3 aminophtalhydrazide) and 100 µl of peroxide (7% *tert*-butyl hydroperoxide), both dissolved in $NaOH/Na_2CO_3$ solution, light emitted in the presence of Fe^{3+} (present in the haematin core) was measured during one second using a Thermo Luminoskan Ascent apparatus. Peroxide catalysis into oxygen by Fe^{3+} is a fast reaction. Therefore, special care was taken to keep the time between the addition of the peroxide and the luminescence measurements minimal and as similar as possible between the different wells. A diluition series of haematin (10 µM-1.2 nM) was used as a standard. The unknown

Hz concentration (nM) was calculated from the calibration curve of the haematin concentration (nM) *versus* luminescence (events/sec).
The amount of Hz (pmol/mg tissue) was multiplied with the total weight of the concerning organ and expressed as pmol or nmol haematin/organ.

3.9 Histological analyses

Livers were perfused to remove circulating blood, dilated with 0.75 ml neutral buffered formalin solution (4%) by intratracheal instillation with subsequent ligation, removed, fixed in the same solution for 24 hours and embedded in paraffin. Histological assessment was done by hematoxylin-eosin staining and immunohistochemistry. Immunohistochemistry was performed on paraffin-embedded section with monoclonal anti-mouse F4/80 IgG2b (CI: A3-1, Abcam, Cambridge, UK, diluition 1/50). Paraffin sections were pretreated with EnVision FLEX Target Retrieval Solution, low pH (Dako, Heverlee, Belgium) for 10 min at 97°C. Endogenous peroxidase activity was blocked using EnVision FLEX Peroxidase-Blocking Reagent (Dako) for 5 min. The sections were incubated with the primary antibodies for 30 min at room temperature. Subsequently, slides were incubated with peroxidase labelled rabbit anti-mouse (Dako; diluition1/100) to enhance sensitivity. Visualization was by reaction with 3.3'-diaminobenzidine wich produces a brown color in the presence of peroxide. Negative controls consisted of omission of the primary antibody. Transmitted light images were taken trough a 40x/1.3 oil Plan-Apochromat objective of an Axiovert 200 M microscope equipped with AxioCamMRm camera (Zeiss, Gottingen, Germany). Image adjustements (Sigma, unsharp masking and gamma) were performed with the AxioVision 4.6 software.

3.10 Lung leukocytes analyses

The analyses of leukocytes in lung tissue were performed in Leuven, Belgium, at the laboratory of the professor Van den Steen (Rega Institute). Leukocytes were isolated from the lungs and counted with a Burker hemacytometer (excluding erythrocytes and dead cells), and the relative proportions of various leukocyte subclasses were analyzed by fluorescence-activated cell sorting. Total number of each subclass were calculated by multiplication of the relative proportion with the total leukocyte cell numbers.

3.11 Statistical analysis

Results are reported as mean ± standard deviation (SD). Comparison between groups was performed using Student's *t*-test. Differences were considered statistically significant when $p < 0.05$.

4 RESULTS

Pulmonary tissue. The macroscopical analyses of the lungs showed that 10 days post infection, differently from *Pc*AS mice, the lungs of *Pb*NK65 infected mice were significantly affected as indicated by the swollen and dark brown aspect (Figure 8) and by the increased lung weight (Figure 9).

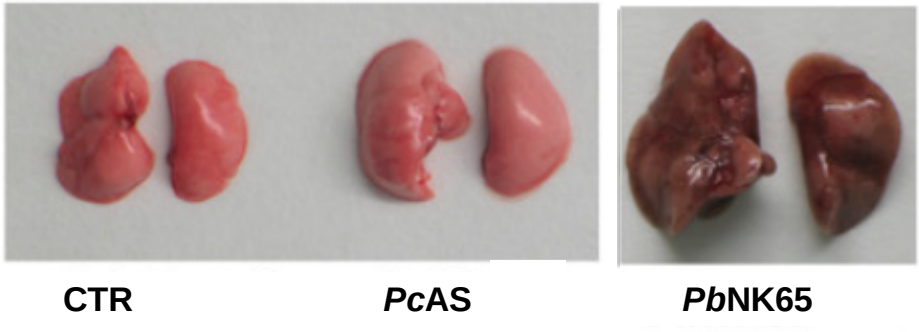

Figure 8- Lungs from uninfected mice and mice infected with PcAS or PbNK65 (10 days post infection)

The increase in lung weight started 8 days post infection and was approximately twofold that in *Pc*AS infected mice at the time of death, with peripheral parasitaemia around 20 %.

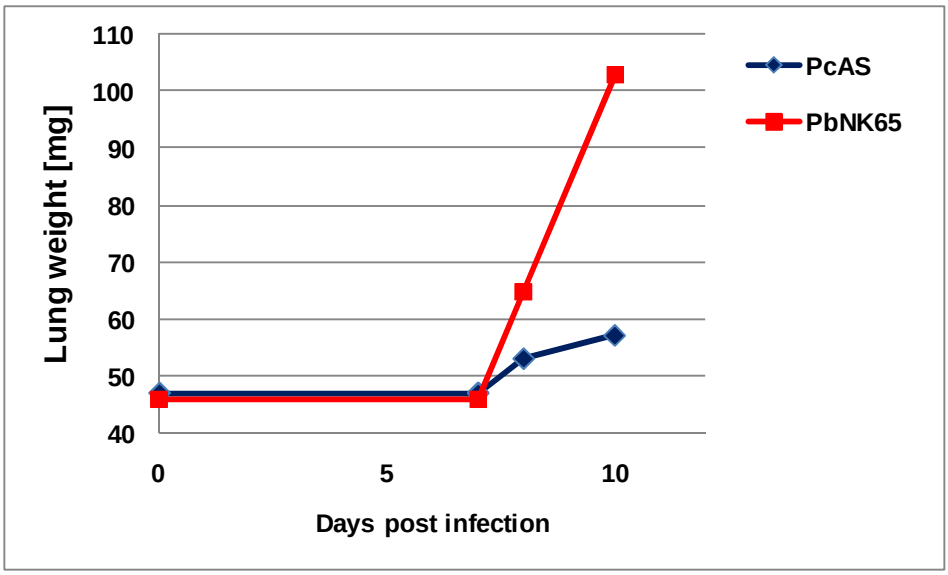

Figure 9- Weights of the lungs of mice infected with PbNK65 or PcAS were determinated at various times post-infection (day 8, 9 and 10).
n=6 for each time point and strain

The dark brown aspect of *Pb*NK65 mice was due to the deposition of the black malaria pigment (Hz): at day 10 post infection we found a significantly higher content of Hz in the lungs of P.*berghei* (*Pb*NK65) mice while in P.*chabaudi* (*Pc*AS) infected mice only traces of malaria pigment were present (Figure 10).

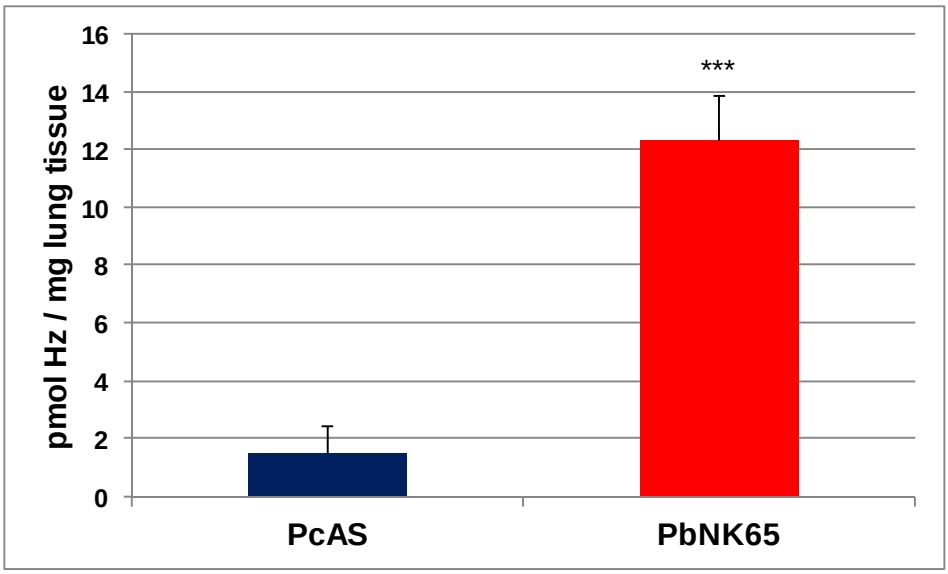

Figure 10- Hz levels in perfused right lungs. Hz from 30-60 mg of tissue was quantified as described in Materials and Methods expressed as pmol Hz/mg lung tissue.

*n=10/12; ***p<0,001 vs CTR.*

*Pc*AS infection was not lethal and did not result in any lung pathology, although the parasitaemia of *Pc*As infected mice at day 10 post infection was similar to that of *Pb*NK65 mice (Figure 11).

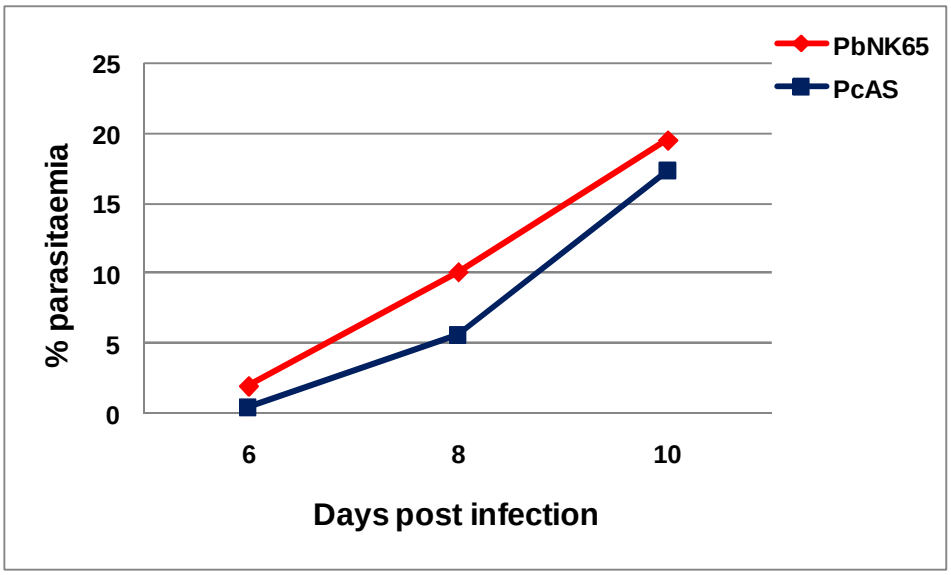

Figure 11- Peripheral parasitaemia of mice infected with PbNK65 or PcAS was determinated 6, 8 and 10 days post infection.

n=6

Despite the proven lung pathology of *Pb*NK65 infected mice, in the total lung homogenate we did not detect at day 8 or 10 post infection neither collagen increase due to fibrotic degeneration as suggested by the normal hydroxyproline levels, nor lipoperoxidation products due to oxidative stress (data not shown).

Since Hz has inflammatory properties and a strong pulmonary inflammatory response is induced in MA-ARDS, we investigated the expression of some cytokines at various times post infection. A significant increase of mRNA of TNF-α and IL-10 was detected only in *Pb*NK65 infected mice and not in *Pc*AS (Figure 12).

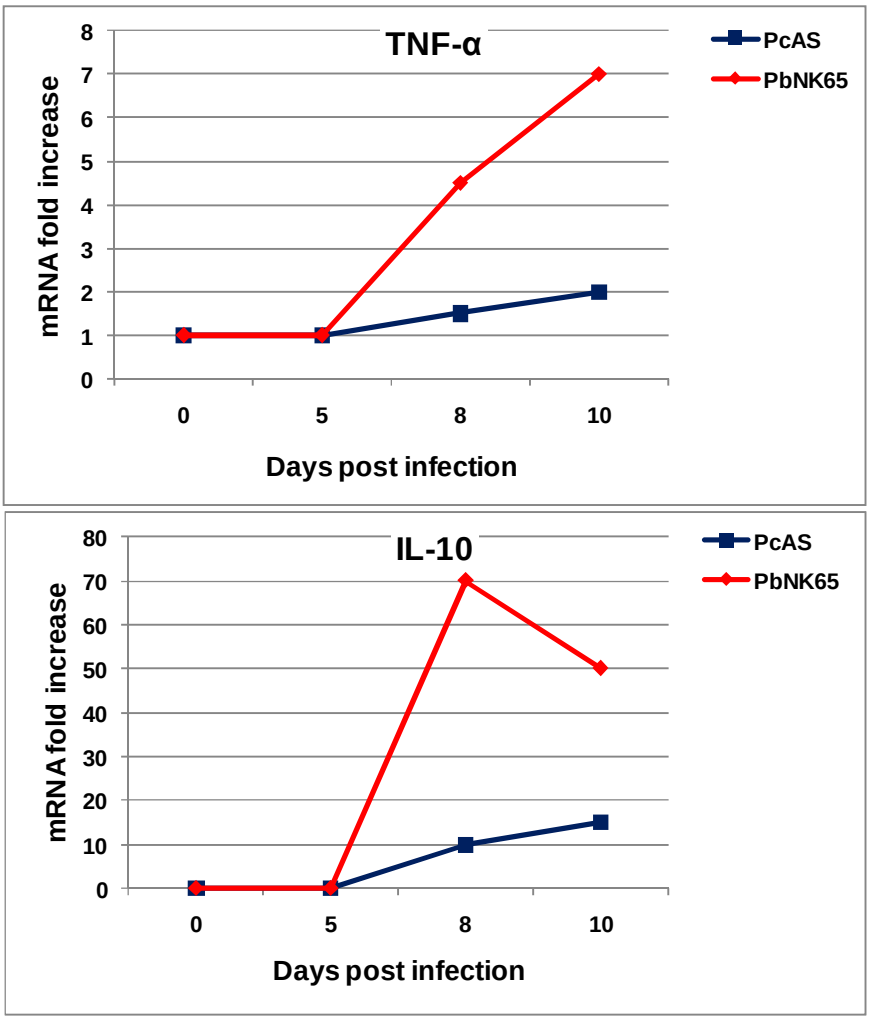

Figure 12- Cytokine expression in lungs of PbNK65 or PcAS infected mice. mRNA expression was analyzed at different time points by quantitative reverse transcription polymerase chain reaction.
n=4/6 for each time point and each parasite strain.

The cytokines increase indicated that a pathogenic inflammatory reaction caused the pulmonary pathology. Therefore, the effects of treatment with dexamethasone (DEX), a common anti-inflammatory glucocorticoid, were

evaluated in *Pb*NK65 infected mice. Daily intraperitoneal injection of DEX was made starting at day 6 or 7 post infection as described in materials and methods. Survival of *Pb*NK65 mice was significantly extended (Figure 13, Panel A) and the lung oedema was reduced by DEX treatment (Figure 13, Panel B).

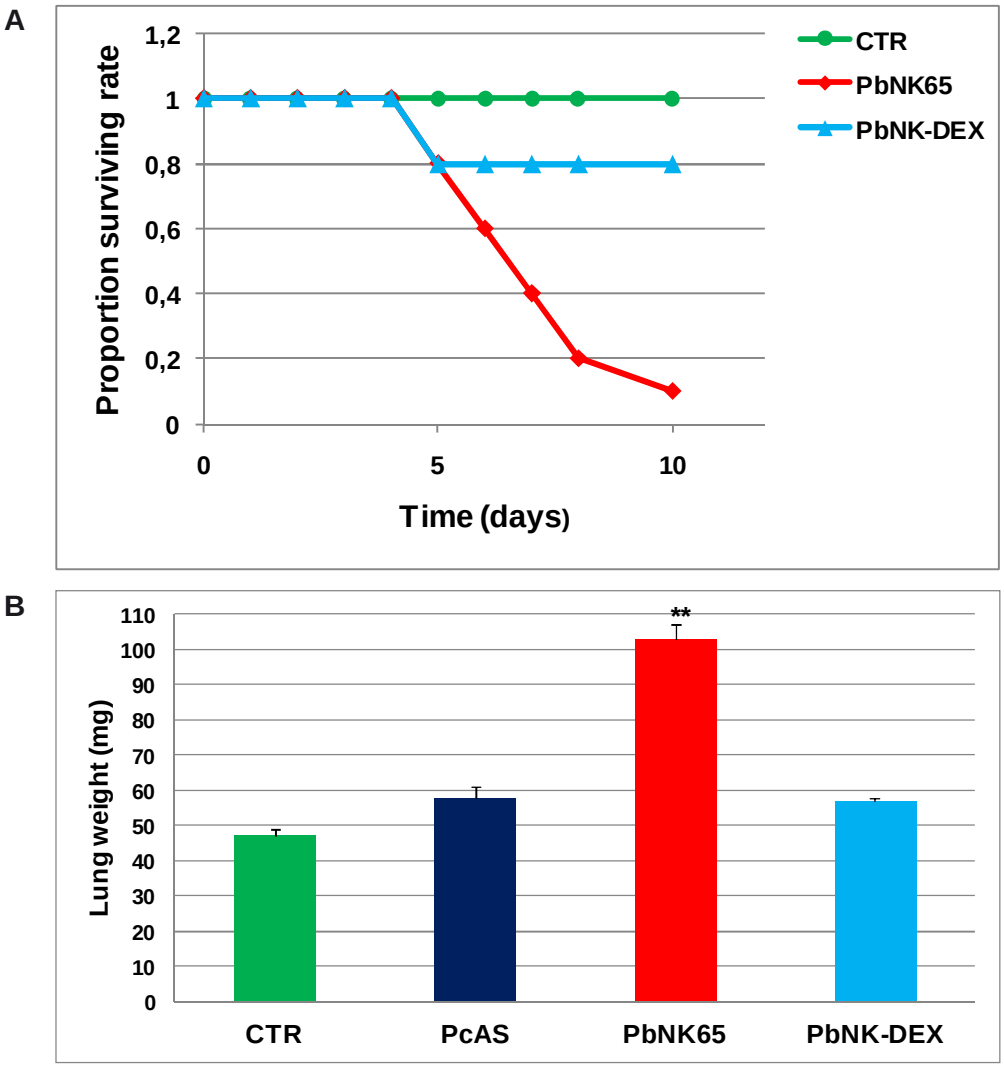

*Figure 13- **Panel A**: Infected mice with PbNK65 were treated with DEX and survival of mice was monitorated daily. n=16 for each group.*

***Panel B**: Lung weight of PbNK65 or PcAS infected mice and PbNK65 infected mice treated daily with DEX starting 6 days after the infection. n=10; ** p<0,01 vs CTR*

DEX acted on the cytokine and inflammatory response present in MA-ARDS decreasing the infiltration of CD8+ cells into lungs and the levels of IFN-γ (Figure 14, Panel A and B).

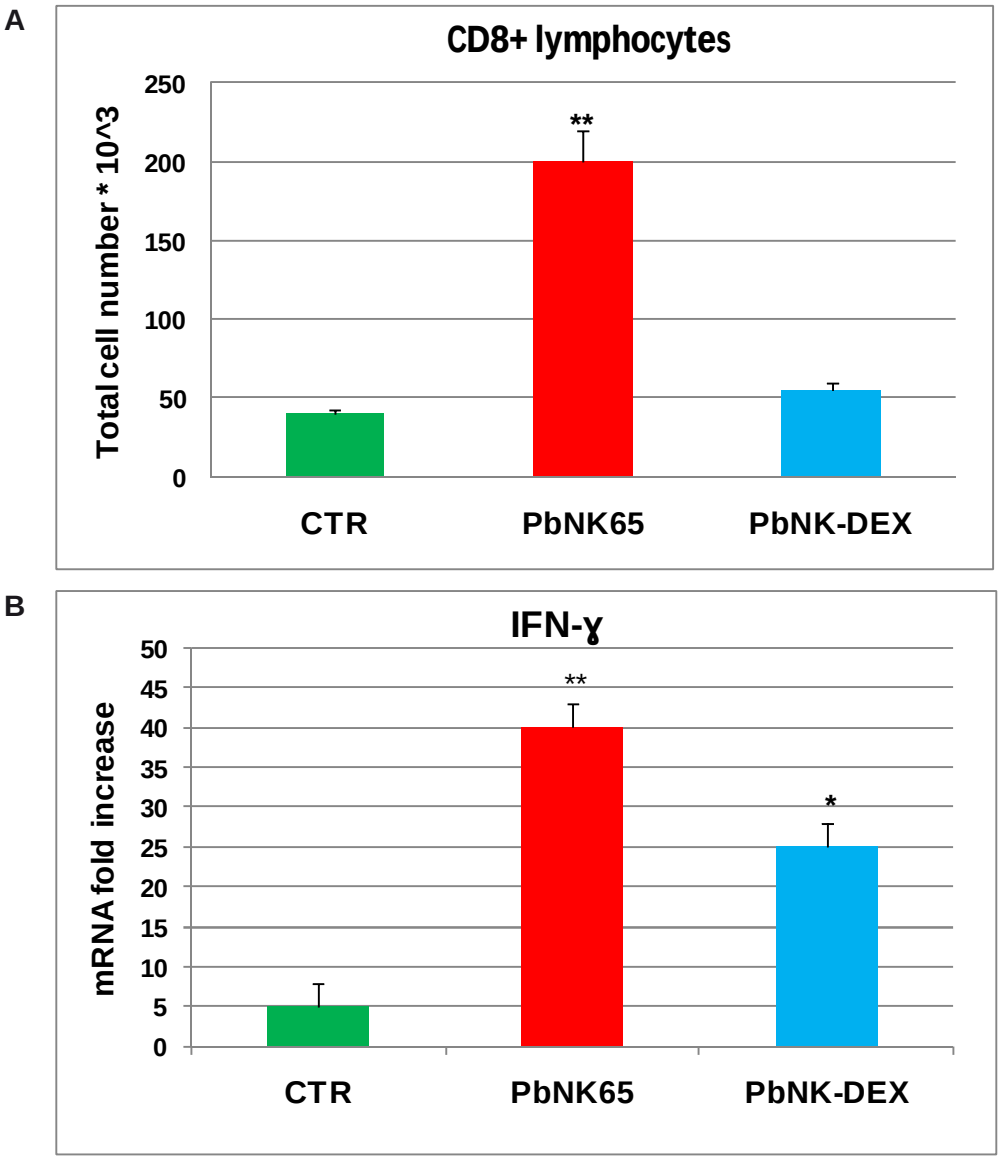

*Figure 14- **Panel A**: CD8+cells infiltration in lungs of PbNK65 infected mice and PbNK65 infected mice treated with DEX. n= 5/7 for each group; **p<0,01 vs CTR.*

***Panel B**: Effect of DEX on IFN-γ expression in PbNK65 infected mice and in PbNK65 infected mice treated with DEX. n=8/10 * p< 0,05; **p<0,01 vs CTR*

However, DEX treatment did not reduce the peripheral parasitaemia that was, on the contrary, slightly but significantly increased (Figure 15).

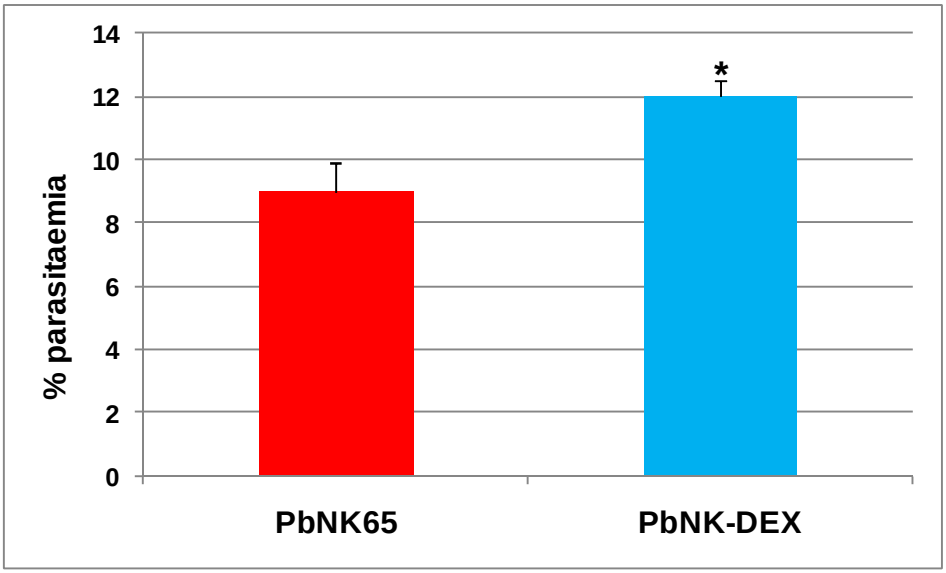

*Figure 15- Peripheral parasitaemia of PbNK65 infected mice treated or not with DEX was determined at 10 days post infection by Giemsa staining of blood smears. n=10; *p<0,05 vs not treated mice*

The pathogenesis of MA-ARDS in PbNK65 mice was investigated by studying the changes in the lipid profile of lung tissue.

Strain-related differences in the lipid composition were present in the membrane enriched fraction of lungs: in *Pb*NK65 infected mice the total content of phospholipids (PL) and cholesterol esters (ChoE) was significantly higher than in control or in *Pc*AS-infected mice both at day 8 and 10 post infection, (Figure 16, Panel A and B) and PL increase was accounted by the higher amount of phosphatidylcholine (PC), corresponding to 30% or 50% of total PL respectively at day 8 and 10 post infection (Figure 17).

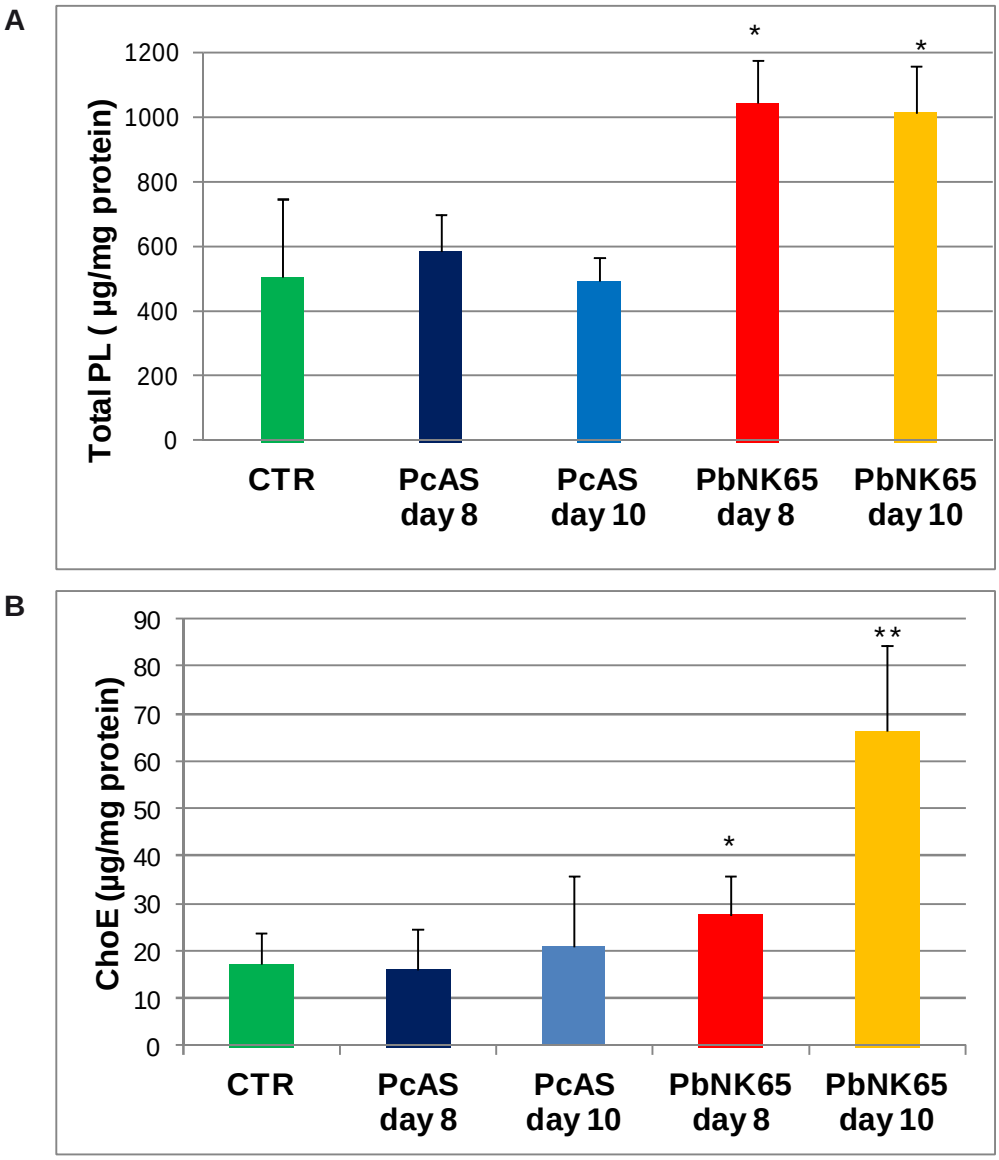

*Figure 16- **Panel A**: Phospholipid content of the lung membrane enriched fraction at different times post infection. n=9/15; * p<0,05 vs CTR*

***Panel B**: ChoE content of the lung membrane enriched fraction at different times post infection. n=6; *p<0,05; **p<0,01 vs CTR*

The content of phosphatidylethanolamine (PE), phosphatidilserine (PS), phosphatidilinositol (PI) and sphingomyelin (SM) was similar to that of CTR and *Pc*AS groups (Figure 17).

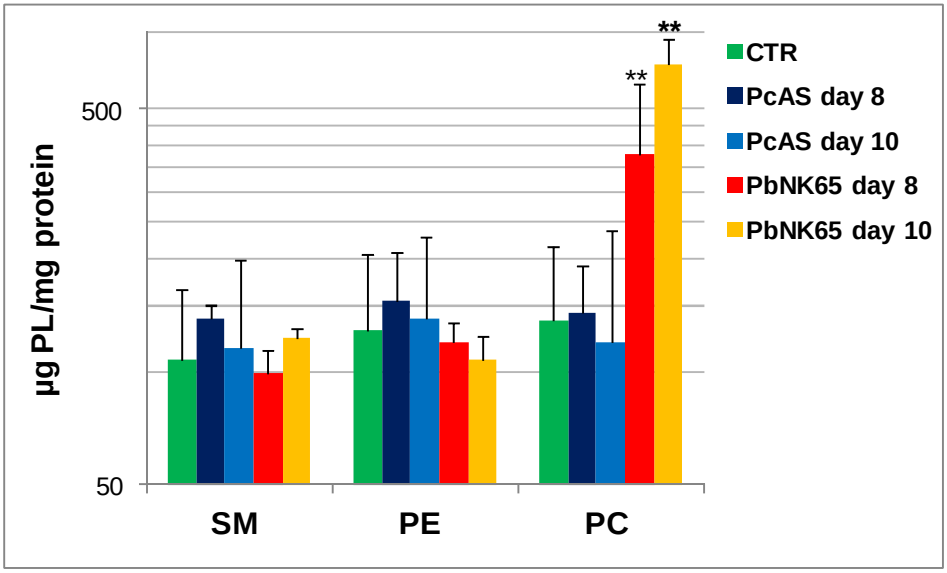

Figure 17- PL composition of the membrane enriched fraction of PcAS or PbNk65 infected mice at day 8 and 10 post infection.
*n=6/7; **p<0,01 vs CTR*

When the analyses were performed in the membrane enriched fraction of non perfused lungs the increase of ChoE and PL of *Pb*NK65 mice was significantly higherTable 1 and Figure 18).

	CTR	PcAS	PbNK65	PbNK-DEX
µg/mg protein	12,68 ± 2,0	31,70 ± 9,5	**348,90 ± 43,0****	34,30 ± 5,1

*Table 1- ChoE content of the lung membrane enriched fraction (µg ChoE/mg protein) of PcAS or PbNk65 infected mice and PbNK65 infected mice treated with DEX. Lungs not perfused n=9/15; **p<0,001 vs CTR*

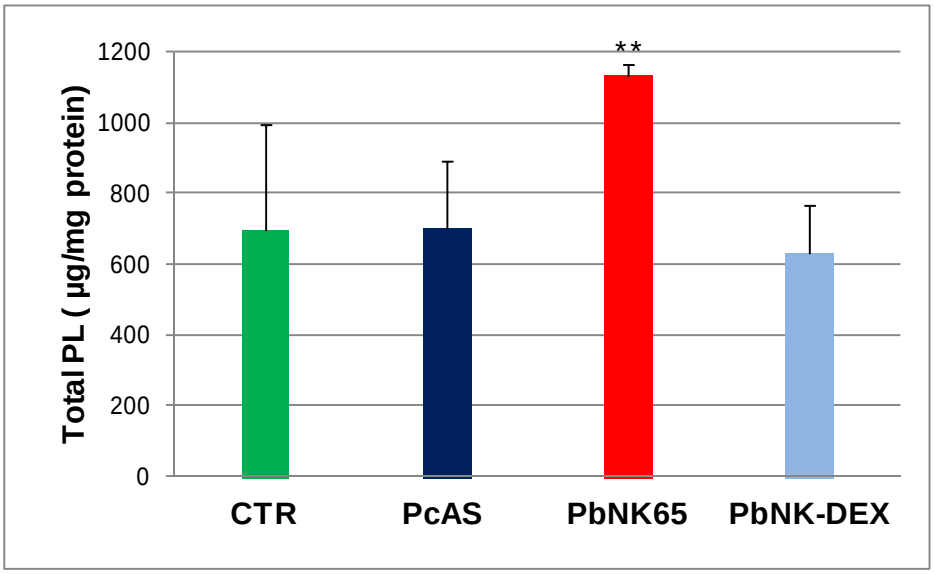

Figure 18- PL content of the membrane enriched fraction of PcAS or PbNk65 infected mice and of PbNK65 infected mice treated with DEX.
Lungs not perfused
*n=9/15; **p<0,001 vs CTR*

Further, the increase of PL was accounted not only by the higher content of PC (370,4 µg/mg protein corresponding to 35,9%) but also by a significant increase of PE (417 µg/mg protein corresponding to 40,4%) (Figure 19).

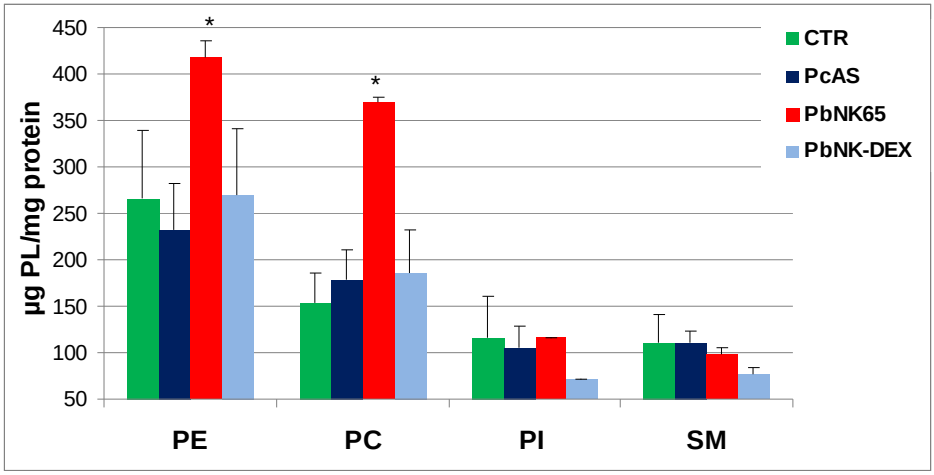

Figure 19- PL composition of the membrane enriched fraction of PcAS or PbNk65 infected mice and PbNK65 infected mice treated with DEX.

The mice were not perfused

*n=9/15; *p<0,05 vs CTR*

The increase of the total content of PL, in particular of PC and PE (Figure 18 and Figure 19), and ChoE Table 1) was almost completely reduced by the treatment with DEX.

The fatty acid distribution of the total lung lipids was altered as well at day 10 post infection, being characterized by higher levels of palmitic (C16:0, n-7) and docosahexenoic (C22:6 n-3, DHA) fatty acids (Table 2).

Table 2- Percentage distribution of fatty acid in the lung tissue (day 10 post infection)

	CTR	*Pc* AS	*Pb* NK65	*Pb* NK-DEX
C14:1	1,88 ± 1,1	0,81 ± 0,4	1,62 ± 0,8	0,54 ± 0,3
C16:0	33,15 ± 5,5	31,45 ± 9,6	**38,78 ± 5,8 ***	32,99 ± 8,8
C16:1	3,54 ± 1,0	1,37 ± 0,9	4,78 ± 1,5	2,95 ± 1,3
C18:0	12,50 ± 1,8	13,73 ± 2,4	**10,19 ± 2,2 ****	14,03 ± 4,1
C18:1	14,16 ± 1,0	11,85 ± 0,6	**10,09 ± 1,4 *****	**11,20 ± 1,2 ***
C18:2 n-6	12,71 ± 1,6	11,23 ± 1,0	**10,21 ± 1,8 ****	**11,66 ± 1,2 ***
C18:3 α	1,38 ± 1,3	0,42 ± 0,2	1,55 ± 1,6	0,25 ± 0,1
C18:3 γ	1,85 ± 1,4	1,24 ± 0,5	1,50 ± 1,2	0,82 ± 0,1
C20:3 n-6	1,65 ± 0,8	1,62 ± 1,2	1,25 ± 0,6	1,60 ± 0,3
C20:4 n-6	11,82 ± 2,8	15,65 ± 2,5	11,65 ± 2,6	13,97 ± 2,8
C20:5 n-3	0,29 ± 0,2	0,39 ± 0,4	0,22 ± 0,1	0,18 ± 0,2
C22:5 n-3	1,09 ± 0,5	2,06 ± 0,6	0,92 ± 0,2	2,06 ± 0,8
C22:6 n-3	3,93 ± 1,1	**8,16 ± 1,4****	**7,24 ± 1,6 *****	**7,72 ± 0,9 ****
PI [a]	110,10 ± 23,9	**160,74 ± 18,2****	**130,59 ± 19,4 ****	**148,51 ± 20,1 ****
*** p< 0,05 vs CTR**				
**** p< 0,01 vs CTR**				
*****p< 0,001 vs CTR**				

[a]PI: Relative oxidizability of lipid. The value is calculated based on the relative oxidation rate of unsatured fatty acid as follows:

PI=(%monoenoic x 0,025)+(%dienoic x 1)+(%trienoic x 3)+ (%tetraenoic x 4)+ (%pentaenoic x 6)+(%hexaenoic x 8)

*n= 5/11; *p<0,05; **p<0,01; ***p<0,001 vs CTR*

DHA was similarly increased in *Pc*AS-infected mice and not affected by DEX treatment. Table 2 also includes the Peroxidability Index (PI) value, which is calculated by the formula specified in Table 2 caption. Due to the high content of DHA, the PI value of lung tissue from infected mice is significantly higher compared to CTR mice indicating a higher relative oxidability of the membranes. Preliminary results showed that in *Pb*NK65-

infected mice higher percentages of DHA are also present in the lung ChoE fraction (6,9% vs 3,8% of CTR). The *Pb*NK65 ChoE fraction is also characterized by higher levels of linoleic acid (C18:2, n-6, LA= 25,4 % vs 16,2 % of CTR), arachidonic acid (C20:4, n-6, AA= 26,4 % vs 13,7% of CTR) and an higher linoleic/oleic acid (C18:1, n-9) ratio (2,3 vs 1,0 of CTR).

Brochoalveolar lavage. Since ARDS pathology is often associated with surfactant disorder, in the present study we analyzed the bronchoalveolar lavage fluid (BAL) from *P.berghei* and *P.chabaudi* infected mice. The data from BAL analyses further documented the gravity of the lung pathology, present especially in *Pb*NK65 group.

The total (cell-free) BAL fluid of *Pb*NK65-infected mice showed highly increased protein levels from day 8 post infection, greater at day 10 post infection and absent in *Pc*AS infected mice (Figure 20).

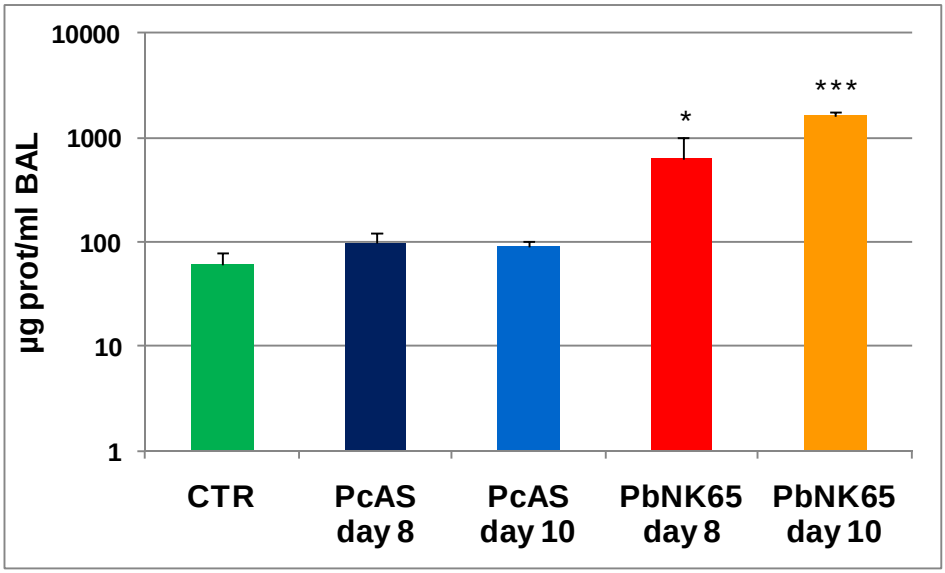

Figure 20- Protein content of BAL fluid of PbNK65 or PcAS infected mice at day 8 or 10 post infection.

*n=4/6; *p< 0,01; ***p<0,0001 vs CTR*

Considerable number of erythrocytes were observed in the BAL fluid of *Pb*NK65-infected mice, showing that haemorrhages had occurred. Importantly, leukocyte numbers were strikingly increased in the BAL fluid 10 days post infection with *Pb*NK65, whereas in *Pc*AS infected mice, BAL leukocytes were barely or not increased. The different leukocyte subpopulations of BAL fluid were determined by microscopy enumeration of Cytospin preparations, and the absolute numbers of macrophages, lymphocytes and neutrophils were calculated. All three different cells populations were significantly increased already from 8 days post infection with *Pb*NK65 (Table 3).

Table 3- Cell numbers in BAL fluids (day 10 post infection)

	CTR	PcAS	PbNK65
Leukocytes	107,3 ± 10,3	106,1 ± 17,5	**668,5 ± 173,1 ****
Erytrocytes	31,0 ± 10,0	11,6 ± 3,8	**2386,8 ± 898,1 ****
Macrophages	103,8 ± 12,4	100,7 ± 19,6	**569,5 ± 141,5 ****
Neutrophils	1,1 ± 0,3	**0,4 ± 0,2 ***	**28,3 ± 14,3 ****
Lymphocytes	2,5 ± 0,5	**5,8 ± 1,4 ***	**68,7 ± 24,6 ****

*n=4/6; ***p<0,0001 vs CTR*

Similarly to the *Pc*AS group, the PL content of *Pb*NK65 infected mice was slightly higher compared to CTR at day 8 post infection, although not significantly different, and further increased at day 10 (Table 4). The ratio protein/PL of total BAL was higher in *Pb*NK65 mice than *Pc*AS at both time points (Table 4).

Table 4- BAL fluid: total PL content and prot/PL ratio

	ug PL/ml	prot/PL
CTR	56,00 ± 5,2	1,71 ± 0,5
PcAS day 8	91,76 ± 32,0	1,06 ± 1,0
PcAS day 10	80,12 ± 50,6	1,09 ± 0,6
PbNK65 day 8	77,63 ± 53,8	**8,18 ± 8,05*** **
PbNK65 day 10	162,30 ± 75,8	**10,05 ± 5,5*** **

*n=4/6; ***p<0,0001 vs CTR*

The BAL large aggregate fraction (LA) of *Pb*NK65 infected mice was similar to that of CTR mice at day 8 and 10 post infection (Figure 21, Panel A), showing substantial increases in both protein content (not shown) and protein/PL ratio (Figure 21, Panel B). These alterations are absent in the *Pc*AS group.

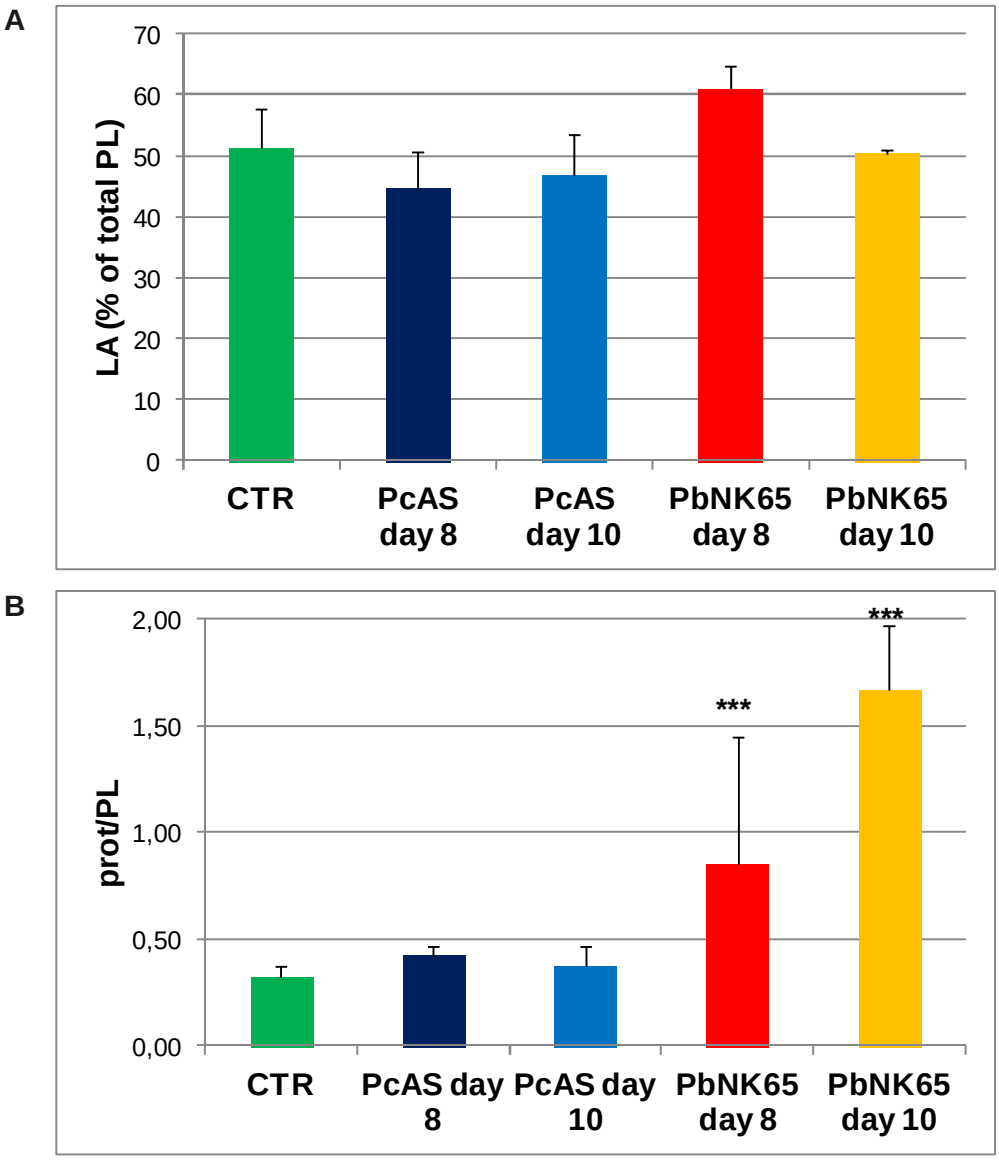

*Figure 21- Percentage of the total PL **(Panel A)** and protein/PL ratio **(Panel B)** of BAL large aggregate(LA) fraction at day 8 or 10 post infection in PbNK65 and PcAS infected mice.*

*n=4/6; ***p< 0,001 vs CTR*

In addition, in the *Pb*NK65-infected mice the PL profile of LA fraction was significantly modified at both days post infection, showing a significant increase in the relative amounts of SM and a decrease in phosphatidylglycerol (PG) (Figure 22, Panel A). The same changes of the PL profile were observed in the small aggregates fraction. In this fraction, PG was almost undetectable and lysophosphatidylcholine (LPC) was dramatically increased (Figure 22, Panel B).

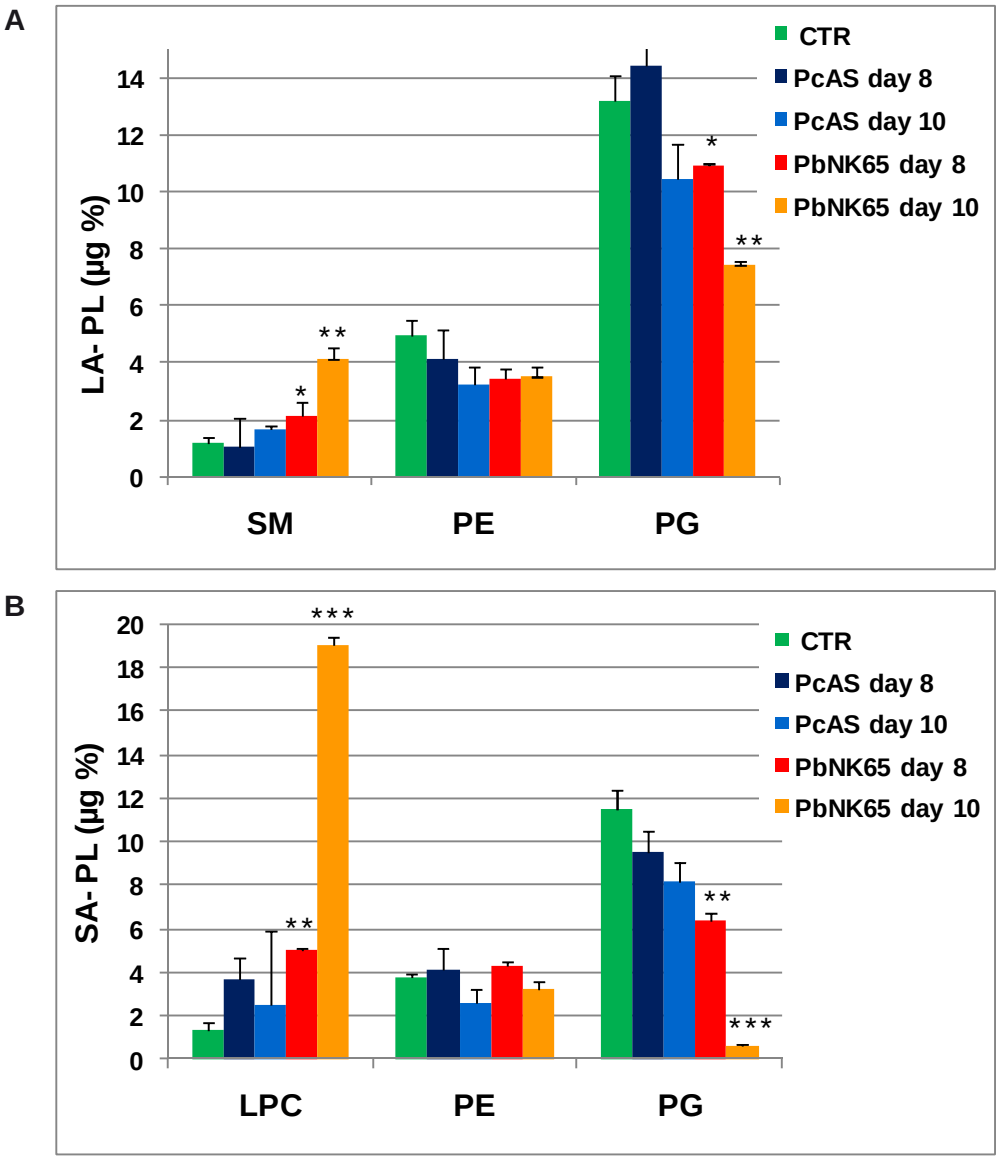

*Figure 22- Percentage distribution of PL in LA **(Panel A)** and SA **(Panel B)** fractions of PbNK65 and PcAS infected mice at day 8 or 10 post infection. n=4; *p<0,05; **p<0,001; ***p<0,0001 vs CTR*

***Plasma*.** Since plasma reflects the status of host homeostasis and is also an excellent reporter of disturbances caused by environmental stressors, we explored the plasma lipid profile.

Compared to CTR and *Pc*AS the plasma lipid profile of *Pb*NK65 mice was characterized by an higher PL content (Figure 23).

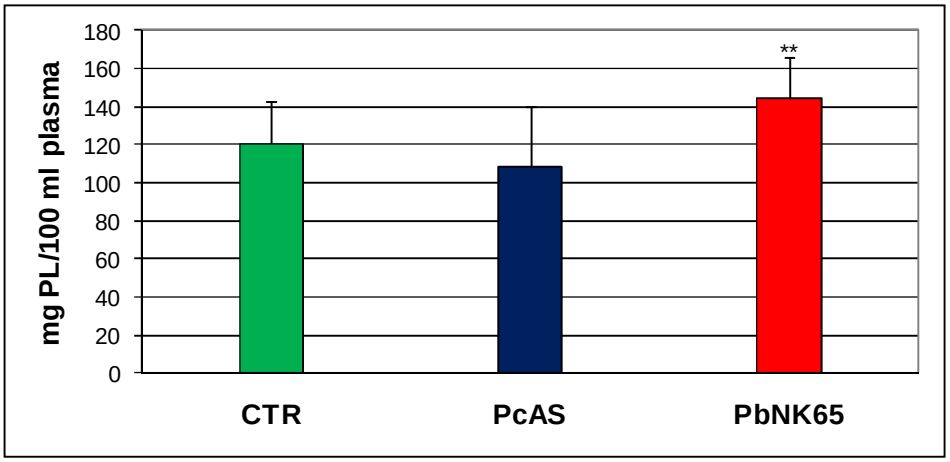

Figure 23- PL content in plasma (mg/100 ml) of PbNK65 and PcAS infected mice at day 8 post infection.

*n=8/12; **p<0,01 vs CTR*

Specifically, we found a significant increase in SM, PC and PE content in *Pb*NK65 infected mice paralleled by lower levels of LysoPC that led to an higher PC/lysoPC ratio (Figure 24).

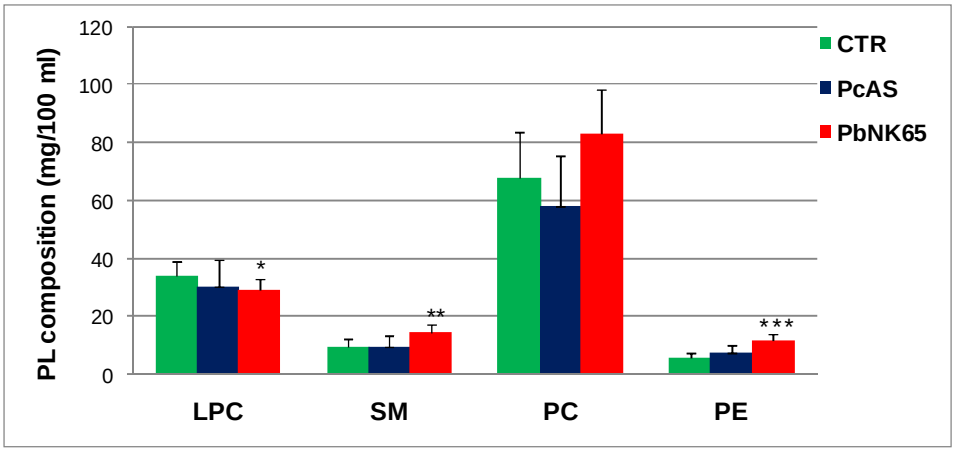

Figure 24- PL composition of plasma (mg/100 ml) of infected and non infected mice at day 8 post infection.

*n=6/8; *p<0,05; **p<0,01; ***p<0,001 vs CTR*

The neutral lipid content was changed as well. In particular the total triacylglycerol (TG) and free cholesterol (Cho) content were significantly increased while ChoE content was unchanged in the two different strains (Figure 25).

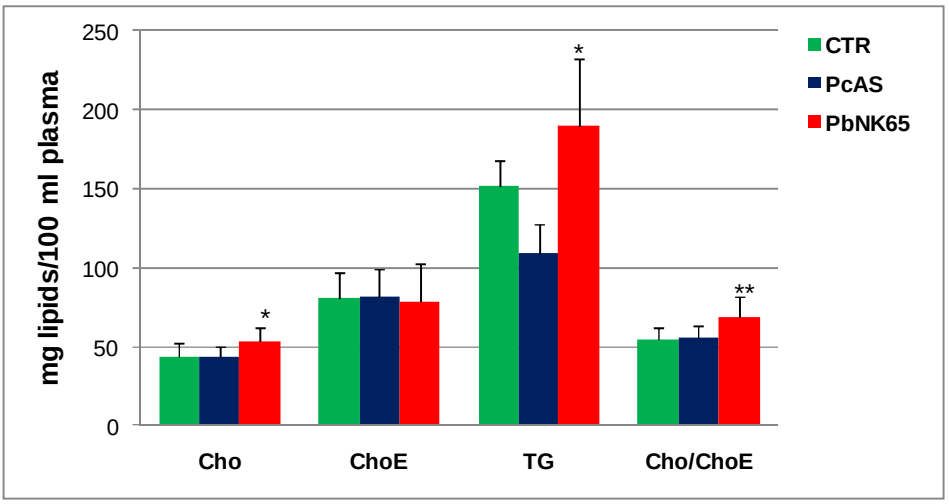

Figure 25- Plasma neutral lipid content (mg lipids/mg protein) of infected and non infected mice at day 8 post infection.
*n=8/12 *p<0,05; **p<0,01 vs CTR*

The total fatty acid profile of plasma showed in *Pb*NK65-infected mice lower levels of linoleic acid (C18:2) and higher levels of arachidonic acid (AA) and DHA at both day 8 and 10 post infection (Table 5). Lower levels of C18:3 and higher levels of AA and DHA fatty acids were also present in the purified PL and ChoE fractions (not shown).
Treatment by DEX only partially reduced the DHA levels (Table 6).

Table 5- Plasma fatty acid distribution (%) of PbNK65 or PcAS infected mice at day 8 and 10 post infection

	CTR	PcAS day 8	PcAS day 10	PbNK65 day 8	PbNK65 day 10
C16	23,24 ± 0,1	23,92 ± 0,03	24,68 ± 0,5	18,67 ± 1,0	20,57 ± 0,6
C16:1	1,89 ± 0,1	1,38 ± 0,4	**0,55 ± 0,1 ***	**0,61 ± 0,05 ***	**0,66 ± 0,05 ***
C18	9,94 ± 0,08	10,06 ± 0,1	10,84 ± 1,1	18,22 ± 0,05	13,79 ± 0,06
C18:1	13,46 ± 0,8	13,48 ± 0,01	11,25 ± 1,2	8,03 ± 0,2	9,03 ± 0,2
C18:2 n-6	30,90 ± 0,6	31,36 ± 0,1	31,11 ± 2,5	**25,26 ± 0,6 ***	**25,94 ± 0,6 ***
C18:3 γ	0,76 ± 0,5	1,14 ± 0,1	0,94 ± 0,2	**0,51 ± 0,01 ****	**0,16 ± 0,07 ****
C20:3 n-6	1,00 ± 0,01	0,85 ± 0,2	0,66 ± 0,0,1	**0,71 ± 0,01 ****	**0,41 ± 0,04 ****
C20:4 n-6	12,92 ± 1,08	12,28 ± 0,2	14,09 ± 2,3	19,24 ± 0,9	17,98 ± 0,6
C20:5 n-3	0,42 ± 0,01	0,36 ± 0,01	0,33 ± 0,03	0,36 ± 0,01	0,51 ± 0,08
C22:5 n-3	0,40 ± 0,01	0,39 ± 0,03	0,45 ± 0,01	**0,31 ± 0,03 ***	0,47 ± 0,03
C22:6 n-3	4,52 ± 0,14	4,26 ± 0,2	4,66 ± 0,7	**7,74 ± 0,4 ****	**10,18 ± 0,4 *****
PI	128,67 ± 8,5	124,48 ± 10,1	133,84 ± 6,1	171,48 ± 9,7	187,25 ± 11,8
C18:2/C20:4	2,70 ± 0,9	2,55 ± 0,05	2,25 ± 0,4	1,31 ± 0,03	1,45 ± 0,1

*n=4; *p<0,05; **p<0,01; ***p<0,0001 vs CTR*

Table 6- Plasma fatty acid distribution (%) of mice infected with PcAS, PbNK65 and PbNK65 treated with DEX (day 10 post infection)

	CTR	PcAS	PbNK65	PbNK-DEX
C16	19,06 ± 2,8	21,71 ± 1,8	18,11 ± 2,2	16,64 ± 1,3
C16:1	1,90 ± 1,0	1,27 ± 0,4	**0,72 ± 1,1 ***	**0,90 ± 0,5 ***
C18	11,75 ± 3,5	10,54 ± 2,3	11,48 ± 2,0	10,71 ± 1,2
C18:1	13,63 ± 1,9	12,98 ± 1,7	13,10 ± 3,7	17,43 ± 3,7
C18:2 n-6	33,02 ± 4,8	30,43 ± 3,7	**26,90 ± 0,2 ***	31,53 ± 0,8
C18:3 γ	0,98 ± 0,4	0,95 ± 0,2	**0,47 ± 0,2 ***	1,17 ± 0,2
C20:3 n-6	1,14 ± 0,1	1,17 ± 2,5	**0,66 ± 0,3 ***	**0,69 ± 0,2 ****
C20:4 n-6	13,42 ± 4,8	14,13 ± 2,5	16,25 ± 1,9	11,98 ± 1,8
C20:5 n-3	0,49 ± 0,1	0,36 ± 0,1	0,43 ± 0,1	0,36 ± 0,1
C22:5 n-3	0,39 ± 0,02	**0,57± 0,1 ***	**0,59 ± 0,1 ****	**0,87 ± 0,2 *****
C22:6 n-3	4,21 ± 1,3	**6,48 ± 0,2 ***	**10,87 ± 1,0 ****	**7,26 ± 1,6 ****
PI	130,29 ± 28,5	177 ± 21,6	**187,78 ± 14,2 ***	149,31 ± 14,7
C18:2/C20:4	2,70 ± 0,9	2,18 ± 0,5	**1,68 ± 0,4 ***	2,69 ± 0,5

*n=5; *p<0,05; **p<0,01; ***p<0,0001 vs CTR*

Liver. We also investigated the liver pathology present in *Pc*AS and *Pb*NK65 infected mice. The weight of liver was significant increased, at day 8 post infection, in *Pb*NK65 infected mice and at a greater extent in *Pc*AS infected mice, while at day 10 post infection hepatomegaly was present only in *Pc*AS group (Figure 26). The content of total protein/gr liver was significantly lower, compared to CTR, in both models of infection, with levels in *Pb*NK65 mice significantly lower compared to *Pc*AS ($p < 0,05$) (Figure 27).

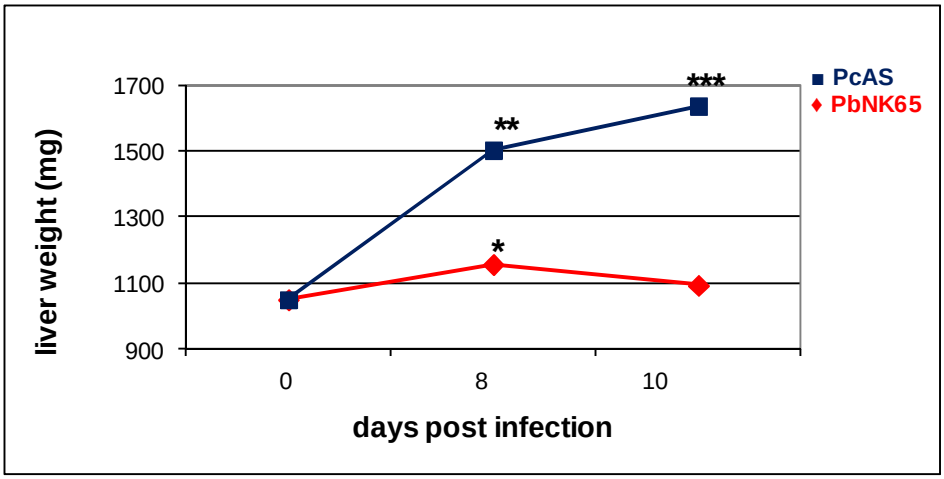

Figure 26- Liver weights of PbNK65 and PcAS infected mice.
*n=6; *p<0,05; **p<0,01; ***p<0,001 vs CTR*

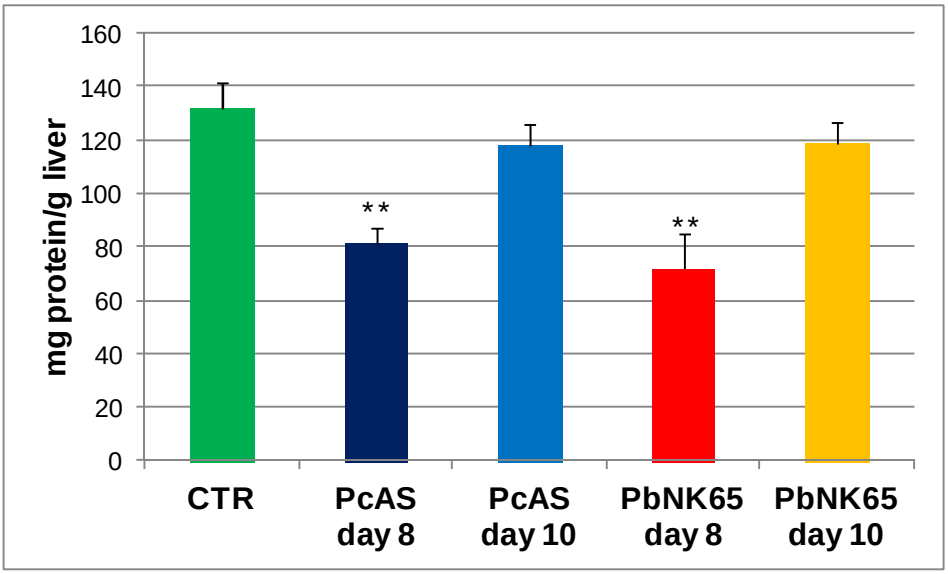

Figure 27- Protein content (mg protein/g liver) in the liver of infected and not infected mice at different times post infection.
*n=6; **p<0,01 vs CTR*

Analogously to lungs, livers from *Pb*NK65-infected mice had a dark-brown coloration due to HZ deposition. The amount of malaria pigment increased progressively during infection and was higher in *Pb*NK65 group compared to PcAS (Figure 28).

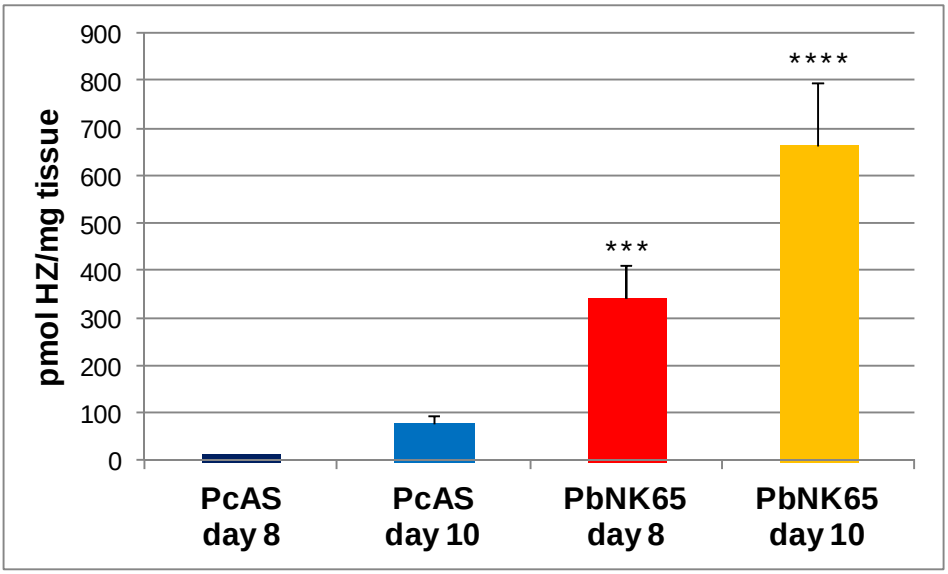

Figure 28- pmol HZ/mg liver at different time points after infection with PbNK65 or PcAS.

*n=5/6; ***p<0,001; ****p<0,0001 vs PcAs day 10*

As shown in Figure 29 the cryosections from perfused livers, stained with hematoxylin-eosin, demonstrated larger and more abundant clusters of HZ in *Pb*NK65 mice compared to *Pc*AS group. No major morphological changes were noticeable in the liver architecture of the two parasite strains.

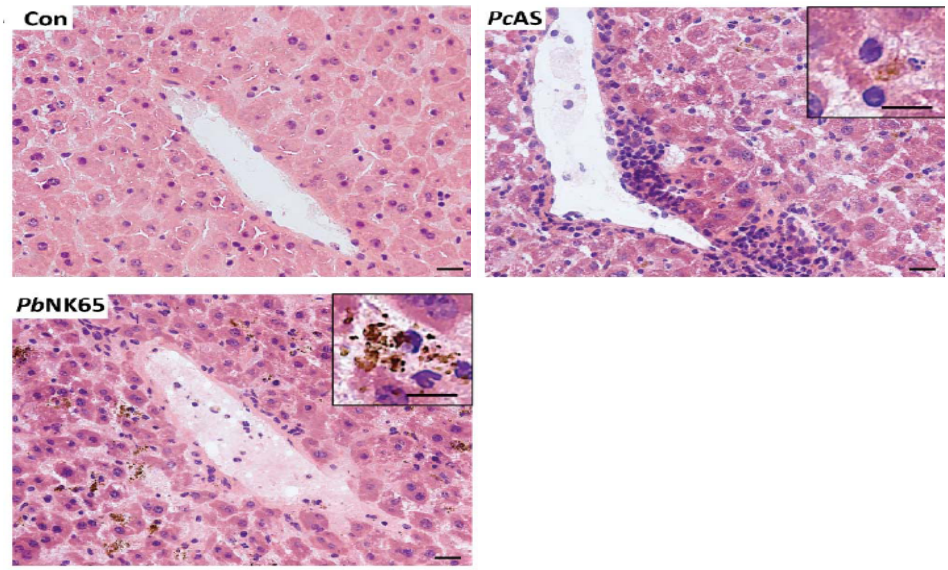

Figure 29- Cryosections were prepared from livers of mice uninfected (Con) and infected with PbNK65 or PcAS at day 10 post infection and stained with hematoxylin-eosin. Insets show cluster of Hz (dark brown crystals). Representative images are shown.

However, submicroscopical signs of liver fibrosis were evident in *Pc*AS and *Pb*NK65 infected mice at day 8 post infection as demonstrated by the increased levels of hydroxyproline. However, in both strains, the amount of hydroxyproline decreased at day 10 post infection returning to values similar to those of CTR group (Figure 30).

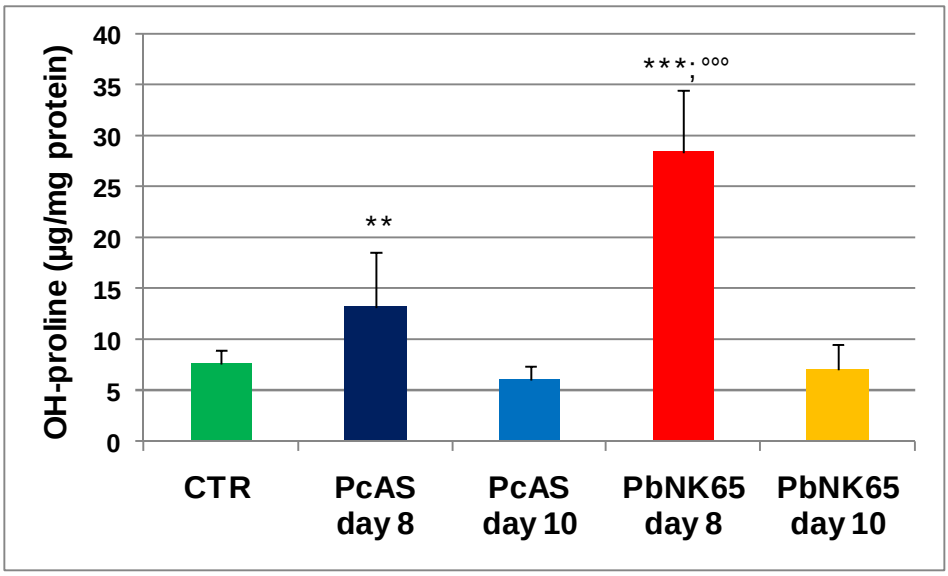

Figure 30- OH proline content in liver of infected mice at different time points (day 8 or 10 post infection)

*n=4/9; **p<0,01; ***p<0,0001 vs CTR*

°°°p<0,001 vs PcAS day 8

In agreement with the high HZ deposition present in the liver of *Pb*NK65-infected mice we found higher levels of mRNA TNF-α (Figure 31) and TNF-α protein (Figure 32).

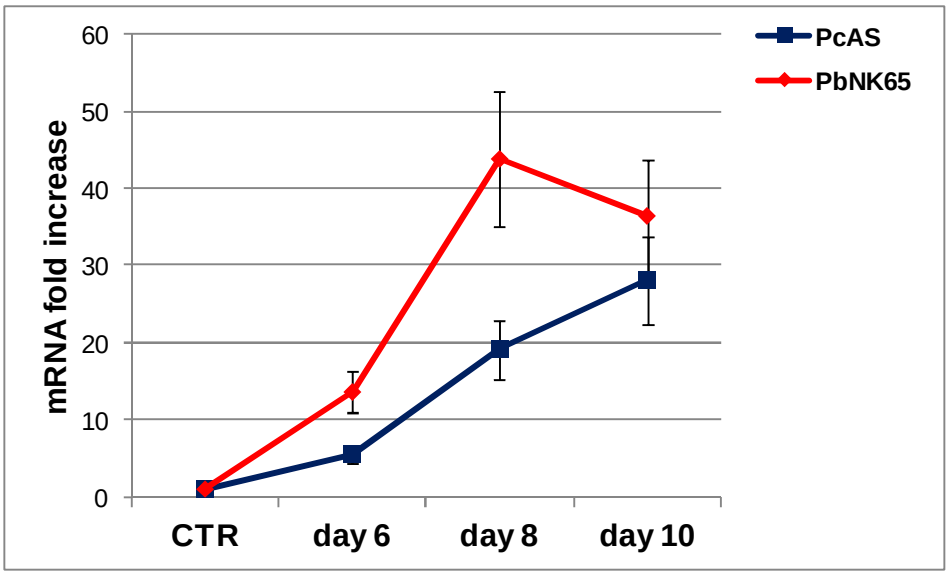

Figure 31- TNF-α expression in PbNK65 and PcAS infected mice at different times post infection. mRNA expression kinetic was analyzed by quantitative reverse transcription-polymerase chain reaction. n=6

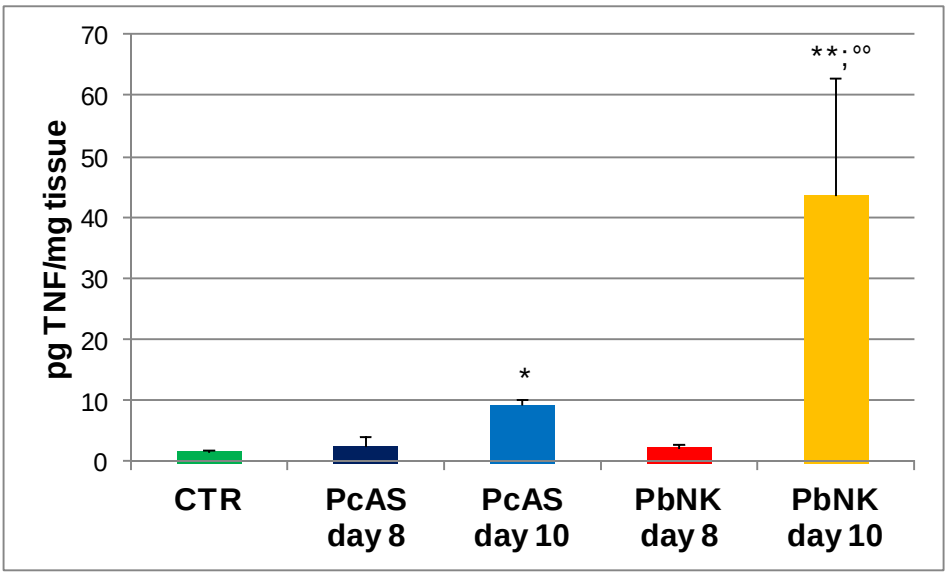

Figure 32- TNF-α protein in mice infected with PbNK65 or PcAS at day 8 or 10 post infection.

*n= 5; * p<0,05; ** p<0,01 vs CTR; °° p<0,01 vs PcAS day 10*

The expression of the inflammatory mediator TNF-α was strictly correlated to the HZ deposition in *Pb*NK65 infected mice (Figure 33).

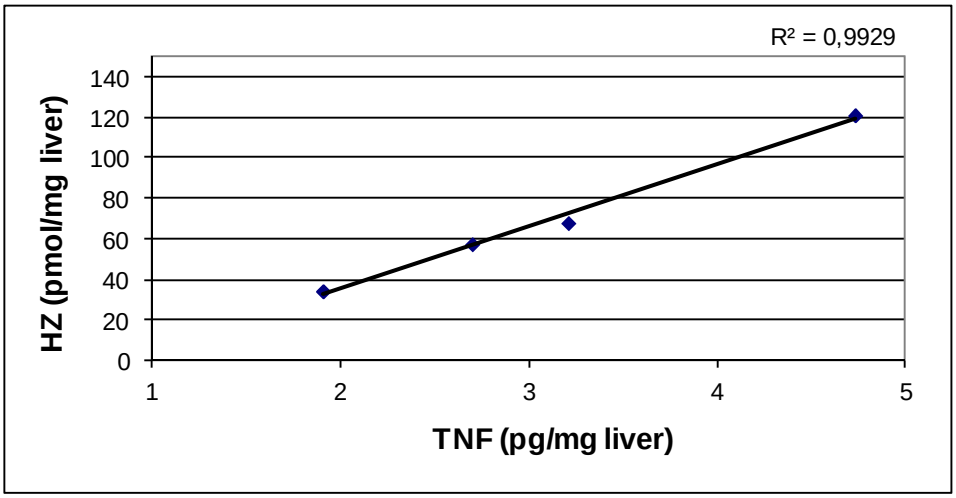

Figure 33- Speraman correlation between Hz and TNF-α expression in liver of PbNK65 infected mice at day 8 and 10 post infection.
n= 5/6

Lipid peroxidation was also investigated and expressed as pmol of malondialdehyde (MDA)/mg protein. MDA levels were significantly higher in livers from *Pb*NK65-infected mice at day 8 and further increased at day 10 post infection, while in *Pc*AS infected mice they were similar to CTR at both days post infection (Figure 34).

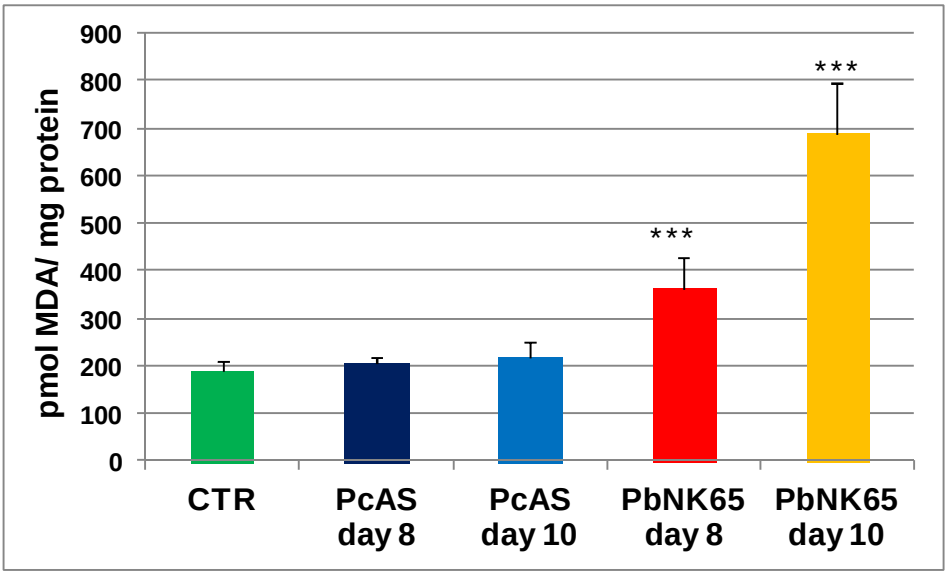

Figure 34- MDA content in the liver of PbNK65 or PcAS infected mice 8 or 10 days post infection.

*n=6/8; ***p<0,0001 vs CTR*

The activity of glutathione reductase (GR) was significantly enhanced at day 8 and 10 post infection in both parasite strains. SOD activity was similar to CTR at day 8 post infection but, with the progression of the pathology, its activity was significantly enhanced. Catalase (CAT) activity and total glutathione content increased at day 8 and 10 post infection in *Pc*AS infected mice, while in PbNK65 infected mice they significantly decreased, compared to CTR, at day 10 post infection (Table 7).

Table 7- Enzymatic activities and total GSH content

	CAT	GR	SOD	Total GSH
	mU/mg prot	mU/mg prot	U/mg prot	nmol/mg prot
CTR	182,12 ± 23,1	108,48 ± 7,8	84,64 ± 27,2	87,43 ± 14,6
PcAS day 8	301,32 ± 59,2*	220,18 ± 5,4***	99,98 ± 23,7	158,24 ± 3,5*
PcAS day10	284,15 ± 72,3**	260,97 ± 65,1***	**199,17 ± 54,5*** **	**165,62 ± 30,7*** **
PbNK65 day 8	236,31 ± 27,8	189,37 ± 35,7***	74,57 ± 19,6	102,58 ± 17,0
PbNK65 day 10	121,17 ± 11,2*	162,7 ± 21,5***	**165,79 ± 34,1*** **	**65,06 ± 14,9****

*n=6; *p<0,05;**p<0,01; ***p<0,0001 vs CTR*

The lipid profile of livers of *Pb*NK65 mice was significantly affected, showing higher levels of TG, free fatty acid (FFA) and ChoE, whereas free Cho was not significantly changed. These alterations were present at day 8 and 10 post infection (Table 8).

Table 8- Cholesterol (Cho), Cholesterol Esters (ChoE), Triacylglycerol (TG) and free fatty acid (FFA) content (mg lipid /g protein) in PcAs and PbNk65 infected mice at day 8 or 10 post infection.

	Cho	ChoE	TG	FFA
CTR	18,99 ± 7,4	0,74 ± 0,6	25,92 ± 3,6	21,58 ± 6,5
PcAS day 8	34,86 ± 17,2	1,9 ± 1,3	**37,4+19****	**33,04 ± 7,5***
PcAS day10	28,6 ± 4,8	2,13 ± 1,8	55,81 ± 39,8	36,28 ± 19,0
PbNK65 day 8	26,24 ± 3,7	**3,92 ± 2,5***	**159,3 ± 54,3*** **	**46,87 ± 8,8*** **
PbNK65 day 10	18,9 ± 13,9	**3,47 ± 0,3*** **	**144,79 ± 12,4*** **	**39,7 ± 16,6*** **

*n=6; *p<0,05; **p<0,01; ***p<0,0001 vs CTR*

In contrast, the total content of PL and the PL pattern were unchanged (not shown). The total fatty acid pattern of *Pb*NK65 livers was characterized by higher levels of linoleic acid and lower levels of eicosatrienoic (C20:3 n-6) and arachidonic acids compared to CTR (Table 9).

The same fatty acid profile and differences compared to the CTR group were present in the isolated PC fraction (the most abundant, more than 30% of the liver phospholipids). In addition, PC showed higher levels of DHA (9,0% vs 7,1% of CTR, p <0.05, not shown).

Table 9- Fatty acid distribution (%) in liver

	CTR	PcAS	PbNK65
C16:0	22,76 ± 1,0	**25,04 ± 0,8 ***	**20,39 ± 0,9 ***
C16:1	1,4 ± 0,2	1,24 ± 0,1	**0,63 ± 0,3 ***
C18:0	14,25 ± 1,6	13,90 ± 0,7	14,47 ± 1,7
C18:1	11,34 ± 1,5	11,48± 1,5	12,67 ± 1,5
C18:2 n-6	17,93 ± 1,4	18,24 ± 0,6	**24,32 ± 2,4 ****
C18:3 α	0,34 ± 0,1	0,25 ± 0,1	0,24 ± 0,1
C18:3 γ	0,16 ± 0,1	0,15 ± 0,1	0,12 ± 0,1
C20:3 n-6	1,01 ± 0,1	0,95 ± 0,2	**0,48 ± 0,1 *****
C20:4 n-6	21,82 ± 1,1	**19,82 ± 0,8 ***	**17,41 ± 1,4 *****
C20:5 n-3	0,31 ± 0,1	0,24 ± 0,1	0,18 ± 0,1
C22:5 n-3	0,36 ± 0,1	**0,52 ± 0,1 ***	0,45 ± 0,1
C22:6 n-3	8,31 ± 0,7	8,16 ± 1,2	8,64 ± 0,6
PI	179,05 ± 8,9	170,34 ± 8,6	168,86 ± 9,4
C18:2/C20:4	0,82 ± 0,1	**0,92 ± 0,1 ***	**1,41 ± 0,2 *****

*n= 4; *p<0,05; **p<0,01; ***p<0,001 vs CTR*

5 DISCUSSION

As outlined in the introduction, MA-ARDS is a common, often lethal pathological complication in adult patients with *P.falciparum* malaria. According to the WHO classification, deep breathing, respiratory distress and pulmonary oedema are among the clinical feature defining severe malaria (*166*). MA-ARDS is really important in malaria-endemic areas with low transmission (where adults get complications because they have no semi-immunity). In a survey conducted in India, malaria was the second cause of ARDS after sepsis (*167*). MA-ARDS is characterized by acute pulmonary inflammation, increased capillary endothelial and alveolar permeability leading to interstitial and alveolar oedema and hyaline-membrane formation and results in ventilation-perfusion mismatch and impairment of gas exchange. The pronounced inflammatory response in MA-ARDS (both human and murine) is characterized by leukocyte and a limited number of neutrophil infiltration (*130*). Chronic and poorly regulated inflammation can often lead to fibrosis and macrophages are also considered important in this progression. The idea that inflammatory reactions may participate in the pathogenesis of MA-ARDS is reinforced by the fact that MA-ARDS is sometimes observed in patients with malaria during or even after treatment, when most of parasites are cleared from the circulation (*112*).

We developed, in collaboration with professor Van den Steen of the University of Leuven, a new animal model for MA-ARDS with many similarities to human MA-ARDS. The infection of C57Bl/6 mice with *P. berghei* NK65 resulted in severe MA-ARDS with initial interstitial oedema and cell infiltration and progression to severe alveolar oedema, and the pathology developed to a full extent without cerebral malaria, creating a sufficient time window to study the pulmonary complications.

Lungs from *Pb*NK65-infected mice had a brown-greyish colour due to hemorrhages and Hz deposition, in addition to significantly increased weights. The lung weight of *Pb*NK65-infected mice was about twofold that of *Pc*AS. This increase is due to the oedema formation and cells infiltration. Pulmonary Hz levels increased progressively during infection with *Pb*NK65 whereas lungs from *Pc*AS-infected mice contained significantly less Hz. As previously demonstrated (*130, 131*) the strain-specific differences in pulmonary Hz levels were due to differences in Hz production by the parasite and not to differences in Hz degradation rate by the host. Even thought the amount of Hz decreased in the lungs after therapeutic parasite clearance, no Hz degradation was found during a four months observation period (*168*).

Since Hz has inflammatory properties and tissue inflammation and cell migration are orchestrated by the expression of cytokines and chemokines, we measured mRNAs of some cytokines and in particular we studied the expression of TNF-α and IL-10 in lung homogenates at different times post infection. The comparison between *Pb*NK65 and *Pc*AS infections is important to discriminate between cytokines induced specifically during MA-ARDS or as a consequence of systemic malaria infection. We found a major expression of TNF-α as well as IL-10 in the lungs of *Pb*NK65-infected mice compared to mice infected with *Pc*AS, indicating that these cytokines are induced specifically during MA-ARDS and they are not a consequence of the systemic malaria infection. The pulmonary expression of TNF-α and IL-10 present only in *Pb*NK65 mice confirm the important role of Hz in pulmonary inflammation. The association between Hz, lung pathology and the induction of these mediators was determinated by Spearmen correlation analyses (data not shown). A positive correlation with both the amount of Hz/lung tissue and lung pathology was found for mRNA expression of TNF-α and IL-10 only in *Pb*NK65-infected mice. Van de

Steen et al. demonstrated in a multiple regression model, that the relationship was statistically significant and was independent of sex and peripheral parasitaemia (*131*). A similar relation was found between Hz/mg lung tissue and lung weight and this relation was dependent on TNF-α and vascular endothelial growth factor (VEGF) (*131*).

It's known that TNF-α, induced in the lungs by Hz, can increase vascular permeability (*128*). Moreover, TNF-α reduces the pulmonary expression of the amiloride-sensitive epithelial sodium channel in the alveoli, thereby altering alveolar fluid clearance (*136*). Additionally, TNF-α triggers the release of NO, which can reduce alveolar epithelial sodium transport by reducing the activity of epithelial sodium channel and sodium/potassium ATPase (*129*). It has been shown that the alveolar epithelial sodium channel expression is also decreased during pulmonary pathology in mice infected with the *P.berghei* (*136*) and this may contribute to the observed interstitial oedema.

The increased cytokine expression suggested that inflammatory reaction may participate in the pathogenesis of MA-ARDS. Therefore, in a different experiment we analyzed the effects of the anti-inflammatory DEX. The results showed that DEX is therapeutically effective against *Pb*NK65 induced MA-ARDS as indicated by the significant increased survival and reduced lung oedema. In agreement DEX reduced the pulmonary levels of some cytokines as IFN-γ. In addition to its known inhibitory influence on the expression of inflammatory cytokines, DEX exerted also an antiproliferative effect on leukocytes, in particular T lymphocytes. In fact in *Pb*NK65 mice treated with DEX the number of CD8+ T lymphocytes was significantly decreased However, DEX treatment did not reduce the peripheral parasitaemia that was, on the contrary, slightly but significantly increased. Therefore, DEX inhibited MA-ARDS, not inhibiting parasite growth but rather modulating immunopathology. Altogether these data suggest that

anti- inflammatory treatment has the potential to improve the outcome of MA-ARDS.

In addition to the inflammatory effects, Hz has a strong prooxidant activity (*169*). However, in spite of the high Hz concentration, in the present investigation we did not detect markers of increased lipid peroxidation, nor did we see signs of lung fibrosis. This is consistent with the particularly acute nature of MA-ARDS since fibroproliferation may progress in the second, more chronic phase of ARDS. In post-mortem analyses of patients with MA-ARDS, fibrosis is usually also not observed, although some exceptions have been reported of patients who died after a long chronic period of MA-ARDS and with interstitial pulmonary fibrosis (*170, 171*).

In the membrane-enriched fraction of the pulmonary tissue of *Pb*NK65-infected mice we found a significant increase of the content of PL and ChoE. In particular the increase in the total content of PL is accounted by the higher levels of PC. The increase in lung PL is a common, although not universal response to alveolar inflammation and may be contributed to increased levels of intracellular surfactant (*172*). PC, the main PL of surfactant, is indeed increased in *Pb*NK65-infected mice and contains a high percentage of palmitic acid, the most abundant fatty acid of surfactant (48%, not shown). The PL and ChoE levels of lung homogenates were significantly higher when the lungs were dissected without previous perfusion. In this case PE was also significantly increased. This phospholipid was present in higher concentrations also in plasma of *Pb*NK65 infected mice suggesting a correlation with interstitial oedema and lipoprotein infiltration during MA-ARDS. This hypothesis was confirmed by the observation that PL and ChoE were not increased in *Pc*AS-infected mice whereas they are reverted by DEX treatment in *Pb*NK65-infected mice. Lipoprotein infiltration is suggested also by the fatty acid composition of ChoE from *Pb*NK65-infected lungs, reflecting the peculiar fatty acid

composition of *Pb*NK65 ChoE in plasma: high linoleic acid arachidonic acid (AA) and DHA fatty acids and high ratio linoleic/oleic fatty acids (*173*). The high linoleic/oleic ratio is typical of plasma ChoE where the majority of ChoE derives from the activity of the plasma Lecithin Cholesterol AcylCoA Transferase (LCAT) highly specific for linoleic acid rather than from the hepatic AcylCoA Cholesterol Acyl Transferase (ACAT) activity, more specific for oleic acid. On the contrary, the high level of DHA observed not only in the lung of *Pb*NK65-infected mice but also in *Pc*AS-infected mice and not reverted by DEX, merely reflects the high levels of DHA present in plasma excluding a correlation with the malaria caused lung pathology.

Since ARDS is often associated with surfactant disorder we investigated the changes in lung surfactant of infected and non infected mice.

Proposed mechanisms of lung surfactant disorders in ARDS include destruction of the air-water interface by alveolar oedema, phospholipid and protein degradation by secretory phospholipases and proteases (*174*), and decreased synthesis of surfactant components by damaged type II cells (*175*). Leakage of plasma proteins into the alveoli is thought to contribute to the lower alveolar stability (*176*).

In *Pb*NK65-infected mice, oedema and alveolar leakage due to the lung pathology are responsible for increased protein levels, either in the total cell-free BAL fraction or in the BAL LA fraction, probably due to blood-derived proteins being incorporated into or associated with these microstructures in the alveolar hypophase. Van den Steen et al. (*130*) demonstrated that the protein profile of BAL fluid was comparable with that of plasma. At day 10 post infection with *Pb*NK65 a considerable volume of plasma had leaked out from the blood vessels into alveoli. Concurrent with the oedema formation and alveolar leakage, the protein concentration of plasma was significantly decreased in *Pb*NK65-infected mice (*130*).

The different leukocyte subpopulations of BAL fluid, calculated by microscopy enumeration of Cytospin preparations, were significantly increased already from day 8 post infection with *Pb*NK65, showing that large numbers of leukocytes had infiltrated into the alveoli during *Pb*NK65 induced MA-ARDS. The leukocyte infiltration confirmed the already discussed hypothesis i.e that inflammatory reactions participate in the pathogenesis of MA-ARDS.

It's well known that oedema formation and blood protein infiltration decrease the intrinsic surface activity of LA fraction that represents the more active form of surfactant (*177*). A lower surface activity may also contribute to pathology in *Pb*NK65-infected mice, as indicated by the altered PL profile of the LA fraction, characterized since day 8 post infection by higher levels of SM and lower levels of PG. PG was dramatically decreased also in the SA fraction where it was almost undetectable. These changes have been reported also in other animal models of lung injury and in patients with established ARDS (*178, 179*) and may be related to the altered surfactant reuptake and synthesis by injured alveolar cells or to PL contamination due to inflammatory cells or damaged alveolar type II cells. The increase of lysophosphatidylcholine (LPC), a known inhibitor of surfactant activity (*180*), in the SA fraction is consistent with the action of secretory phospholipases A_2 (sPLA2) whose activity has been detected in ARDS patients in BAL fluid, in particular in the SA aggregates (*181*). Interestingly, it has been suggested that during severe liver pathology, as that demonstrated in the present work in *Pb*NK65 mice, $sPLA_2$ may be activated and related to lung injury (*182*). Since plasma reflects the status of host homeostasis and it's also an excellent reporter of disturbances caused by environmental stressors we the content and composition of plasma lipids was also investigated.

As expected, in *Pb*NK65-infected mice the lipid profile of plasma appeared altered as well. Most of the observed alterations may be related to a delayed catabolism of VLDL due to the TNF-α induced reduction of lipoprotein lipase (LPL) activity (*183*). The impairment of LPL activity in *Pb*NK65-infected mice may account for the higher levels of TG and Cho, as well as PE. In fact, PE is a phospholipid enriched in nascent VLDL particles and is cleared from the plasma during the metabolism of VLDL by LPL and the delivery to high density lipoprotein (HDL), by the action of hepatic lipase (HL) (*184*). Interestingly, HL activity too has been found to be reduced in some models of infection and inflammation (*185, 186*). Likewise, a delayed VLDL catabolism may account for the increase of plasma SM whose plasma concentration is higher in hyperlipidemia models related to infection and inflammation (*187*). These models are characterized by a higher Cho/ChoE ratio and an increased VLDL production and/or a delayed VLDL clearance (*187, 188*). In addition, high levels of TNF-α have been shown to reduce LCAT activity (*188*). In *Pb*NK65-infected mice, a lower activity of LCAT can be hypothesized from the lower percentage of plasma LPC and the higher Cho/ChoE ratio.

The fatty acid profile of the total lipids from plasma was in good agreement with the literature (*189*). Since the three main lipid classes (PL, TG and ChoE) of plasma have a peculiar fatty acid pattern, the change in their concentration or their molecular species can account for differences in total plasma fatty acids. The most important observation was the higher levels of polyunsaturated fatty acids (PUFA), in particular DHA, that may be related to the higher proportion of PE, the phospholipid carrying the most of this fatty acid, as confirmed by the higher DHA level also in the isolated PL fraction (not shown). The DHA levels were only partially reverted by DEX treatment. This finding suggests that their increase is not related to lung pathology but rather to the malaria infection.

The fatty acid composition of plasma ChoE showed an higher proportions of linoleic acid than oleic acid, suggesting that also in *Pb*NK65-infected mice the majority of plasma ChoE derives from LCAT rather than ACAT activity (*190*).

In agreement with literature, our findings on plasma lipid alterations demonstrated that infection or inflammation can severely impair the activity of enzymes involved in the metabolism of lipoprotein. Together with a delayed or modified metabolism of lipoproteins, the increase of plasma lipids may be due to an enhanced hepatic lipogenesis. To verify this last hypothesis we found of interest to extend our investigation to liver tissue.

The incidence of hepatopathy is high in patients with severe malaria and MA-ARDS (*191*) and it is characterized by Kupffer cell hyperplasia with haemozoin deposition. In our models of murine infection hepatomegaly was observed with both parasite strains at day 8 post infection while, 10 days post infection hepatomegaly was present only in *Pc*AS infected mice, whereas liver weights were slightly decreased in *P.berghey* NK65. The infected mice liver showed also a decrease in total protein contents. This finding suggests that continuous extensive proteolysis may provide a readily available pool of free amino acids to parasites for their rapid proliferation.

Upon intraerythrocytic parasite replication and subsequent schizont rupture, newly formed merozoites are released into the blood together with high amounts of Hz, which are rapidly removed by phagocytosis. The liver significantly contributes to the phagocytosis of infected RBC and Hz, as evidenced by the high hepatic Hz levels. The amount of Hz/mg liver tissue was higher in *Pb*NK65 mice and the level progressively increased during infection, indicating that when infection progresses, more Hz is released into the circulation and trapped in the liver. To analyze whether liver histology is differently affected by the two parasite strains, cryosections

from perfused livers were stained with hematoxylin-eosin. No major morphological changes were noticeable in the liver architecture of both *Pb*NK65 or *Pc*AS infected mice, but the livers of *Pb*NK65 mice 10 days after infection contained more abundant and larger clusters of Hz, than livers from *Pc*As infected mice, corroborating the Hz quantification data. Higher levels of TNF-α, as mRNA and protein, were detected in *Pb*NK65-infected mice compared to *Pc*AS group. TNF-α expression was correlated to Hz deposition. Hz levels, which are significantly higher in *Pb*NK65-infected mice than in mice with a self-resolving *Pc*AS infection, may activate Kupffer cells to release TNF-α, which may be involved in liver damage and may play a key role, in the early stages, in the lipogenetic activity of the liver (*192*). Infection and inflammation have been shown to induce multiple alterations in hepatic lipid and lipoprotein metabolism (*186*). In fact, in rodents TNF-α rapidly increases adipose tissue lipolysis and hepatic fatty acid, Cho and TG synthesis (*186, 193*) and hepatic lipotoxicity, at least in part, by inducing hepatocyte lysosomial destabilization (*194*). In agreement with these findings we have observed important alterations in liver lipids of *Pb*NK65-infected mice. The significant increase of TG, FFA and ChoE in *Pb*NK65-infected livers is in agreement with literature data showing that livers from *P. berghei*-infected mice contain lipid droplets and myelin-like figures (*151*) and suggesting that malaria parasites are able to influence the hepatic lipogenesis.

In addition, TNF-α damages the mitochondrial membrane enhancing the production of anion superoxide radicals and therefore reactive oxygen species (ROS) and triggering a vicious cycle since it has been proposed that ROS further promotes TNF-α synthesis through the activation of NF-kB transcription factor (*185*). Subsequently, mitochondria themselves become the target of ROS, thereby promoting, through the further impairment of the electron flow, the production of other radicals and inducing lipoperoxidation

of unsaturated lipids in hepatic fat deposits. ROS-induced lipoperoxidation and/or ROS-induced impairment of the elongation/desaturation pathway from linoleic acid (LA) to arachidonic acid (AA) (*195*), may explain the higher LA/AA ratio in the liver of *Pb*NK65-infected mice. The higher production of ROS in *Pb*NK65-infected mice was evidenced by the elevated MDA concentration present at day 8 and 10 post infection. MDA remained similar to CTR in *Pc*AS-infected mice. We studied also the enzymes involved in the antioxidant defence and we found that catalase activity in both parasite strains increased at day 8 post infection. With the progression of the pathology (10 days post infection) in *Pb*NK65 infected mice, the activity of the enzyme decreased becoming significantly lower than CTR.

A similar trend was observed for hepatic glutathione levels while SOD activity increases only at day 10 post infection in both parasite strains. GR and SOD are known to exert a protective role in minimizing oxidative stress, largely derived from the production of superoxide anion radicals. These findings suggest that the increase of ROS may initially trigger the elevation of the endogenous antioxidant defences that are later depleted due to the liver damage caused by the aggressive progression of the pathology.

Imbalances in the oxidative status of *Pb*NK65-infected livers may be involved in the progression of liver disease. In fact, it is known that the expression of transforming growth factor-β (TGF-β) is enhanced in ROS-activated macrophages (*192*). In turn, TGF-β plays a role in the recruitment of neutrophils and in the activation of hepatic stellate cells, which increase the secretion of type I collagen (*196*). This contributes to the development of hepatic fibrosis, as shown in *Pb*NK65-infected mice by the high hepatic levels of hydroxyproline. Submicroscopical signs of fibrosis, determinated by hydroxyproline quantification analyses, were evident not only in *Pb*NK65 infected mice but also, although at a lower level, in *Pc*AS group, starting

from day 8 post infection. Interestingly, at day 10 post infection the quantity of hydroxyproline decreased in both parasite strains, becoming similar to CTR mice. The hypothesis that inflammation may lead to the activation of metalloproteinase (MMPs) is under investigation. MMPs are proteolytic enzymes able to degrade different proteins of the extracellular matrix (e.g. collagen, laminin, fibronectin) and modulate cytokine and chemokine activity in a variety of physiological processes and pathological conditions such as inflammation. Van de Steen et al demonstrated, in the liver of C57Bl/6J mice infected with *Pb*NK65, a significant increase of the activity of MMPs (*197*). Furthermore several in vitro studies have shown an induction TNF-α dependent of MMPs mRNA and protein by monocytes fed with natural Hz (*198-200*).

6 CONCLUSIONS

We performed a comprehensive analyses of the lipid content and inflammatory response of different organs in a murine model of MA-ARDS.
Hypoxia, cytoadhesion and inflammation, all observed in the lung of our model, can deregulated or disrupt the alveola endothelial barrier resulting in extravasation of protein rich fluid characteristic of vascular hyper-permeability. Under normal circumstances, increases in vascular permeability result in leakage of protein rich fluid into perivascular spaces between the vasculature and the alveoli with subsequent fluid removal by the lymphatic system. However, when fluid filtration exceeds fluid removal, vasogenic oedema develops as is observed in both mice and patients with MA-ARDS (63,112).
The precise mediators responsible for this hyper-permeability state and the pathways by which molecules can cross the endothelial barrier under pathologic circumstances are heterogeneous and not well understood.
In our model we found an imbalance between immune mechanisms generated by the host and immune evasion mechanisms by the parasite, in particular there is an increase in the lung expression of several cytokines (TNF-α; IL-10; IFN-γ) and leukocyte and macrophages infiltrations. Since natural Hz has multiple effects on monocytes in vitro, and was localized insides monocytes and macrophages in lung, we investigated whether Hz might have a role in the pathogenesis of malaria complications. The symptoms of lung pathology are more severe in C57Bl/6J mice infected with the *Pb*NK65 strain which succumb from MA-ARDS. In particular cytokines and chemokines are increased in the lung of *Pb*NK65 infected mice and lipids of lung tissue and bronchoalveolar lavage fluid are qualitative and quantitative changed. At the same time in the liver of *Pb*NK65 infected mice are present high levels of Hz.

When we investigated Hz levels and disease parameters we found a strong correlation between Hz concentration and pulmonary or hepatic pathology. These results suggest that Hz might have a pathological role in these complications. Hz is not an inert crystal, due to the presence of multiple Fe3+ ions in the haemin components constituting the Hz crystals, and causes lipoperoxidation when interacting with membranes containing polyunsaturated fatty acids. The different lipoperoxidation products and reactive oxygen species (ROS) that are generated during this process may have opposite effects, since both inhibition of important monocyte functions (such as phagocitosis and antigen presentation), and the induction of pro-inflammatory cytokine expression, in particular TNF-α, through nuclear factor-κB (NF-Kb) activation (132, 200). TNF-α on the one hand damages mitochondrial membrane further enhancing the production of ROS, on the other one induces lipogenesis conducing to steatosis. Subsequently, mitochondria themselves become the target of ROS, thereby promoting, through the further impairment of the electron flow, the production of other radicals and inducing lipoperoxidation of unsaturated lipids in hepatic fat deposits.

We demonstrated a pulmonary-liver metabolic interplay in wich Hz is not merely a waste product of the metabolic activity of the parasite, but it is an important inflammatory virulence factor. The pathogenesis of the lung tissue injury, is related to the hepatic generation of the pro-inflammatory cytokine TNF-α. TNF-α, generated by liver, translocates to lung where it initiates a mediator cascade result in pulmonary neutrophil accumulation and ensuing lung injury.

Since inflammation plays an important role in different organs, may be worthwhile to test anti-inflammatory drugs in clinical trials in addition to anti-malaria drugs.

REFERENCES

1. White, N. J., Pukrittayakamee, S., Hien, T. T., Faiz, M. A., Mokuolu, O. A., and Dondorp, A. M. (2013) Malaria, *Lancet*.
2. Lang-Unnasch, N., and Murphy, A. D. (1998) Metabolic changes of the malaria parasite during the transition from the human to the mosquito host, *Annual review of microbiology 52*, 561-590.
3. Monti, D., Vodopivec, B., Basilico, N., Olliaro, P., and Taramelli, D. (1999) A novel endogenous antimalarial: Fe(II)-protoporphyrin IX alpha (heme) inhibits hematin polymerization to beta-hematin (malaria pigment) and kills malaria parasites, *Biochemistry 38*, 8858-8863.
4. Chou, A. C., and Fitch, C. D. (1981) Mechanism of hemolysis induced by ferriprotoporphyrin IX, *The Journal of clinical investigation 68*, 672-677.
5. Vincent, S. H. (1989) Oxidative effects of heme and porphyrins on proteins and lipids, *Seminars in hematology 26*, 105-113.
6. Omodeo-Sale, F., Monti, D., Olliaro, P., and Taramelli, D. (2001) Prooxidant activity of beta-hematin (synthetic malaria pigment) in arachidonic acid micelles and phospholipid large unilamellar vesicles, *Biochemical pharmacology 61*, 999-1009.
7. Slater, A. F., Swiggard, W. J., Orton, B. R., Flitter, W. D., Goldberg, D. E., Cerami, A., and Henderson, G. B. (1991) An iron-carboxylate bond links the heme units of malaria pigment, *Proceedings of the National Academy of Sciences of the United States of America 88*, 325-329.
8. Hempelmann, E., and Egan, T. J. (2002) Pigment biocrystallization in Plasmodium falciparum, *Trends in parasitology 18*, 11.

9. Kapishnikov, S., Weiner, A., Shimoni, E., Guttmann, P., Schneider, G., Dahan-Pasternak, N., Dzikowski, R., Leiserowitz, L., and Elbaum, M. Oriented nucleation of hemozoin at the digestive vacuole membrane in Plasmodium falciparum, *Proceedings of the National Academy of Sciences of the United States of America 109*, 11188-11193.
10. Pisciotta, J. M., Coppens, I., Tripathi, A. K., Scholl, P. F., Shuman, J., Bajad, S., Shulaev, V., and Sullivan, D. J., Jr. (2007) The role of neutral lipid nanospheres in Plasmodium falciparum haem crystallization, *The Biochemical journal 402*, 197-204.
11. Jani, D., Nagarkatti, R., Beatty, W., Angel, R., Slebodnick, C., Andersen, J., Kumar, S., and Rathore, D. (2008) HDP-a novel heme detoxification protein from the malaria parasite, *PLoS pathogens 4*, e1000053.
12. Omodeo-Sale, F., Motti, A., Dondorp, A., White, N. J., and Taramelli, D. (2005) Destabilisation and subsequent lysis of human erythrocytes induced by Plasmodium falciparum haem products, *European journal of haematology 74*, 324-332.
13. Weissbuch, I., and Leiserowitz, L. (2008) Interplay between malaria, crystalline hemozoin formation, and antimalarial drug action and design, *Chemical reviews 108*, 4899-4914.
14. Tekwani, B. L., and Walker, L. A. (2005) Targeting the hemozoin synthesis pathway for new antimalarial drug discovery: technologies for in vitro beta-hematin formation assay, *Combinatorial chemistry & high throughput screening 8*, 63-79.
15. Loup, C., Lelievre, J., Benoit-Vical, F., and Meunier, B. (2007) Trioxaquines and heme-artemisinin adducts inhibit the in vitro formation of hemozoin better than chloroquine, *Antimicrobial agents and chemotherapy 51*, 3768-3770.

16. Chugh, M., Sundararaman, V., Kumar, S., Reddy, V. S., Siddiqui, W. A., Stuart, K. D., and Malhotra, P. Protein complex directs hemoglobin-to-hemozoin formation in Plasmodium falciparum, *Proceedings of the National Academy of Sciences of the United States of America 110*, 5392-5397.
17. Munoz-Durango, K., Maciuk, A., Harfouche, A., Torijano-Gutierrez, S., Jullian, J. C., Quintin, J., Spelman, K., Mouray, E., Grellier, P., and Figadere, B. Detection, characterization, and screening of heme-binding molecules by mass spectrometry for malaria drug discovery, *Analytical chemistry 84*, 3324-3329.
18. Hanscheid, T., Valadas, E., and Grobusch, M. P. (2000) Automated malaria diagnosis using pigment detection, *Parasitology today (Personal ed 16*, 549-551.
19. Mens, P. F., Matelon, R. J., Nour, B. Y., Newman, D. M., and Schallig, H. D. Laboratory evaluation on the sensitivity and specificity of a novel and rapid detection method for malaria diagnosis based on magneto-optical technology (MOT), *Malaria journal 9*, 207.
20. Hanscheid, T., Langin, M., Lell, B., Potschke, M., Oyakhirome, S., Kremsner, P. G., and Grobusch, M. P. (2008) Full blood count and haemozoin-containing leukocytes in children with malaria: diagnostic value and association with disease severity, *Malaria journal 7*, 109.
21. Lyke, K. E., Diallo, D. A., Dicko, A., Kone, A., Coulibaly, D., Guindo, A., Cissoko, Y., Sangare, L., Coulibaly, S., Dakouo, B., Taylor, T. E., Doumbo, O. K., and Plowe, C. V. (2003) Association of intraleukocytic Plasmodium falciparum malaria pigment with disease severity, clinical manifestations, and prognosis in severe malaria, *The American journal of tropical medicine and hygiene 69*, 253-259.

22. Nguyen, P. H., Day, N., Pram, T. D., Ferguson, D. J., and White, N. J. (1995) Intraleucocytic malaria pigment and prognosis in severe malaria, *Transactions of the Royal Society of Tropical Medicine and Hygiene 89*, 200-204.
23. Hanscheid, T., Egan, T. J., and Grobusch, M. P. (2007) Haemozoin: from melatonin pigment to drug target, diagnostic tool, and immune modulator, *The Lancet infectious diseases 7*, 675-685.
24. Shio, M. T., Kassa, F. A., Bellemare, M. J., and Olivier, M. Innate inflammatory response to the malarial pigment hemozoin, *Microbes and infection / Institut Pasteur 12*, 889-899.
25. Were, T., Davenport, G. C., Yamo, E. O., Hittner, J. B., Awandare, G. A., Otieno, M. F., Ouma, C., Orago, A. S., Vulule, J. M., Ong'echa, J. M., and Perkins, D. J. (2009) Naturally acquired hemozoin by monocytes promotes suppression of RANTES in children with malarial anemia through an IL-10-dependent mechanism, *Microbes and infection / Institut Pasteur 11*, 811-819.
26. Awandare, G. A., Ouma, Y., Ouma, C., Were, T., Otieno, R., Keller, C. C., Davenport, G. C., Hittner, J. B., Vulule, J., Ferrell, R., Ong'echa, J. M., and Perkins, D. J. (2007) Role of monocyte-acquired hemozoin in suppression of macrophage migration inhibitory factor in children with severe malarial anemia, *Infection and immunity 75*, 201-210.
27. Davenport, G. C., Ouma, C., Hittner, J. B., Were, T., Ouma, Y., Ong'echa, J. M., and Perkins, D. J. Hematological predictors of increased severe anemia in Kenyan children coinfected with Plasmodium falciparum and HIV-1, *American journal of hematology 85*, 227-233.
28. Deroost, K., Tyberghein, A., Lays, N., Noppen, S., Schwarzer, E., Vanstreels, E., Komuta, M., Prato, M., Lin, J. W., Pamplona, A.,

Janse, C. J., Arese, P., Roskams, T., Daelemans, D., Opdenakker, G., and Van den Steen, P. E. Hemozoin induces lung inflammation and correlates with malaria-associated acute respiratory distress syndrome, *American journal of respiratory cell and molecular biology 48*, 589-600.

29. Coban, C., Yagi, M., Ohata, K., Igari, Y., Tsukui, T., Horii, T., Ishii, K. J., and Akira, S. The malarial metabolite hemozoin and its potential use as a vaccine adjuvant, *Allergol Int 59*, 115-124.
30. Parroche, P., Lauw, F. N., Goutagny, N., Latz, E., Monks, B. G., Visintin, A., Halmen, K. A., Lamphier, M., Olivier, M., Bartholomeu, D. C., Gazzinelli, R. T., and Golenbock, D. T. (2007) Malaria hemozoin is immunologically inert but radically enhances innate responses by presenting malaria DNA to Toll-like receptor 9, *Proceedings of the National Academy of Sciences of the United States of America 104*, 1919-1924.
31. Coban, C., Ishii, K. J., Kawai, T., Hemmi, H., Sato, S., Uematsu, S., Yamamoto, M., Takeuchi, O., Itagaki, S., Kumar, N., Horii, T., and Akira, S. (2005) Toll-like receptor 9 mediates innate immune activation by the malaria pigment hemozoin, *The Journal of experimental medicine 201*, 19-25.
32. Barrera, V., Skorokhod, O. A., Baci, D., Gremo, G., Arese, P., and Schwarzer, E. Host fibrinogen stably bound to hemozoin rapidly activates monocytes via TLR-4 and CD11b/CD18-integrin: a new paradigm of hemozoin action, *Blood 117*, 5674-5682.
33. Carney, C. K., Schrimpe, A. C., Halfpenny, K., Harry, R. S., Miller, C. M., Broncel, M., Sewell, S. L., Schaff, J. E., Deol, R., Carter, M. D., and Wright, D. W. (2006) The basis of the immunomodulatory activity of malaria pigment (hemozoin), *J Biol Inorg Chem 11*, 917-929.

34. Egan, T. J., Hempelmann, E., and Mavuso, W. W. (1999) Characterisation of synthetic beta-haematin and effects of the antimalarial drugs quinidine, halofantrine, desbutylhalofantrine and mefloquine on its formation, *Journal of inorganic biochemistry 73*, 101-107.
35. Scorza, T., Magez, S., Brys, L., and De Baetselier, P. (1999) Hemozoin is a key factor in the induction of malaria-associated immunosuppression, *Parasite immunology 21*, 545-554.
36. Skorokhod, O. A., Schwarzer, E., Ceretto, M., and Arese, P. (2007) Malarial pigment haemozoin, IFN-gamma, TNF-alpha, IL-1beta and LPS do not stimulate expression of inducible nitric oxide synthase and production of nitric oxide in immuno-purified human monocytes, *Malaria journal 6*, 73.
37. Jaramillo, M., Gowda, D. C., Radzioch, D., and Olivier, M. (2003) Hemozoin increases IFN-gamma-inducible macrophage nitric oxide generation through extracellular signal-regulated kinase- and NF-kappa B-dependent pathways, *J Immunol 171*, 4243-4253.
38. Coban, C., Ishii, K. J., Sullivan, D. J., and Kumar, N. (2002) Purified malaria pigment (hemozoin) enhances dendritic cell maturation and modulates the isotype of antibodies induced by a DNA vaccine, *Infection and immunity 70*, 3939-3943.
39. Williams, T. N. Balancing act: haemoglobinopathies and malaria, *The Lancet infectious diseases 12*, 427-428.
40. Cyrklaff, M., Sanchez, C. P., Kilian, N., Bisseye, C., Simpore, J., Frischknecht, F., and Lanzer, M. Hemoglobins S and C interfere with actin remodeling in Plasmodium falciparum-infected erythrocytes, *Science (New York, N.Y 334*, 1283-1286.
41. Cholera, R., Brittain, N. J., Gillrie, M. R., Lopera-Mesa, T. M., Diakite, S. A., Arie, T., Krause, M. A., Guindo, A., Tubman, A.,

Fujioka, H., Diallo, D. A., Doumbo, O. K., Ho, M., Wellems, T. E., and Fairhurst, R. M. (2008) Impaired cytoadherence of Plasmodium falciparum-infected erythrocytes containing sickle hemoglobin, *Proceedings of the National Academy of Sciences of the United States of America 105*, 991-996.

42. Taylor, S. M., Parobek, C. M., and Fairhurst, R. M. Haemoglobinopathies and the clinical epidemiology of malaria: a systematic review and meta-analysis, *The Lancet infectious diseases 12*, 457-468.
43. Cordery, D. V., and Urban, B. C. (2009) Immune recognition of Plasmodium-infected erythrocytes, *Advances in experimental medicine and biology 653*, 175-184.
44. Cooke, B., Coppel, R., and Wahlgren, M. (2000) Falciparum malaria: sticking up, standing out and out-standing, *Parasitology today (Personal ed 16*, 416-420.
45. Pain, A., Ferguson, D. J., Kai, O., Urban, B. C., Lowe, B., Marsh, K., and Roberts, D. J. (2001) Platelet-mediated clumping of Plasmodium falciparum-infected erythrocytes is a common adhesive phenotype and is associated with severe malaria, *Proceedings of the National Academy of Sciences of the United States of America 98*, 1805-1810.
46. Doumbo, O. K., Thera, M. A., Kone, A. K., Raza, A., Tempest, L. J., Lyke, K. E., Plowe, C. V., and Rowe, J. A. (2009) High levels of Plasmodium falciparum rosetting in all clinical forms of severe malaria in African children, *The American journal of tropical medicine and hygiene 81*, 987-993.
47. Pongponratn, E., Turner, G. D., Day, N. P., Phu, N. H., Simpson, J. A., Stepniewska, K., Mai, N. T., Viriyavejakul, P., Looareesuwan, S., Hien, T. T., Ferguson, D. J., and White, N. J. (2003) An

ultrastructural study of the brain in fatal Plasmodium falciparum malaria, *The American journal of tropical medicine and hygiene 69*, 345-359.

48. Simpson, J. A., Silamut, K., Chotivanich, K., Pukrittayakamee, S., and White, N. J. (1999) Red cell selectivity in malaria: a study of multiple-infected erythrocytes, *Transactions of the Royal Society of Tropical Medicine and Hygiene 93*, 165-168.
49. Looareesuwan, S., Ho, M., Wattanagoon, Y., White, N. J., Warrell, D. A., Bunnag, D., Harinasuta, T., and Wyler, D. J. (1987) Dynamic alteration in splenic function during acute falciparum malaria, *The New England journal of medicine 317*, 675-679.
50. Ayimba, E., Hegewald, J., Segbena, A. Y., Gantin, R. G., Lechner, C. J., Agosssou, A., Banla, M., and Soboslay, P. T. Proinflammatory and regulatory cytokines and chemokines in infants with uncomplicated and severe Plasmodium falciparum malaria, *Clinical and experimental immunology 166*, 218-226.
51. Karunaweera, N. D., Grau, G. E., Gamage, P., Carter, R., and Mendis, K. N. (1992) Dynamics of fever and serum levels of tumor necrosis factor are closely associated during clinical paroxysms in Plasmodium vivax malaria, *Proceedings of the National Academy of Sciences of the United States of America 89*, 3200-3203.
52. Simpson, J. A., Aarons, L., Collins, W. E., Jeffery, G. M., and White, N. J. (2002) Population dynamics of untreated Plasmodium falciparum malaria within the adult human host during the expansion phase of the infection, *Parasitology 124*, 247-263.
53. Dondorp, A. M., Lee, S. J., Faiz, M. A., Mishra, S., Price, R., Tjitra, E., Than, M., Htut, Y., Mohanty, S., Yunus, E. B., Rahman, R., Nosten, F., Anstey, N. M., Day, N. P., and White, N. J. (2008) The

relationship between age and the manifestations of and mortality associated with severe malaria, *Clin Infect Dis 47*, 151-157.

54. White, N. J., Turner, G. D., Day, N. P., and Dondorp, A. M. Lethal malaria: Marchiafava and Bignami were right, *The Journal of infectious diseases 208*, 192-198.

55. Silamut, K., Phu, N. H., Whitty, C., Turner, G. D., Louwrier, K., Mai, N. T., Simpson, J. A., Hien, T. T., and White, N. J. (1999) A quantitative analysis of the microvascular sequestration of malaria parasites in the human brain, *The American journal of pathology 155*, 395-410.

56. Day, N. P., Phu, N. H., Mai, N. T., Chau, T. T., Loc, P. P., Chuong, L. V., Sinh, D. X., Holloway, P., Hien, T. T., and White, N. J. (2000) The pathophysiologic and prognostic significance of acidosis in severe adult malaria, *Critical care medicine 28*, 1833-1840.

57. MacPherson, G. G., Warrell, M. J., White, N. J., Looareesuwan, S., and Warrell, D. A. (1985) Human cerebral malaria. A quantitative ultrastructural analysis of parasitized erythrocyte sequestration, *The American journal of pathology 119*, 385-401.

58. Medana, I. M., and Turner, G. D. (2007) Plasmodium falciparum and the blood-brain barrier--contacts and consequences, *The Journal of infectious diseases 195*, 921-923.

59. Warrell, D. A., Looareesuwan, S., Phillips, R. E., White, N. J., Warrell, M. J., Chapel, H. M., Areekul, S., and Tharavanij, S. (1986) Function of the blood-cerebrospinal fluid barrier in human cerebral malaria: rejection of the permeability hypothesis, *The American journal of tropical medicine and hygiene 35*, 882-889.

60. Calis, J. C., Phiri, K. S., Faragher, E. B., Brabin, B. J., Bates, I., Cuevas, L. E., de Haan, R. J., Phiri, A. I., Malange, P., Khoka, M., Hulshof, P. J., van Lieshout, L., Beld, M. G., Teo, Y. Y., Rockett, K.

A., Richardson, A., Kwiatkowski, D. P., Molyneux, M. E., and van Hensbroek, M. B. (2008) Severe anemia in Malawian children, *The New England journal of medicine 358*, 888-899.

61. Buffet, P. A., Safeukui, I., Deplaine, G., Brousse, V., Prendki, V., Thellier, M., Turner, G. D., and Mercereau-Puijalon, O. The pathogenesis of Plasmodium falciparum malaria in humans: insights from splenic physiology, *Blood 117*, 381-392.
62. Price, R. N., Simpson, J. A., Nosten, F., Luxemburger, C., Hkirjaroen, L., ter Kuile, F., Chongsuphajaisiddhi, T., and White, N. J. (2001) Factors contributing to anemia after uncomplicated falciparum malaria, *The American journal of tropical medicine and hygiene 65*, 614-622.
63. Anstey, N. M., Handojo, T., Pain, M. C., Kenangalem, E., Tjitra, E., Price, R. N., and Maguire, G. P. (2007) Lung injury in vivax malaria: pathophysiological evidence for pulmonary vascular sequestration and posttreatment alveolar-capillary inflammation, *The Journal of infectious diseases 195*, 589-596.
64. Daneshvar, C., Davis, T. M., Cox-Singh, J., Rafa'ee, M. Z., Zakaria, S. K., Divis, P. C., and Singh, B. (2009) Clinical and laboratory features of human Plasmodium knowlesi infection, *Clin Infect Dis 49*, 852-860.
65. Taylor, W. R., Hanson, J., Turner, G. D., White, N. J., and Dondorp, A. M. Respiratory manifestations of malaria, *Chest 142*, 492-505.
66. Hanson, J. P., Lam, S. W., Mohanty, S., Alam, S., Pattnaik, R., Mahanta, K. C., Hasan, M. U., Charunwatthana, P., Mishra, S. K., Day, N. P., White, N. J., and Dondorp, A. M. Fluid resuscitation of adults with severe falciparum malaria: effects on Acid-base status, renal function, and extravascular lung water, *Critical care medicine 41*, 972-981.

67. Nguansangiam, S., Day, N. P., Hien, T. T., Mai, N. T., Chaisri, U., Riganti, M., Dondorp, A. M., Lee, S. J., Phu, N. H., Turner, G. D., White, N. J., Ferguson, D. J., and Pongponratn, E. (2007) A quantitative ultrastructural study of renal pathology in fatal Plasmodium falciparum malaria, *Trop Med Int Health 12*, 1037-1050.

68. Trang, T. T., Phu, N. H., Vinh, H., Hien, T. T., Cuong, B. M., Chau, T. T., Mai, N. T., Waller, D. J., and White, N. J. (1992) Acute renal failure in patients with severe falciparum malaria, *Clin Infect Dis 15*, 874-880.

69. Phu, N. H., Hien, T. T., Mai, N. T., Chau, T. T., Chuong, L. V., Loc, P. P., Winearls, C., Farrar, J., White, N., and Day, N. (2002) Hemofiltration and peritoneal dialysis in infection-associated acute renal failure in Vietnam, *The New England journal of medicine 347*, 895-902.

70. Desai, M., ter Kuile, F. O., Nosten, F., McGready, R., Asamoa, K., Brabin, B., and Newman, R. D. (2007) Epidemiology and burden of malaria in pregnancy, *The Lancet infectious diseases 7*, 93-104.

71. Falade, C., Mokuolu, O., Okafor, H., Orogade, A., Falade, A., Adedoyin, O., Oguonu, T., Aisha, M., Hamer, D. H., and Callahan, M. V. (2007) Epidemiology of congenital malaria in Nigeria: a multi-centre study, *Trop Med Int Health 12*, 1279-1287.

72. Steketee, R. W., Nahlen, B. L., Parise, M. E., and Menendez, C. (2001) The burden of malaria in pregnancy in malaria-endemic areas, *The American journal of tropical medicine and hygiene 64*, 28-35.

73. Bardaji, A., Sigauque, B., Sanz, S., Maixenchs, M., Ordi, J., Aponte, J. J., Mabunda, S., Alonso, P. L., and Menendez, C. Impact of

malaria at the end of pregnancy on infant mortality and morbidity, *The Journal of infectious diseases 203*, 691-699.

74. Rijken, M. J., McGready, R., Boel, M. E., Poespoprodjo, R., Singh, N., Syafruddin, D., Rogerson, S., and Nosten, F. Malaria in pregnancy in the Asia-Pacific region, *The Lancet infectious diseases 12*, 75-88.

75. McGready, R., Lee, S. J., Wiladphaingern, J., Ashley, E. A., Rijken, M. J., Boel, M., Simpson, J. A., Paw, M. K., Pimanpanarak, M., Mu, O., Singhasivanon, P., White, N. J., and Nosten, F. H. Adverse effects of falciparum and vivax malaria and the safety of antimalarial treatment in early pregnancy: a population-based study, *The Lancet infectious diseases 12*, 388-396.

76. Agnandji, S. T., Lell, B., Soulanoudjingar, S. S., Fernandes, J. F., Abossolo, B. P., Conzelmann, C., Methogo, B. G., Doucka, Y., Flamen, A., Mordmuller, B., Issifou, S., Kremsner, P. G., Sacarlal, J., Aide, P., Lanaspa, M., Aponte, J. J., Nhamuave, A., Quelhas, D., Bassat, Q., Mandjate, S., Macete, E., Alonso, P., Abdulla, S., Salim, N., Juma, O., Shomari, M., Shubis, K., Machera, F., Hamad, A. S., Minja, R., Mtoro, A., Sykes, A., Ahmed, S., Urassa, A. M., Ali, A. M., Mwangoka, G., Tanner, M., Tinto, H., D'Alessandro, U., Sorgho, H., Valea, I., Tahita, M. C., Kabore, W., Ouedraogo, S., Sandrine, Y., Guiguemde, R. T., Ouedraogo, J. B., Hamel, M. J., Kariuki, S., Odero, C., Oneko, M., Otieno, K., Awino, N., Omoto, J., Williamson, J., Muturi-Kioi, V., Laserson, K. F., Slutsker, L., Otieno, W., Otieno, L., Nekoye, O., Gondi, S., Otieno, A., Ogutu, B., Wasuna, R., Owira, V., Jones, D., Onyango, A. A., Njuguna, P., Chilengi, R., Akoo, P., Kerubo, C., Gitaka, J., Maingi, C., Lang, T., Olotu, A., Tsofa, B., Bejon, P., Peshu, N., Marsh, K., Owusu-Agyei, S., Asante, K. P., Osei-Kwakye, K., Boahen, O., Ayamba, S., Kayan, K., Owusu-Ofori,

R., Dosoo, D., Asante, I., Adjei, G., Adjei, G., Chandramohan, D., Greenwood, B., Lusingu, J., Gesase, S., Malabeja, A., Abdul, O., Kilavo, H., Mahende, C., Liheluka, E., Lemnge, M., Theander, T., Drakeley, C., Ansong, D., Agbenyega, T., Adjei, S., Boateng, H. O., Rettig, T., Bawa, J., Sylverken, J., Sambian, D., Agyekum, A., Owusu, L., Martinson, F., Hoffman, I., Mvalo, T., Kamthunzi, P., Nkomo, R., Msika, A., Jumbe, A., Chome, N., Nyakuipa, D., Chintedza, J., Ballou, W. R., Bruls, M., Cohen, J., Guerra, Y., Jongert, E., Lapierre, D., Leach, A., Lievens, M., Ofori-Anyinam, O., Vekemans, J., Carter, T., Leboulleux, D., Loucq, C., Radford, A., Savarese, B., Schellenberg, D., Sillman, M., and Vansadia, P. First results of phase 3 trial of RTS,S/AS01 malaria vaccine in African children, *The New England journal of medicine 365*, 1863-1875.

77. Phillips-Howard, P. A., Nahlen, B. L., Kolczak, M. S., Hightower, A. W., ter Kuile, F. O., Alaii, J. A., Gimnig, J. E., Arudo, J., Vulule, J. M., Odhacha, A., Kachur, S. P., Schoute, E., Rosen, D. H., Sexton, J. D., Oloo, A. J., and Hawley, W. A. (2003) Efficacy of permethrin-treated bed nets in the prevention of mortality in young children in an area of high perennial malaria transmission in western Kenya, *The American journal of tropical medicine and hygiene 68*, 23-29.

78. Moonen, B., Cohen, J. M., Snow, R. W., Slutsker, L., Drakeley, C., Smith, D. L., Abeyasinghe, R. R., Rodriguez, M. H., Maharaj, R., Tanner, M., and Targett, G. Operational strategies to achieve and maintain malaria elimination, *Lancet 376*, 1592-1603.

79. Godfray, H. C. Mosquito ecology and control of malaria, *The Journal of animal ecology 82*, 15-25.

80. Barnes, K. I., Durrheim, D. N., Little, F., Jackson, A., Mehta, U., Allen, E., Dlamini, S. S., Tsoka, J., Bredenkamp, B., Mthembu, D. J., White, N. J., and Sharp, B. L. (2005) Effect of artemether-

lumefantrine policy and improved vector control on malaria burden in KwaZulu-Natal, South Africa, *PLoS medicine 2*, e330.

81. Enayati, A., and Hemingway, J. Malaria management: past, present, and future, *Annual review of entomology 55*, 569-591.
82. Pluess, B., Tanser, F. C., Lengeler, C., and Sharp, B. L. Indoor residual spraying for preventing malaria, *The Cochrane database of systematic reviews*, CD006657.
83. Aneck-Hahn, N. H., Schulenburg, G. W., Bornman, M. S., Farias, P., and de Jager, C. (2007) Impaired semen quality associated with environmental DDT exposure in young men living in a malaria area in the Limpopo Province, South Africa, *Journal of andrology 28*, 423-434.
84. van den Berg, H. (2009) Global status of DDT and its alternatives for use in vector control to prevent disease, *Environmental health perspectives 117*, 1656-1663.
85. Chen, L. H., Wilson, M. E., and Schlagenhauf, P. (2006) Prevention of malaria in long-term travelers, *Jama 296*, 2234-2244.
86. Schlagenhauf, P., Blumentals, W. A., Suter, P., Regep, L., Vital-Durand, G., Schaerer, M. T., Boutros, M. S., Rhein, H. G., and Adamcova, M. Pregnancy and fetal outcomes after exposure to mefloquine in the pre- and periconception period and during pregnancy, *Clin Infect Dis 54*, e124-131.
87. Clarke, S. E., Jukes, M. C., Njagi, J. K., Khasakhala, L., Cundill, B., Otido, J., Crudder, C., Estambale, B. B., and Brooker, S. (2008) Effect of intermittent preventive treatment of malaria on health and education in schoolchildren: a cluster-randomised, double-blind, placebo-controlled trial, *Lancet 372*, 127-138.

88. von Seidlein, L., and Greenwood, B. M. (2003) Mass administrations of antimalarial drugs, *Trends in parasitology 19*, 452-460.

89. Dondorp, A. M., Fanello, C. I., Hendriksen, I. C., Gomes, E., Seni, A., Chhaganlal, K. D., Bojang, K., Olaosebikan, R., Anunobi, N., Maitland, K., Kivaya, E., Agbenyega, T., Nguah, S. B., Evans, J., Gesase, S., Kahabuka, C., Mtove, G., Nadjm, B., Deen, J., Mwanga-Amumpaire, J., Nansumba, M., Karema, C., Umulisa, N., Uwimana, A., Mokuolu, O. A., Adedoyin, O. T., Johnson, W. B., Tshefu, A. K., Onyamboko, M. A., Sakulthaew, T., Ngum, W. P., Silamut, K., Stepniewska, K., Woodrow, C. J., Bethell, D., Wills, B., Oneko, M., Peto, T. E., von Seidlein, L., Day, N. P., and White, N. J. Artesunate versus quinine in the treatment of severe falciparum malaria in African children (AQUAMAT): an open-label, randomised trial, *Lancet 376*, 1647-1657.

90. Kreeftmeijer-Vegter, A. R., van Genderen, P. J., Visser, L. G., Bierman, W. F., Clerinx, J., van Veldhuizen, C. K., and de Vries, P. J. Treatment outcome of intravenous artesunate in patients with severe malaria in the Netherlands and Belgium, *Malaria journal 11*, 102.

91. Gomes, M. F., Faiz, M. A., Gyapong, J. O., Warsame, M., Agbenyega, T., Babiker, A., Baiden, F., Yunus, E. B., Binka, F., Clerk, C., Folb, P., Hassan, R., Hossain, M. A., Kimbute, O., Kitua, A., Krishna, S., Makasi, C., Mensah, N., Mrango, Z., Olliaro, P., Peto, R., Peto, T. J., Rahman, M. R., Ribeiro, I., Samad, R., and White, N. J. (2009) Pre-referral rectal artesunate to prevent death and disability in severe malaria: a placebo-controlled trial, *Lancet 373*, 557-566.

92. Crawley, J., Waruiru, C., Mithwani, S., Mwangi, I., Watkins, W., Ouma, D., Winstanley, P., Peto, T., and Marsh, K. (2000) Effect of phenobarbital on seizure frequency and mortality in childhood cerebral malaria: a randomised, controlled intervention study, *Lancet 355*, 701-706.

93. Maitland, K., Kiguli, S., Opoka, R. O., Engoru, C., Olupot-Olupot, P., Akech, S. O., Nyeko, R., Mtove, G., Reyburn, H., Lang, T., Brent, B., Evans, J. A., Tibenderana, J. K., Crawley, J., Russell, E. C., Levin, M., Babiker, A. G., and Gibb, D. M. Mortality after fluid bolus in African children with severe infection, *The New England journal of medicine 364*, 2483-2495.

94. Maude, R. J., Hoque, G., Hasan, M. U., Sayeed, A., Akter, S., Samad, R., Alam, B., Yunus, E. B., Rahman, R., Rahman, W., Chowdhury, R., Seal, T., Charunwatthana, P., Chang, C. C., White, N. J., Faiz, M. A., Day, N. P., Dondorp, A. M., and Hossain, A. Timing of enteral feeding in cerebral malaria in resource-poor settings: a randomized trial, *PloS one 6*, e27273.

95. Farnert, A., Gwer, S., and Berkley, J. A. Clinical considerations for antibiotic choices in the treatment of severe malaria, *Trends in parasitology 26*, 465-466.

96. Dondorp, A. M., Nosten, F., Yi, P., Das, D., Phyo, A. P., Tarning, J., Lwin, K. M., Ariey, F., Hanpithakpong, W., Lee, S. J., Ringwald, P., Silamut, K., Imwong, M., Chotivanich, K., Lim, P., Herdman, T., An, S. S., Yeung, S., Singhasivanon, P., Day, N. P., Lindegardh, N., Socheat, D., and White, N. J. (2009) Artemisinin resistance in Plasmodium falciparum malaria, *The New England journal of medicine 361*, 455-467.

97. Phyo, A. P., Nkhoma, S., Stepniewska, K., Ashley, E. A., Nair, S., McGready, R., Ier Moo, C., Al-Saai, S., Dondorp, A. M., Lwin, K. M.,

Singhasivanon, P., Day, N. P., White, N. J., Anderson, T. J., and Nosten, F. Emergence of artemisinin-resistant malaria on the western border of Thailand: a longitudinal study, *Lancet 379*, 1960-1966.

98. Baer, K., Klotz, C., Kappe, S. H., Schnieder, T., and Frevert, U. (2007) Release of hepatic Plasmodium yoelii merozoites into the pulmonary microvasculature, *PLoS pathogens 3*, e171.

99. Frevert, U., Nacer, A., Cabrera, M., Movila, A., and Leberl, M. Imaging Plasmodium immunobiology in the liver, brain, and lung, *Parasitology international*.

100. Luxemburger, C., Nosten, F., Kyle, D. E., Kiricharoen, L., Chongsuphajaisiddhi, T., and White, N. J. (1998) Clinical features cannot predict a diagnosis of malaria or differentiate the infecting species in children living in an area of low transmission, *Transactions of the Royal Society of Tropical Medicine and Hygiene 92*, 45-49.

101. Anstey, N. M., Jacups, S. P., Cain, T., Pearson, T., Ziesing, P. J., Fisher, D. A., Currie, B. J., Marks, P. J., and Maguire, G. P. (2002) Pulmonary manifestations of uncomplicated falciparum and vivax malaria: cough, small airways obstruction, impaired gas transfer, and increased pulmonary phagocytic activity, *The Journal of infectious diseases 185*, 1326-1334.

102. Hovette, P., Touze, J. E., and Laroche, R. (1990) [Pulmonary manifestations of malaria], *Bulletin de la Societe de pathologie exotique (1990) 83*, 479-486.

103. Maguire, G. P., Handojo, T., Pain, M. C., Kenangalem, E., Price, R. N., Tjitra, E., and Anstey, N. M. (2005) Lung injury in uncomplicated and severe falciparum malaria: a longitudinal study in papua, Indonesia, *The Journal of infectious diseases 192*, 1966-1974.

104. Nayak, K. C., Mohini, Kumar, S., Tanwar, R. S., Kulkarni, V., Gupta, A., Sharma, P., Sirohi, P., and Ratan, P. A study on pulmonary manifestations in patients with malaria from northwestern India (Bikaner), *Journal of vector borne diseases 48*, 219-223.

105. Van den Steen, P. E., Deroost, K., Deckers, J., Van Herck, E., Struyf, S., and Opdenakker, G. Pathogenesis of malaria-associated acute respiratory distress syndrome, *Trends in parasitology 29*, 346-358.

106. English, M., Muambi, B., Mithwani, S., and Marsh, K. (1997) Lactic acidosis and oxygen debt in African children with severe anaemia, *Qjm 90*, 563-569.

107. Krishna, S., Waller, D. W., ter Kuile, F., Kwiatkowski, D., Crawley, J., Craddock, C. F., Nosten, F., Chapman, D., Brewster, D., Holloway, P. A., and et al. (1994) Lactic acidosis and hypoglycaemia in children with severe malaria: pathophysiological and prognostic significance, *Transactions of the Royal Society of Tropical Medicine and Hygiene 88*, 67-73.

108. Zolg, J. W., Macleod, A. J., Scaife, J. G., and Beaudoin, R. L. (1984) The accumulation of lactic acid and its influence on the growth of Plasmodium falciparum in synchronized cultures, *In vitro 20*, 205-215.

109. Marsh, K., Forster, D., Waruiru, C., Mwangi, I., Winstanley, M., Marsh, V., Newton, C., Winstanley, P., Warn, P., Peshu, N., and et al. (1995) Indicators of life-threatening malaria in African children, *The New England journal of medicine 332*, 1399-1404.

110. English, M., Waruiru, C., Amukoye, E., Murphy, S., Crawley, J., Mwangi, I., Peshu, N., and Marsh, K. (1996) Deep breathing in children with severe malaria: indicator of metabolic acidosis and

poor outcome, *The American journal of tropical medicine and hygiene 55*, 521-524.

111. Krishnan, A., and Karnad, D. R. (2003) Severe falciparum malaria: an important cause of multiple organ failure in Indian intensive care unit patients, *Critical care medicine 31*, 2278-2284.

112. Mohan, A., Sharma, S. K., and Bollineni, S. (2008) Acute lung injury and acute respiratory distress syndrome in malaria, *Journal of vector borne diseases 45*, 179-193.

113. Taylor, W. R., Canon, V., and White, N. J. (2006) Pulmonary manifestations of malaria : recognition and management, *Treatments in respiratory medicine 5*, 419-428.

114. Taylor, W. R., and White, N. J. (2002) Malaria and the lung, *Clinics in chest medicine 23*, 457-468.

115. Cox-Singh, J., Hiu, J., Lucas, S. B., Divis, P. C., Zulkarnaen, M., Chandran, P., Wong, K. T., Adem, P., Zaki, S. R., Singh, B., and Krishna, S. Severe malaria - a case of fatal Plasmodium knowlesi infection with post-mortem findings: a case report, *Malaria journal 9*, 10.

116. Day, N. P., Hien, T. T., Schollaardt, T., Loc, P. P., Chuong, L. V., Chau, T. T., Mai, N. T., Phu, N. H., Sinh, D. X., White, N. J., and Ho, M. (1999) The prognostic and pathophysiologic role of pro- and antiinflammatory cytokines in severe malaria, *The Journal of infectious diseases 180*, 1288-1297.

117. Yeo, T. W., Lampah, D. A., Gitawati, R., Tjitra, E., Kenangalem, E., McNeil, Y. R., Darcy, C. J., Granger, D. L., Weinberg, J. B., Lopansri, B. K., Price, R. N., Duffull, S. B., Celermajer, D. S., and Anstey, N. M. (2007) Impaired nitric oxide bioavailability and L-arginine reversible endothelial dysfunction in adults with falciparum malaria, *The Journal of experimental medicine 204*, 2693-2704.

118. Zwissler, B., Kemming, G., Habler, O., Kleen, M., Merkel, M., Haller, M., Briegel, J., Welte, M., and Peter, K. (1996) Inhaled prostacyclin (PGI2) versus inhaled nitric oxide in adult respiratory distress syndrome, *American journal of respiratory and critical care medicine 154*, 1671-1677.

119. Yeo, T. W., Lampah, D. A., Tjitra, E., Gitawati, R., Darcy, C. J., Jones, C., Kenangalem, E., McNeil, Y. R., Granger, D. L., Lopansri, B. K., Weinberg, J. B., Price, R. N., Duffull, S. B., Celermajer, D. S., and Anstey, N. M. Increased asymmetric dimethylarginine in severe falciparum malaria: association with impaired nitric oxide bioavailability and fatal outcome, *PLoS pathogens 6*, e1000868.

120. Epiphanio, S., Campos, M. G., Pamplona, A., Carapau, D., Pena, A. C., Ataide, R., Monteiro, C. A., Felix, N., Costa-Silva, A., Marinho, C. R., Dias, S., and Mota, M. M. VEGF promotes malaria-associated acute lung injury in mice, *PLoS pathogens 6*, e1000916.

121. Davis, J. S., Yeo, T. W., Piera, K. A., Woodberry, T., Celermajer, D. S., Stephens, D. P., and Anstey, N. M. Angiopoietin-2 is increased in sepsis and inversely associated with nitric oxide-dependent microvascular reactivity, *Critical care (London, England) 14*, R89.

122. Jain, V., Armah, H. B., Tongren, J. E., Ned, R. M., Wilson, N. O., Crawford, S., Joel, P. K., Singh, M. P., Nagpal, A. C., Dash, A. P., Udhayakumar, V., Singh, N., and Stiles, J. K. (2008) Plasma IP-10, apoptotic and angiogenic factors associated with fatal cerebral malaria in India, *Malaria journal 7*, 83.

123. Maniatis, N. A., Kotanidou, A., Catravas, J. D., and Orfanos, S. E. (2008) Endothelial pathomechanisms in acute lung injury, *Vascular pharmacology 49*, 119-133.

124. Valecha, N., Pinto, R. G., Turner, G. D., Kumar, A., Rodrigues, S., Dubhashi, N. G., Rodrigues, E., Banaulikar, S. S., Singh, R., Dash,

A. P., and Baird, J. K. (2009) Histopathology of fatal respiratory distress caused by Plasmodium vivax malaria, *The American journal of tropical medicine and hygiene 81*, 758-762.

125. Rogerson, S. J., Grau, G. E., and Hunt, N. H. (2004) The microcirculation in severe malaria, *Microcirculation 11*, 559-576.
126. Roberts, A., Deming, D., Paddock, C. D., Cheng, A., Yount, B., Vogel, L., Herman, B. D., Sheahan, T., Heise, M., Genrich, G. L., Zaki, S. R., Baric, R., and Subbarao, K. (2007) A mouse-adapted SARS-coronavirus causes disease and mortality in BALB/c mice, *PLoS pathogens 3*, e5.
127. Serghides, L., Smith, T. G., Patel, S. N., and Kain, K. C. (2003) CD36 and malaria: friends or foes?, *Trends in parasitology 19*, 461-469.
128. Mura, M., dos Santos, C. C., Stewart, D., and Liu, M. (2004) Vascular endothelial growth factor and related molecules in acute lung injury, *J Appl Physiol (1985) 97*, 1605-1617.
129. Eisenhut, M. (2006) Changes in renal sodium transport during a systemic inflammatory response, *Pediatric nephrology (Berlin, Germany) 21*, 1487-1488; author reply 1489.
130. Van den Steen, P. E., Geurts, N., Deroost, K., Van Aelst, I., Verhenne, S., Heremans, H., Van Damme, J., and Opdenakker, G. Immunopathology and dexamethasone therapy in a new model for malaria-associated acute respiratory distress syndrome, *Am J Respir Crit Care Med 181*, 957-968.
131. Deroost, K., Tyberghein, A., Lays, N., Noppen, S., Schwarzer, E., Vanstreels, E., Komuta, M., Prato, M., Lin, J. W., Pamplona, A., Janse, C. J., Arese, P., Roskams, T., Daelemans, D., Opdenakker, G., and Van den Steen, P. E. Hemozoin Induces Lung Inflammation

and Correlates with Malaria-Associated Acute Respiratory Distress Syndrome, *Am J Respir Cell Mol Biol*.

132. Polimeni, M., Valente, E., Aldieri, E., Khadjavi, A., Giribaldi, G., and Prato, M. Haemozoin induces early cytokine-mediated lysozyme release from human monocytes through p38 MAPK- and NF-kappaB-dependent mechanisms, *PloS one 7*, e39497.
133. Lovegrove, F. E., Gharib, S. A., Pena-Castillo, L., Patel, S. N., Ruzinski, J. T., Hughes, T. R., Liles, W. C., and Kain, K. C. (2008) Parasite burden and CD36-mediated sequestration are determinants of acute lung injury in an experimental malaria model, *PLoS pathogens 4*, e1000068.
134. Senaldi, G., Vesin, C., Chang, R., Grau, G. E., and Piguet, P. F. (1994) Role of polymorphonuclear neutrophil leukocytes and their integrin CD11a (LFA-1) in the pathogenesis of severe murine malaria, *Infection and immunity 62*, 1144-1149.
135. Carvalho, L. J., Lenzi, H. L., Pelajo-Machado, M., Oliveira, D. N., Daniel-Ribeiro, C. T., and Ferreira-da-Cruz, M. F. (2000) Plasmodium berghei: cerebral malaria in CBA mice is not clearly related to plasma TNF levels or intensity of histopathological changes, *Experimental parasitology 95*, 1-7.
136. Hee, L., Dinudom, A., Mitchell, A. J., Grau, G. E., Cook, D. I., Hunt, N. H., and Ball, H. J. Reduced activity of the epithelial sodium channel in malaria-induced pulmonary oedema in mice, *International journal for parasitology 41*, 81-88.
137. Schofield, L., and Grau, G. E. (2005) Immunological processes in malaria pathogenesis, *Nature reviews 5*, 722-735.
138. Andrade Junior, H. F., Corbett, C. E., Laurenti, M. D., and Duarte, M. I. (1991) Comparative and sequential histopathology of Plasmodium chabaudi-infected Balb/c mice, *Brazilian journal of*

medical and biological research = Revista brasileira de pesquisas medicas e biologicas / Sociedade Brasileira de Biofisica ... [et al 24, 1209-1218.

139. Briel, M., Meade, M., Mercat, A., Brower, R. G., Talmor, D., Walter, S. D., Slutsky, A. S., Pullenayegum, E., Zhou, Q., Cook, D., Brochard, L., Richard, J. C., Lamontagne, F., Bhatnagar, N., Stewart, T. E., and Guyatt, G. Higher vs lower positive end-expiratory pressure in patients with acute lung injury and acute respiratory distress syndrome: systematic review and meta-analysis, *Jama 303*, 865-873.

140. Lamontagne, F., Briel, M., Guyatt, G. H., Cook, D. J., Bhatnagar, N., and Meade, M. Corticosteroid therapy for acute lung injury, acute respiratory distress syndrome, and severe pneumonia: a meta-analysis of randomized controlled trials, *Journal of critical care 25*, 420-435.

141. Putensen, C., Theuerkauf, N., Zinserling, J., Wrigge, H., and Pelosi, P. (2009) Meta-analysis: ventilation strategies and outcomes of the acute respiratory distress syndrome and acute lung injury, *Annals of internal medicine 151*, 566-576.

142. Dellinger, R. P., Levy, M. M., Carlet, J. M., Bion, J., Parker, M. M., Jaeschke, R., Reinhart, K., Angus, D. C., Brun-Buisson, C., Beale, R., Calandra, T., Dhainaut, J. F., Gerlach, H., Harvey, M., Marini, J. J., Marshall, J., Ranieri, M., Ramsay, G., Sevransky, J., Thompson, B. T., Townsend, S., Vender, J. S., Zimmerman, J. L., and Vincent, J. L. (2008) Surviving Sepsis Campaign: international guidelines for management of severe sepsis and septic shock: 2008, *Critical care medicine 36*, 296-327.

143. Cordeiro, R. S., Assreuy Filho, J., Flores, C. A., Cunha, F. Q., Martins, M. A., and Vasconcelos, H. N. (1984) Pulmonary edema in

mice infected with Plasmodium berghei. Involvement of catecholamines, *Experientia 40*, 301-302.

144. Pena, A. C., Penacho, N., Mancio-Silva, L., Neres, R., Seixas, J. D., Fernandes, A. C., Romao, C. C., Mota, M. M., Bernardes, G. J., and Pamplona, A. A novel carbon monoxide-releasing molecule fully protects mice from severe malaria, *Antimicrobial agents and chemotherapy 56*, 1281-1290.

145. Cordeiro, R. S., Cunha, F. Q., Filho, J. A., Flores, C. A., Vasconcelos, H. N., and Martins, M. A. (1983) Plasmodium berghei: physiopathological changes during infections in mice, *Annals of tropical medicine and parasitology 77*, 455-465.

146. Piguet, P. F., Kan, C. D., Vesin, C., Rochat, A., Donati, Y., and Barazzone, C. (2001) Role of CD40-CVD40L in mouse severe malaria, *The American journal of pathology 159*, 733-742.

147. Togbe, D., Schofield, L., Grau, G. E., Schnyder, B., Boissay, V., Charron, S., Rose, S., Beutler, B., Quesniaux, V. F., and Ryffel, B. (2007) Murine cerebral malaria development is independent of toll-like receptor signaling, *The American journal of pathology 170*, 1640-1648.

148. Greenwood, B. M., Fidock, D. A., Kyle, D. E., Kappe, S. H., Alonso, P. L., Collins, F. H., and Duffy, P. E. (2008) Malaria: progress, perils, and prospects for eradication, *J Clin Invest 118*, 1266-1276.

149. Srivastava, A., Khanduri, A., Lakhtakia, S., Pandey, R., and Choudhuri, G. (1996) Falciparum malaria with acute liver failure, *Trop Gastroenterol 17*, 172-174.

150. Dey, S., Guha, M., Alam, A., Goyal, M., Bindu, S., Pal, C., Maity, P., Mitra, K., and Bandyopadhyay, U. (2009) Malarial infection develops mitochondrial pathology and mitochondrial oxidative stress to promote hepatocyte apoptosis, *Free Radic Biol Med 46*, 271-281.

151. Rodriguez-Acosta, A., Finol, H. J., Pulido-Mendez, M., Marquez, A., Andrade, G., Gonzalez, N., Aguilar, I., Giron, M. E., and Pinto, A. (1998) Liver ultrastructural pathology in mice infected with Plasmodium berghei, *J Submicrosc Cytol Pathol 30*, 299-307.
152. Davidson, B. A., Knight, P. R., Wang, Z., Chess, P. R., Holm, B. A., Russo, T. A., Hutson, A., and Notter, R. H. (2005) Surfactant alterations in acute inflammatory lung injury from aspiration of acid and gastric particulates, *American journal of physiology 288*, L699-708.
153. Folch, J., Lees, M., and Sloane Stanley, G. H. (1957) A simple method for the isolation and purification of total lipides from animal tissues, *The Journal of biological chemistry 226*, 497-509.
154. Vance, D. E., and Sweeley, C. C. (1967) Quantitative determination of the neutral glycosyl ceramides in human blood, *Journal of lipid research 8*, 621-630.
155. Horning, M. G., Williams, E. A., and Horning, E. C. (1960) Separation of tissue cholesterol esters and triglycerides by silicic acid chromatography, *Journal of lipid research 1*, 482-484.
156. Bartlett, G. R. (1959) Phosphorus assay in column chromatography, *The Journal of biological chemistry 234*, 466-468.
157. Svennerholm, L. (1956) The quantitative estimation of cerebrosides in nervous tissue, *Journal of neurochemistry 1*, 42-53.
158. Corsetto, P. A., Montorfano, G., Zava, S., Jovenitti, I. E., Cremona, A., Berra, B., and Rizzo, A. M. Effects of n-3 PUFAs on breast cancer cells through their incorporation in plasma membrane, *Lipids in health and disease 10*, 73.
159. D'Alessandro, S., Basilico, N., Corbett, Y., Scaccabarozzi, D., Omodeo-Sale, F., Saresella, M., Marventano, I., Vaillant, M., Olliaro, P., and Taramelli, D. Hypoxia modulates the effect of

dihydroartemisinin on endothelial cells, *Biochemical pharmacology 82*, 476-484.

160. Bradford, M. M. (1976) A rapid and sensitive method for the quantitation of microgram quantities of protein utilizing the principle of protein-dye binding, *Analytical biochemistry 72*, 248-254.
161. Aebi, H. (1984) Catalase in vitro, *Methods in enzymology 105*, 121-126.
162. Pinto, M. C., Mata, A. M., and Lopez-Barea, J. (1984) Reversible inactivation of Saccharomyces cerevisiae glutathione reductase under reducing conditions, *Archives of biochemistry and biophysics 228*, 1-12.
163. Beutler. (1984) Red cell metabolism A manual of Biochemical Methods, (Grune and Stratton, O., Ed.) 3rd edn ed.
164. Tager, A. M., Kradin, R. L., LaCamera, P., Bercury, S. D., Campanella, G. S., Leary, C. P., Polosukhin, V., Zhao, L. H., Sakamoto, H., Blackwell, T. S., and Luster, A. D. (2004) Inhibition of pulmonary fibrosis by the chemokine IP-10/CXCL10, *American journal of respiratory cell and molecular biology 31*, 395-404.
165. Deroost, K., Lays, N., Noppen, S., Martens, E., Opdenakker, G., and Van den Steen, P. E. Improved methods for haemozoin quantification in tissues yield organ-and parasite-specific information in malaria-infected mice, *Malaria journal 11*, 166.
166. WHO. (2010) Guidelines for the treatment of malaria, *World Health Organization 2nd Ed., Geneva*.
167. Gupta, D., Ramanathan, R. P., Aggarwal, A. N., and Jindal, S. K. (2001) Assessment of factors predicting outcome of acute respiratory distress syndrome in North India, *Respirology 6*, 125-130.

168. Frita, R., Carapau, D., Mota, M. M., and Hanscheid, T. In Vivo Hemozoin Kinetics after Clearance of Plasmodium berghei Infection in Mice, *Malaria research and treatment 2012*, 373086.

169. Schwarzer, E., Muller, O., Arese, P., Siems, W. G., and Grune, T. (1996) Increased levels of 4-hydroxynonenal in human monocytes fed with malarial pigment hemozoin. A possible clue for hemozoin toxicity, *FEBS letters 388*, 119-122.

170. Charoenpan, P., Indraprasit, S., Kiatboonsri, S., Suvachittanont, O., and Tanomsup, S. (1990) Pulmonary edema in severe falciparum malaria. Hemodynamic study and clinicophysiologic correlation, *Chest 97*, 1190-1197.

171. Feldman, R. M., and Singer, C. (1987) Noncardiogenic pulmonary edema and pulmonary fibrosis in falciparum malaria, *Reviews of infectious diseases 9*, 134-139.

172. Viviano, C. J., Bakewell, W. E., Dixon, D., Dethloff, L. A., and Hook, G. E. (1995) Altered regulation of surfactant phospholipid and protein A during acute pulmonary inflammation, *Biochim Biophys Acta 1259*, 235-244.

173. Hodson, L., Skeaff, C. M., and Fielding, B. A. (2008) Fatty acid composition of adipose tissue and blood in humans and its use as a biomarker of dietary intake, *Prog Lipid Res 47*, 348-380.

174. Baker, C. S., Evans, T. W., Randle, B. J., and Haslam, P. L. (1999) Damage to surfactant-specific protein in acute respiratory distress syndrome, *Lancet 353*, 1232-1237.

175. Rodriguez-Capote, K., Manzanares, D., Haines, T., and Possmayer, F. (2006) Reactive oxygen species inactivation of surfactant involves structural and functional alterations to surfactant proteins SP-B and SP-C, *Biophys J 90*, 2808-2821.

176. Frerking, I., Gunther, A., Seeger, W., and Pison, U. (2001) Pulmonary surfactant: functions, abnormalities and therapeutic options, *Intensive Care Med 27*, 1699-1717.

177. Holm, B. A., Enhorning, G., and Notter, R. H. (1988) A biophysical mechanism by which plasma proteins inhibit lung surfactant activity, *Chem Phys Lipids 49*, 49-55.

178. Veldhuizen, R. A., McCaig, L. A., Akino, T., and Lewis, J. F. (1995) Pulmonary surfactant subfractions in patients with the acute respiratory distress syndrome, *Am J Respir Crit Care Med 152*, 1867-1871.

179. Gunther, A., Schmidt, R., Harodt, J., Schmehl, T., Walmrath, D., Ruppert, C., Grimminger, F., and Seeger, W. (2002) Bronchoscopic administration of bovine natural surfactant in ARDS and septic shock: impact on biophysical and biochemical surfactant properties, *Eur Respir J 19*, 797-804.

180. Wang, Z., and Notter, R. H. (1998) Additivity of protein and nonprotein inhibitors of lung surfactant activity, *Am J Respir Crit Care Med 158*, 28-35.

181. Nakos, G., Kitsiouli, E., Hatzidaki, E., Koulouras, V., Touqui, L., and Lekka, M. E. (2005) Phospholipases A2 and platelet-activating-factor acetylhydrolase in patients with acute respiratory distress syndrome, *Crit Care Med 33*, 772-779.

182. Kostopanagiotou, G., Routsi, C., Smyrniotis, V., Lekka, M., Kitsiouli, E., Arkadopoulos, N., and Nakos, G. (2003) Alterations in bronchoalveolar lavage fluid during ischemia-induced acute hepatic failure in the pig., *Hepatology (Baltimore, Md 37*, 1130-1138.

183. Landin, B., Nilsson, A., Twu, J. S., and Schotz, M. C. (1984) A role for hepatic lipase in chylomicron and high density lipoprotein phospholipid metabolism, *J Lipid Res 25*, 559-563.

184. Feingold, K. R., Memon, R. A., Moser, A. H., Shigenaga, J. K., and Grunfeld, C. (1999) Endotoxin and interleukin-1 decrease hepatic lipase mRNA levels, *Atherosclerosis 142*, 379-387.

185. Catala, A. (2009) Lipid peroxidation of membrane phospholipids generates hydroxy-alkenals and oxidized phospholipids active in physiological and/or pathological conditions, *Chem Phys Lipids 157*, 1-11.

186. Khovidhunkit, W., Kim, M. S., Memon, R. A., Shigenaga, J. K., Moser, A. H., Feingold, K. R., and Grunfeld, C. (2004) Effects of infection and inflammation on lipid and lipoprotein metabolism: mechanisms and consequences to the host, *J Lipid Res 45*, 1169-1196.

187. Nilsson, A., and Duan, R. D. (2006) Absorption and lipoprotein transport of sphingomyelin, *J Lipid Res 47*, 154-171.

188. Ly, H., Francone, O. L., Fielding, C. J., Shigenaga, J. K., Moser, A. H., Grunfeld, C., and Feingold, K. R. (1995) Endotoxin and TNF lead to reduced plasma LCAT activity and decreased hepatic LCAT mRNA levels in Syrian hamsters, *J Lipid Res 36*, 1254-1263.

189. Maldonado, E. N., Furland, N. E., Pennacchiotti, G., and Aveldano, M. I. (2002) Reversibility of the changes induced ny n-3 fatty acids in mouse plasma, liver and blood cell lipids, *Journal of Nutritional Biochemistry 13*, 36-46.

190. Sgoutas, D. S. (1972) Fatty acid specificity of plasma phosphatidylcholine: cholesterol acyltransferase, *Biochemistry 11*, 293-296.

191. Murthy, G. L., Sahay, R. K., Sreenivas, D. V., Sundaram, C., and Shantaram, V. (1998) Hepatitis in falciparum malaria, *Trop Gastroenterol 19*, 152-154.

192. Pessayre, D., and Fromenty, B. (2005) NASH: a mitochondrial disease, *J Hepatol 42*, 928-940.

193. Gabele, E., Froh, M., Arteel, G. E., Uesugi, T., Hellerbrand, C., Scholmerich, J., Brenner, D. A., Thurman, R. G., and Rippe, R. A. (2009) TNFalpha is required for cholestasis-induced liver fibrosis in the mouse, *Biochem Biophys Res Commun 378*, 348-353.

194. Feldstein, A. E., Werneburg, N. W., Canbay, A., Guicciardi, M. E., Bronk, S. F., Rydzewski, R., Burgart, L. J., and Gores, G. J. (2004) Free fatty acids promote hepatic lipotoxicity by stimulating TNF-alpha expression via a lysosomal pathway, *Hepatology (Baltimore, Md 40*, 185-194.

195. Gormaz, J. G., Rodrigo, R., Videla, L. A., and Beems, M. Biosynthesis and bioavailability of long-chain polyunsaturated fatty acids in non-alcoholic fatty liver disease, *Prog Lipid Res 49*, 407-419.

196. Tsukada, S., Parsons, C. J., and Rippe, R. A. (2006) Mechanisms of liver fibrosis, *Clin Chim Acta 364*, 33-60.

197. Van den Steen, P. E., Van Aelst, I., Starckx, S., Maskos, K., Opdenakker, G., and Pagenstecher, A. (2006) Matrix metalloproteinases, tissue inhibitors of MMPs and TACE in experimental cerebral malaria, *Laboratory investigation; a journal of technical methods and pathology 86*, 873-888.

198. Prato, M., Giribaldi, G., Polimeni, M., Gallo, V., and Arese, P. (2005) Phagocytosis of hemozoin enhances matrix metalloproteinase-9 activity and TNF-alpha production in human monocytes: role of matrix metalloproteinases in the pathogenesis of falciparum malaria, *J Immunol 175*, 6436-6442.

199. Prato, M., Gallo, V., Giribaldi, G., Aldieri, E., and Arese, P. Role of the NF-kappaB transcription pathway in the haemozoin- and 15-

HETE-mediated activation of matrix metalloproteinase-9 in human adherent monocytes, *Cellular microbiology 12*, 1780-1791.

200. Giribaldi, G., Prato, M., Ulliers, D., Gallo, V., Schwarzer, E., Akide-Ndunge, O. B., Valente, E., Saviozzi, S., Calogero, R. A., and Arese, P. Involvement of inflammatory chemokines in survival of human monocytes fed with malarial pigment, *Infection and immunity 78*, 4912-4921.

CURRICULUM VITAE

ORAL PRESENTATIONS:

Dipartimento di Scienze Farmacologiche e Biomolecolari (DiSFeB); Università degli Studi di Milano; 12 July 2013

"Malaria acute respiratory distress syndrome (MA-ARDS): modification of the lipid profile, antioxidant defences and cytokine content in different tissues".

POSTER PRESENTATIONS:

9th Annual BioMalPar EVIMalaR Conference - Biology and Pathology of the Malaria Parasite (Heidelberg); 13-15 May 2013

"Effects of the malaria infection on lipid metabolism of plasma and tissues in a murine model of malaria associated acute respiratory distress syndrome"

Italian Malaria Network (Perugia); 18 January 2013

"A murine model of malaria associated acute respiratory distress syndrome (MA-ARDS): effects of the infection on lipid metabolism of host plasma and tissues"

Challenges in Malaria Research Meeting (Basilea); 10-12 October 2012

"Surfactant alterations and lipid profile modifications of the lung tissue and surfactant in a murine model of malaria associated ARDS"

IV Annual Meeting COST Action BM0802- V Annual Meeting: Italian Malaria Network (IMN) (Milano); 19-21 January 2012

"Malaria associated ARDS: surfactant alterations and lipid profile modifications in a murine model"

INTERNATIONAL PUBLICATIONS:

Cattaneo MG, Cappellini E, Ragni M, Tacchini L, **Scaccabarozzi D**, Nisoli E, Vicentini LM "***Chronic nitric oxide deprivation induces an adaptive antioxidant status in human endothelial cells"*** Cell Signal.; 25(11):2290-7; 2013

Santacroce M, Daniele F, Cremona A, **Scaccabarozzi D**, Castagna M, Orsini F. **"*Imaging of Xenopus laevis oocyte plasma membrane in physiological-like conditions by atomic force microscopy"*** Microsc Microanal., 19(5):1358-6; 2013

D'Alessandro S, Basilico N, Corbett Y, **Scaccabarozzi D**, Omodeo-Salè F, Saresella M, Marventano I, Vaillant M, Olliaro P, Taramelli D ***"Hypoxia modulates the effect of dihydroartemisinin on endothelial cells"*** Biochem Pharmacol., 1;82(5):476-84; 2011

Omodeo-Salè F, Cortelezzi L, Vommaro Z, **Scaccabarozzi D**, Dondorp AM. ***"Dysregulation of L-arginine metabolism and bioavailability associated to free plasma heme"*** Am J Physiol Cell Physiol., 299(1):C148-54; 2010

ACKNOWLEDGEMENTS

First of all, I wish to thank Professor Fausta Omodeo Salè for her patience as well as for believing in my skills and in this doctoral project.

Further thanks to Professor Donatella Taramelli for giving me the opportunity to attend a PhD, thus allowing the growth of my love and interest for research.

Thanks to Professor Philippe Van den Steen of the University of Leuven (Belgium) for his priceless collaboration and for teaching me new techniques kindly hosting me in his laboratory.

Many thanks to the girls of his laboratory: Katrien, Natacha and Nathalie who made me feel at home from the first day and enlivened not only the lab life but also the evenings and the weekends.

And finally, I would like to thank my colleagues and friends for their happiness, knowledge and for their help with all the experiments.